Intercarrier Interference Reduction and Channel Estimation in OFDM Systems

by

Yihai Zhang
B.Eng., Beijing University of Posts and Telecommunications, 1996
M.A.Sc., University of Victoria, 2005

A Dissertation Submitted in Partial Fulfillment of the
Requirements for the Degree of

DOCTOR OF PHILOSOPHY

in the Department of Electrical and Computer Engineering

Intercarrier Interference Reduction and Channel Estimation in OFDM Systems

by

Yihai Zhang
B.Eng., Beijing University of Posts and Telecommunications, 1996
M.A.Sc., University of Victoria, 2005

Supervisory Committee

Dr. Wu-Sheng Lu, Co-Supervisor
(Department of Electrical and Computer Engineering)

Dr. T. Aaron Gulliver, Co-Supervisor
(Department of Electrical and Computer Engineering)

Dr. Xiaodai Dong, Departmental Member
(Department of Electrical and Computer Engineering)

Dr. Kui Wu, Outside Member
(Department of Computer Science)

Supervisory Committee

Dr. Wu-Sheng Lu, Co-Supervisor
(Department of Electrical and Computer Engineering)

Dr. T. Aaron Gulliver, Co-Supervisor
(Department of Electrical and Computer Engineering)

Dr. Xiaodai Dong, Departmental Member
(Department of Electrical and Computer Engineering)

Dr. Kui Wu, Outside Member
(Department of Computer Science)

ABSTRACT

With the increasing demand for more wireless multimedia applications, it is desired to design a wireless system with higher data rate. Furthermore, the frequency spectrum has become a limited and valuable resource, making it necessary to utilize the available spectrum efficiently and coexist with other wireless systems. Orthogonal frequency division multiplexing (OFDM) modulation is widely used in communication systems to meet the demand for ever increasing data rates. The major advantage of OFDM over single-carrier transmission is its ability to deal with severe channel conditions without complex equalization. However, OFDM systems suffer from a high peak to average power ratio, and they are sensitive to carrier frequency offset and Doppler spread.

This dissertation first focuses on the development of intercarrier interference (ICI) reduction and signal detection algorithms for OFDM systems over time-varying channels. Several ICI reduction algorithms are proposed for OFDM systems over doubly-selective channels. The OFDM ICI reduction problem over time-varying channels is

formulated as a combinatorial optimization problem based on the maximum likelihood (ML) criterion. First, two relaxation methods are utilized to convert the ICI reduction problem into convex quadratic programming (QP) problems. Next, a low complexity ICI reduction algorithm applicable to M-QAM signal constellations for OFDM systems is proposed. This formulates the ICI reduction problem as a QP problem with non-convex constraints. A successive method is then utilized to deduce a sequence of reduced-size QP problems. For the proposed algorithms, the QP problems are solved by limiting the search in the 2-dimensional subspace spanned by its steepest-descent and Newton directions to reduce the computational complexity. Furthermore, a low-bit descent search (LBDS) is employed to improve the system performance. Performance results are given to demonstrate that the proposed ICI reduction algorithms provide excellent performance with reasonable computational complexity.

A low complexity joint semiblind detection algorithm based on the channel correlation and noise variance is proposed which does not require channel state information. The detection problem is relaxed to a continuous non-convex quadratic programming problem. Then an iterative method is utilized to deduce a sequence of reduced-size quadratic programming problems. A LBDS method is also employed to improve the solution of the derived QP problems. Results are given which demonstrate that the proposed algorithm provides similar performance with lower computational complexity compared to that of a sphere decoder.

A major challenge to OFDM systems is how to obtain accurate channel state information for coherent detection of the transmitted signals. Thus several channel estimation algorithms are proposed for OFDM systems over time-invariant channels. A channel estimation method is developed to utilize the noncircularity of the input signals to obtain an estimate of the channel coefficients. It takes advantage of the nonzero cyclostationary statistics of the transmitted signals, which in turn allows blind polynomial channel estimation using second-order statistics of the OFDM symbol. A set of polynomial equations are formulated based on the correlation of the received signal which can be used to obtain an estimate of the time domain channel coefficients. Performance results are presented which show that the proposed algorithm provides better performance than the least minimum mean-square error (LMMSE) algorithm at high signal to noise ratios (SNRs), with low computational complexity. Near-optimal performance can be achieved with large OFDM systems.

Finally, a CS-based time-domain channel estimation method is presented for

OFDM systems over sparse channels. The channel estimation problem under consideration is formulated as a small-scale l_1-minimization problem which is convex and admits fast and reliable solvers for the globally optimal solution. It is demonstrated that the magnitudes as well as delays of the significant taps of a sparse channel model can be estimated with satisfactory accuracy by using fewer pilot tones than the channel length. Moreover, it is shown that a fast Fourier transform (FFT) matrix of extended size can be used as a set of appropriate basis vectors to enhance the channel sparsity. This technique allows the proposed method to be applicable to less-sparse OFDM channels. In addition, a total-variation (TV) minimization based method is introduced to provide an alternative way to solve the original sparse channel estimation problem. The performance of the proposed method is compared to several established channel estimation algorithms.

Contents

Supervisory Committee ii

Abstract iii

Table of Contents vi

List of Tables ix

List of Figures x

List of Abbreviations xii

Acknowledgements xiv

Dedication xv

1 Introduction 1

1.1 Wireless Communication Channel 2

1.1.1 Delay Spread 2

1.1.2 Doppler Spread 3

1.1.3 WSSUS Channel Model 4

1.2 Principles of OFDM 5

1.2.1 OFDM History 6

1.2.2 The Advantages and Disadvantages of OFDM 7

1.2.3 OFDM System Model 9

1.3 ICI Reduction for OFDM Systems 11

1.4 Channel Estimation in OFDM Systems 13

1.5 Contributions and Organization of the Thesis 14

2 Intercarrier Interference Reduction Algorithms for OFDM Systems 17

2.1 Review of ICI Reduction Algorithms 18
2.1.1 Maximum Likelihood Joint Detection 18
2.1.2 Minimum Mean Square Error (MMSE) Detector 19
2.1.3 Low Complexity MMSE ICI Suppression 19
2.1.4 Decision Feedback Detection 20
2.2 Integer QP Relaxation Based Algorithms for ICI Reduction in OFDM Systems 20
2.2.1 Convex Relaxation 21
2.2.2 2-Dimensional Search Method 23
2.3 A Successive ICI Reduction Algorithm for OFDM Systems 23
2.3.1 A Successive ICI Reduction Algorithm 24
2.3.2 Two Implementation Issues 26
2.3.3 Computational Complexity 27
2.3.4 Extension to 64-QAM OFDM Systems 28
2.4 Performance Enhancement by Low-Bit Descent Search 28
2.5 Simulation Results 29
2.5.1 Performance Evaluation of the Integer QP Relaxation Methods 29
2.5.2 Performance Evaluation of the Successive ICI Reduction Algorithm 31
2.6 Conclusions 32

3 Low Complexity Joint Semiblind Detection for OFDM Systems over Time-Varying Channels 40
3.1 Joint Semiblind Detection Problem 41
3.2 An Iterative Joint Semiblind Detection Algorithm 43
3.2.1 Basic Algorithm 45
3.3 Simulation Results 47
3.4 Conclusions 49

4 Blind Polynomial Channel Estimation for OFDM Systems 55
4.1 Blind Polynomial Channel Estimation for OFDM Systems 56
4.2 An Example 58
4.3 Performance Evaluation 60
4.4 Conclusions 62

5 OFDM Channel Estimation Using Compressive Sensing 66

5.1 Compressive Sensing and TV Minimization 68
5.1.1 Compressive Sensing: Concepts and Key Results 68
5.1.2 Signal Reconstruction via TV Minimization 70
5.2 Sparse Channel Estimation 70
5.2.1 Sparse Channel Estimation with l_1-Minimization 71
5.2.2 Sparse OFDM Channel Estimation by Increasing the FFT Matrix Size 72
5.2.3 Sparse Channel Estimation Using TV Minimization 73
5.3 Performance Evaluation 74
5.4 Conclusions 76

6 Conclusions and Future Work **80**
6.1 Conclusions 80
6.1.1 Intercarrier Interference Reduction Algorithms for OFDM Systems 80
6.1.2 Low Complexity Joint Semiblind Detection for OFDM Systems over Time-Varying Channels 81
6.1.3 Blind Polynomial Channel Estimation for OFDM Systems . . 82
6.1.4 OFDM Channel Estimation Using Compressive Sensing 82
6.2 Future Work 83
6.2.1 ICI Reduction for MIMO OFDM Systems 83
6.2.2 Channel Estimation in OFDM Systems over Doubly-Selective Channels 84
6.2.3 Channel Estimation in MIMO OFDM Systems 84

A Derivation of Constraint (5.11b) **85**

Bibliography **86**

List of Tables

Table 3.1 Computational Complexity Comparison 48

List of Figures

Figure 1.1 Multipath signal propagation [6]. 2
Figure 1.2 Amplitude spectrum of an OFDM symbol. 5
Figure 1.3 The spectrum utilization of an FDM system. 6
Figure 1.4 The spectrum utilization of an OFDM system. 7
Figure 1.5 The basic structure of an OFDM transmitter 10
Figure 1.6 The basic structure of an OFDM receiver. 11
Figure 1.7 Typical training symbol and pilot subcarrier arrangement. . . . 14

Figure 2.1 The feasible set defined by (2.10b) (points on the circle), the feasible region defined by (2.11b) (I), and the feasible region defined by (2.12b) (I+II) [29] 22
Figure 2.2 BER performance of the bounded constraint relaxation method with $f_dT_s = 0.1$ in a 4-QAM OFDM system. 33
Figure 2.3 BER performance of the quadratic constraint relaxation method with $f_dT_s = 0.1$ in a 4-QAM OFDM system. 34
Figure 2.4 BER performance of the 2-dimensional bounded constraint relaxation method with various Doppler spreads in a 4-QAM OFDM system. 35
Figure 2.5 BER performance of the successive ICI reduction algorithm with $f_dT_s = 0.05$ in a 16-QAM OFDM system. 36
Figure 2.6 BER performance of the successive ICI reduction algorithm with $f_dT_s = 0.1$ in a 16-QAM OFDM system. 37
Figure 2.7 BER performance of the successive ICI reduction algorithm with $f_dT_s = 0.3$ in a 16-QAM OFDM system. 38
Figure 2.8 BER performance of the successive ICI reduction algorithm with various Doppler spreads in a 64-QAM OFDM system. 39

Figure 3.1 The feasible regions defined by (3.12b) and (3.13b). 44

Figure 3.2 BPSK OFDM system performance with $f_dT_s = 0.01$, $\alpha = 0.8$ and 4 pilot tones. 50
Figure 3.3 QPSK OFDM system performance with $f_dT_s = 0.01$, $\alpha = 0.8$ and 4 pilot tones. 51
Figure 3.4 QPSK OFDM system performance with $f_dT_s = 0.01$, 4 pilot tones and various thresholds using the proposed IJSD algorithm. 52
Figure 3.5 QPSK OFDM system performance with $\alpha = 0.8$, 4 pilot tones and various Doppler spreads using the proposed IJSD algorithm with LBDS. 53
Figure 3.6 QPSK OFDM system performance with $f_dT_s = 0.01$, $\alpha = 0.8$ and various pilot tones using the proposed IJSD algorithm with LBDS. 54

Figure 4.1 BER performance of a 6-tap 128-subcarrier OFDM system. . . 63
Figure 4.2 Mean-square error of the proposed method for a 128-subcarrier OFDM system with various channel lengths. 64
Figure 4.3 BER performance of the proposed method for an OFDM system with various numbers of subcarriers and a 6-tap channel. 65

Figure 5.1 BER performance of a 20-tap 128-subcarrier OFDM system with 2 nonzero taps. 77
Figure 5.2 BER performance of a 10-tap 128-subcarrier OFDM system with 2 nonzero taps. 78
Figure 5.3 BER performance of a 20-tap 128-subcarrier OFDM system with 4 nonzero taps. 79

List of Abbreviations

4G	Fourth Generation
AWGN	Additive White Gaussian Noise
BER	Bit Error Rate
BP	Basis Pursuit
BPSK	Binary Phase-Shift Keying
CFO	Carrier Frequency Offset
CFR	Channel Frequency Response
CIR	Channel Impulse Response
CP	Cyclic Prefix
CS	Compressive Sensing
CSI	Channel State Information
DAB	Digital Audio Broadcasting
DFE	Decision Feedback Equalizer
DFT	Discrete Fourier Transform
DS-CDMA	Direct Sequence Code Division Multiple Access
DVB	Digital Video Broadcasting
FDM	Frequency Division Multiplexing
FEC	Forward Error Correction
FFT	Fast Fourier Transform
FIR	Finite Impulse Response
GAIC	Generalized Akaike Information Criterion
KKT	Karush-Kuhn-Tucker
ICI	Intercarrier Interference
IFFT	Inverse Fast Fourier Transform
IJSD	Iterative Joint Semiblind Detection
ISI	Inter-Symbol Interference
JD	Joint Detection
LBDS	Low-Bit Descent Search
LMMSE	Least Minimum Mean-Square Error
LOS	Line-of-Sight
LP	Linear Programming

LTE	Long Term Evolution
MMSE	Minimum Mean-Square Error
MIMO	Multiple-Input Multiple-Output
ML	Maximum Likelihood
MUSIC	Multiple Signal Characterization
NLOS	Non-Line-of-Sight
OFDM	Orthogonal Frequency Division Multiplexing
OMP	Orthogonal Matching Pursuit
PAPR	Peak-to-Average Power Ratio
PSK	Phase-Shift Keying
QAM	Quadrature Amplitude Modulation
QP	Quadratic Programming
rms	Root-Mean-Square
SIMO	Single-Input Multiple-Output
SIR	Signal to Interference Ratio
SISO	Single-Input Single Output
SNR	Signal to Noise Ratio
SOCP	Second-order Cone Programming
TDL	Tapped Delay Line
TV	Total-Variation
WIMAX	Worldwide Interoperability for Microwave Access
WSSUS	Wide Sense Stationary Uncorrelated Scattering
ZF	Zero Forcing

ACKNOWLEDGEMENTS

First and foremost, I would like to express my sincere gratitude to my co-supervisors, Dr. Wu-Sheng Lu and Dr. T. Aaron Gulliver for their invaluable guidance and encouragement throughout the journey towards the completion of my PhD degree. Their excellent academic advice and support have been invaluable.

I would like to thank Dr. Xiaodai Dong and Dr. Kui Wu for agreeing to serve on my Supervisory Committee, and for providing insightful suggestions and comments that helped me improve the quality of this dissertation. I would also like to thank the staff of the Department of Electrical and Computer Engineering, Ms. Catherine Chang, Ms. Lynne Barrett, Ms. Vicky Smith, Ms. Moneca Bracken, and Ms. Mary-Anne Teo, and my past and present fellow students and colleagues in the Wireless Communications and Digital Signal Processing research groups, namely Carlos Quiroz Perez, Behzad Bahr-Hosseini, Shiva Kumar Planjery, Dr. Le Yang, Dr. Peng Lu, Dr. Wei Li, Yousry Abdel-Hamid, Dr. Abolfazl Ghassemi, Dr. Yajun Kou, Dr. Parameswaran Ramachandran, Dr. Ana-Maria Sevcenco, Ping Wan, Di Xu, and Jie Yan for their support. Their friendship has made my life in Victoria a wonderful memory.

Most importantly, my deepest thanks go to my parents and brother for their love, understanding and unconditional support in the pursuit of my PhD degree. My wife, Changzheng Liu, has offered me her immense love and encouragement for many years. Without her support, I would not have been able to complete this dissertation.

DEDICATION

to my parents and my wife

Chapter 1

Introduction

With the ever-increasing demand for wireless multimedia applications, it is desirable to design wireless systems with higher data rates. Furthermore, the frequency spectrum has become a limited and valuable resource, making it necessary to utilize the available spectrum efficiently and coexist with other wireless systems. Thus future wireless technology is required to operate at high data rates, at high carrier frequencies under the environment of high mobility and large spectral interference, while the data transmission still remains reliable and supports multiple users. Orthogonal frequency division multiplexing (OFDM) technology is at the core of multicarrier systems that play a crucial role in fulfilling the above requirements.

OFDM modulation is widely used in communication systems to meet the demand for ever increasing data rates. The major advantage of OFDM over single-carrier transmission is its ability to deal with severe channel conditions without complex equalization. An OFDM signal can be viewed as a number of narrowband signals combined together rather than one wideband signal, thus the complexity of the receiver is significantly reduced. The standards employing OFDM modulation include digital video broadcasting (DVB) [1], digital audio broadcasting (DAB) [2], IEEE 802.11a, 802.11g and 802.11n [3] for wireless local area networks, and the fourth generation (4G) wireless standards - long term evolution (LTE) [4] and worldwide interoperability for microwave access (WIMAX) [5].

In this chapter, background on wireless communication channels is first presented, then a brief introduction of OFDM technology is given, followed by an outline of the remainder of this dissertation.

1.1 Wireless Communication Channel

In a wireless system, the radio link between the mobile device and the base station is referred to as the wireless channel. The channel is affected by large-scale and small-scale fading [6]. Large scale fading in a wireless channel is mostly due to the simple attenuations when the radio signal is transmitted through the atmosphere. On the other hand, small-scale fading is the result of the presence of reflectors and scatterers between the mobile device and the base station, which leads to multiple versions of the transmitted signal arriving at the receiver, with different amplitudes, phases and angles of arrival. In this dissertation, only small-scale fading is discussed.

The transmitted signal can arrive at the receiver either directly in a straight line, also known as line-of-sight (LOS) communication, or after being reflected and refracted on buildings, mountains and other surroundings in the environment, also known as non-line-of-sight (NLOS) [6], as shown in Fig. 1.1. Thus the signal transmitted through the wireless channel contains multiple replicas (echoes) of the transmitted signal. At the receiver, the multipath components experience different path loss, delay and angle of arrival, and interfere with each other constructively or destructively. This wireless channel is referred to as a multipath channel, and the multipath components of the wireless channel are characterized by their *delay spread* and *Doppler spread*.

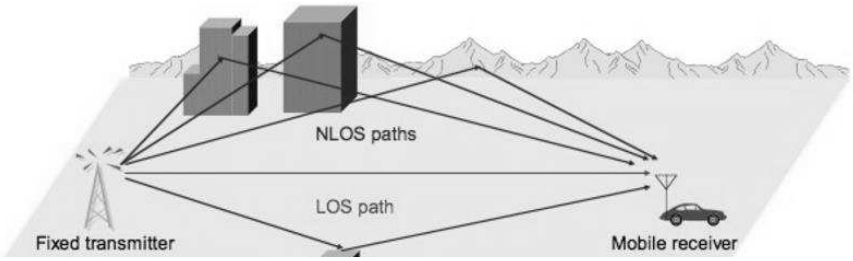

Figure 1.1: Multipath signal propagation [6].

1.1.1 Delay Spread

Delay spread is used to characterize the time dispersion of a wireless channel, which is due to multiple replicas of the transitted signal arriving at the receiver with different

delays. In general, it is a measure of the time difference between the first significant multipath component (usually the LOS component) and the last multipath component. The *delay spread* is usually quantified by the mean excess delay ($\bar{\tau}$) and the root-mean-square (rms) delay spread (σ_τ) [6].

The main effects of *delay spread* on the received signal are frequency-selective fading and inter-symbol interference(ISI). Frequency selective fading means that the channel does not affect all frequency components of the signal equally, which results in distortion of the received signal. On the other hand, ISI is the interference between consecutive symbols. Due to the reception of multiple copies of the signal with different delays, energy from one symbol can spread to the following symbol. If not dealt with, frequency-selective fading and ISI can result in a significant degradation in system performance.

If a channel has a constant gain and linear phase response over a bandwidth greater than the bandwidth of the transmitted signal, the channel is called a flat fading channel. With a frequency flat channel, the delay spread is usually considered to be negligible compared to the symbol duration. If the channel has a constant gain and linear phase response over a bandwidth that is smaller than the bandwidth of the transmitted signal, then the channel is frequency selective [7].

1.1.2 Doppler Spread

In a slow fading channel, the channel impulse response changes much slower than the transmitted signal, hence the channel can be considered constant over time. However, if the transmitted baseband signal changes rapidly compared to the rate of change of the channel, the amplitude and phase change induced by the channel varies over time, resulting in fast fading channel. *Doppler spread* is a commonly used measure of the time variation of a wireless channel, and is related to the mobility of the device and the angle of arrival [6].

In the frequency domain, user mobility leads to a frequency spread of the signal which is dependent on the operating frequency and the relative speed between the transmitter and receiver, i.e., [6]

$$f_m = \frac{v}{c} f_0 \tag{1.1}$$

where v is the mobile speed relative to the base station, c denotes the speed of light, f_0 is the center carrier frequency and f_m is the maximum Doppler frequency.

In the time domain, the coherence time is a statistical measure of the time duration

over which the channel impulse response is invariant. Thus, it is defined as the time duration over which the power of two received signals has a strong correlation. If the coherence time is defined as the time over which the time correlation function is above 0.5, then the coherence time is approximately given by [6]

$$T_c = \frac{9}{16\pi f_m} \tag{1.2}$$

If the symbol duration of the transmitted signal is smaller than the coherence time of the channel, then the effect of *Doppler spread* can be ignored. This is called a slow fading channel. Alternatively, if the symbol duration is greater than the coherence time of the channel, then the channel will change during the transmission of the signal, thus causing distortion at the receiver. This is called a fast fading channel.

1.1.3 WSSUS Channel Model

Due to the randomness of multipath fading channels, statistical models are usually employed to characterize wireless channels [8]. In this dissertation, a wide sense stationary uncorrelated scattering (WSSUS) model is assumed, such that the channel correlation is invariant over time, and scatterers with different path delays are uncorrelated [7]. A WSSUS channel has an impulse response given by

$$h(t;\tau) = \sum_{d=1}^{D} h(t;\tau_d)\delta(\tau - \tau_d) \tag{1.3}$$

where τ_d is the dth path delay with $\tau_1 < \tau_2 < \ \ldots \ < \tau_D$. In a rich scattering environment, the channel autocorrelation function is separable in terms of time and delay, i.e., $\phi_h(\triangle t;\tau) = \phi_t(\triangle t)\phi_\tau(\tau)$, where $\phi_t(\triangle t)$ is the time-correlation function based on Jakes' model, which models the channel as a sum of sinusoids, and $\phi_\tau(\tau)$ is the multipath intensity profile [9]. In (1.3), $h(t;\tau_d)$ is a complex Gaussian process with zero mean and variance $\sigma_d^2 \triangleq \phi_\tau(\tau_d)$.

A discrete version of the WSSUS channel in (1.3) can be modelled as a tapped delay line (TDL) [7]

$$h(n;l) = \sum_{d=1}^{D} h(nT_c;\tau_d)\mathrm{sinc}\left(\frac{\tau_d}{T_c} - l\right) \tag{1.4}$$

where $h(n;l)$ denotes the channel coefficient for the lth tap at the nth sampling instant, $n = 0, \ldots, N-1$, $l = 0, \ldots, L-1$ with $L = \lfloor \tau_D / T_c \rfloor + 1$, and the delay between two taps is T_c.

1.2 Principles of OFDM

In recent years, multicarrier modulation has become a key technology for current and future communication systems. Orthogonal Frequency Division Multiplexing (OFDM) is a form of multicarrier modulation that has become popular due to the fact that it provides efficient usage over the available frequency spectrum and high data rates, and is robust against inter-symbol interference and fading caused by multipath propagation [10]. In an OFDM system, the available frequency band W is divided into a large number (N) of subbands and the user data is modulated onto separate subcarriers. These subcarriers are orthogonal to each other. To achieve orthogonality between subcarriers, the spacing between them is made equal to the reciprocal of the useful symbol period W/N. The spectrum of these subcarriers shows that each has a null at the center frequency of the other subcarriers in the system, as shown in the Fig. 1.3. When the subcarriers are chosen in this fashion, there is no interference between them.

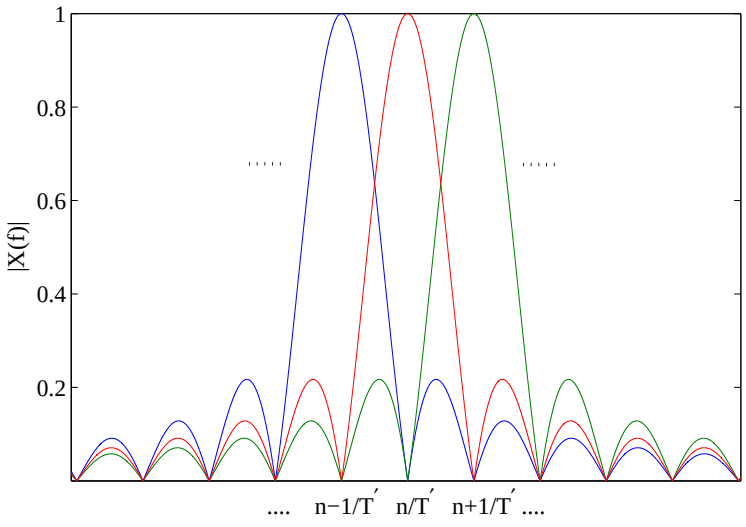

Figure 1.2: Amplitude spectrum of an OFDM symbol.

1.2.1 OFDM History

The concept of frequency division multiplexing (FDM) was introduced around the end of the 1950s for military communications to achieve higher data rates [10]. An FDM system divides the frequency band into non-overlapping frequency bands, and a serial-to-parallel converter divides the incoming message into multiple low rate signals, which in turn are multiplied with separate carrier frequencies. Guard bands or empty spectral regions are inserted between neighbouring bands to eliminate interchannel interference and ensure the data can be separated using filters at the receiver. However, the spectrum utilization of this system is low. The frequency spectrum of an FDM system is depicted in Fig. 1.2. Due to a lack of mature wideband equalization receiver techniques at that time, the parallel system was actually more expensive to implement than a single wideband transceiver, and less efficient in terms of spectrum utilization. In addition, the system performance is affected by ISI due to the short duration of the transmission period and higher distortion due to the wider frequency band.

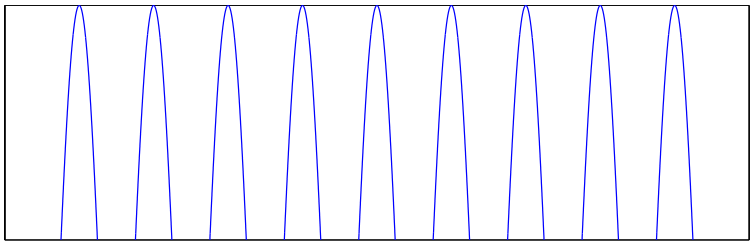

Figure 1.3: The spectrum utilization of an FDM system.

In the middle 1960s, OFDM scheme was introduced by Chang [11] for parallel transmission over a bandlimited channel without intercarrier interference (ICI) and ISI. He proposed dividing a frequency-selective fading channel into a number of flat-fading channels, which simplifies the receiver design. The subchannels are orthogonal to each other, which results in higher spectral efficiency, as shown in Fig. 1.4.

The transmitter and receiver of an OFDM systems must be carefully designed so that orthogonality can be maintained between the subchannels. As the number of subcarriers increases, implementation of an OFDM system becomes more complex considering the requirements of modulation, synchronization and coherent demodulation. In particular, it was impractical to implement the modulation using oscillators at the required frequencies. In the 1970s, the Discrete Fourier Transform (DFT) was

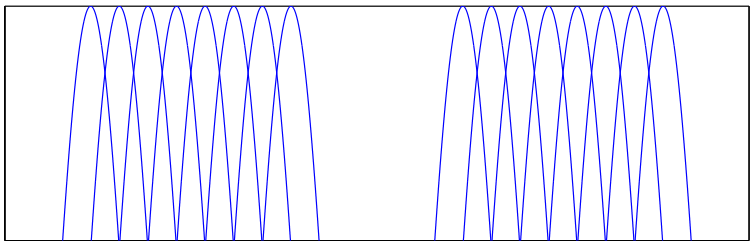

Figure 1.4: The spectrum utilization of an OFDM system.

proposed by Weinstein and Ebert [12] for modulation and demodulation in OFDM systems. This is referred to as DFT-based OFDM, and significantly reduces the implementation complexity of OFDM systems. In a DFT-based OFDM system, the DFT is used to transform the data from the frequency domain to the time domain and provide the orthogonality between subcarriers. A guard interval is employed to reduce the effects of multipath channels. Even though the proposed system does not achieve perfect orthogonality among the subcarriers over a time dispersive channel, it has made modern low-cost OFDM systems possible today.

Another important contribution to OFDM was the cyclic prefix (CP), which was proposed by Peled and Ruiz in 1980 to solve the orthogonality problem [13]. A cyclic prefix, instead of the conventional null band, is added at the beginning of the OFDM symbol after inverse fast Fourier transform (IFFT) procedure. If the length of the cyclic prefix is equal to or longer than the channel length, the linear circular channel is converted into a cyclic circular channel, which ensures orthogonality over a time dispersive channel and eliminates the ISI between subcarriers. The cost is a loss in the effective data rate. With the improvement in implementation technology and increased demand for efficient bandwidth usage, OFDM became a popular wireless technology in the 1990s.

1.2.2 The Advantages and Disadvantages of OFDM

Compared to a single carrier wireless system, OFDM provides several advantages [10] [14]:

Robustness to narrowband interference: The duration of an OFDM symbol is much longer than that from an equivalent single carrier system, and narrowband interference will only affect a small fraction of the OFDM symbol. Channel coding and forward error correction (FEC) codes can be employed to recover the errors caused

by narrowband interference. Thus OFDM is robust against narrowband interference;

Resistance to frequency selective fading: In an OFDM system, the frequency-selective channel is divided into a number of frequency-flat fading subchannels. The OFDM symbol duration is increased by mapping the high rate data stream into several lower rate parallel data streams, which in turn reduces the relative channel delay spread. This effectively randomizes the block errors caused by fading so that symbols are only slightly distorted instead of several adjacent symbols being completely destroyed.

Simple equalization: In an OFDM system, the channel bandwidth is divided into many narrow subbands. The subchannel bandwidth is smaller than the channel coherence bandwidth, so the frequency response over individual subbands is relatively flat. Thus, it is possible to have a simpler equalizer than that of an equivalent single carrier system. Furthermore, if the channel is time-invariant within one OFDM symbol duration, a one tap equalizer can be employed at the receiver, which is much simpler than the adaptive equalizer required in a single carrier system;

Immunity to delay spread and multipath: Generally, a cyclic prefix is appended at the beginning of the OFDM symbol at the transmitter. It is typically a copy of the end of the OFDM symbol. The length of the cyclic prefix should be equal to or longer than that of the channel impulse response. Then the OFDM channel is converted from a linear circular channel into a cyclic circular channel so that the ISI can be eliminated. Use of a cyclic prefix can help preserve orthogonality between subcarriers, and also allow the receiver to capture multipath energy more efficiently.

Efficient bandwidth usage: In an OFDM system, the subcarriers are overlapped and no guard band is required, thus the spectrum efficiency can be close to the Nyquist limit;

Computational efficiency: In an OFDM system, an IFFT and FFT are implemented at the transmitter and receiver for modulation and demodulation, respectively, which significantly reduces the computational complexity of the system.

Although OFDM has been implemented in various applications, there are also some major drawbacks in OFDM systems [10]:

High peak to average power ratio: In an OFDM system, the transmitted symbol is the sum of the signals for all the subcarriers, which results in a high peak-to-average power ratio (PAPR). In this case, the RF power amplifiers must operate over a wider linear region. Otherwise, the maximum power of the signals enters the non-linear region of the power amplifier, which results in signal distortion, and induces

intermodulation among the subcarriers and out of band radiation. However, a wider dynamic range linear power amplifier implies large power back-offs, which leads to inefficient amplification and expensive transmitter designs. Thus, it is desirable to reduce the PAPR in OFDM systems [15].

Sensitivity to carrier frequency offset: Another disadvantage of OFDM systems is the high sensitivity to carrier frequency offset between the oscillators of the transmitter and the receiver. As the bandwidth of each subcarrier is only a small fraction of the total bandwidth, a small carrier frequency offset (CFO) will induce impairments such as attenuation and phase rotation of the subcarriers, and intercarrier interference between subcarriers. Thus precise CFO estimation is needed in OFDM systems. A number of methods have been developed to reduce the sensitivity to frequency offset [10].

Sensitivity to Doppler spread: OFDM is sensitive to Doppler spread caused by user mobility [14], which results in loss of orthogonality among subcarriers. This in turn leads to intercarrier interference and degrades system performance. While it is straightforward to estimate and reduce the ICI induced by phase noise, the ICI introduced by Doppler spread is a more challenging problem.

1.2.3 OFDM System Model

In an OFDM system, the data stream is divided into N parallel lower rate streams and multiplexed onto a number of subcarriers using an IFFT. These subcarriers are overlapped orthogonally to provide bandwidth efficient transmission.

A cyclic prefix is inserted at the beginning of each OFDM symbol before transmission and removed before demodulation. The length of the cyclic prefix is greater than or equal to that of the channel impulse response to eliminate the inter-symbol interference. Generally, a one-tap equalizer is utilized in the frequency-domain to cancel the multipath distortion over time-invariant channels [10].

The system bandwidth is divided into N subchannels, and the data stream is typically modulated onto the subcarriers using quadrature amplitude modulation (QAM) or phase-shift keying (PSK). The transmitted signal is generated using an IFFT

$$x_n = \frac{1}{\sqrt{N}} \sum_{k=0}^{N-1} X_k \exp\left(\frac{j2\pi kn}{N}\right) \text{ for } n = 0, \ldots \ N-1 \tag{1.5}$$

where x_n is the time-domain signal at the nth sampling instant, and X_k is the

frequency-domain data symbol for the kth subcarrier. Equation (1.5) can be written in vector form as

$$\mathbf{x} = \mathbf{F}\mathbf{X} \tag{1.6}$$

where $\mathbf{x} = [x_0\ x_1\ \ldots\ x_{N-1}]^T$ and $\mathbf{X} = [X_0\ X_1\ \ldots\ X_{N-1}]^T$ represent the time-domain and frequency-domain OFDM symbols, respectively, and $\mathbf{F}$ is the IFFT matrix with elements $f_{n,k} = \frac{1}{\sqrt{N}} \exp(\frac{j2\pi kn}{N})$. The OFDM symbol duration is denoted by T_s, so the chip duration of each subchannel is $T_c = T_s/N$. The basic structure of an OFDM transmitter is depicted in Fig. 1.5.

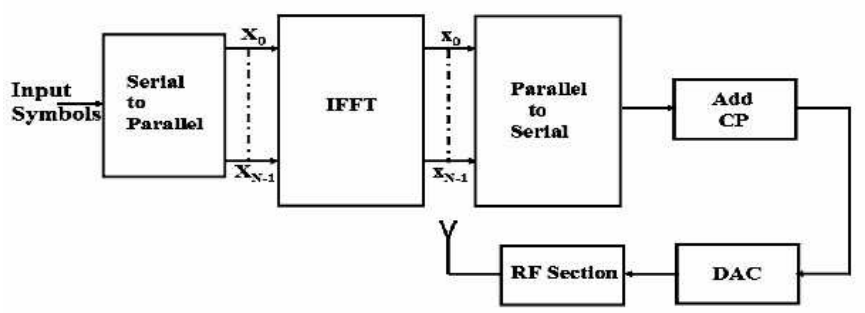

Figure 1.5: The basic structure of an OFDM transmitter

The length N_p of the cyclic prefix is assumed to be greater than or equal to that of the channel impulse response to eliminate intersymbol interference. Thus, the discrete received signal at the nth sampling instant can be expressed as

$$y_n = \sum_{l=0}^{L-1} h(n,l)x(n-l) + w_n \quad \text{for } n = -N_p, \ldots,\ N-1 \tag{1.7}$$

where w_n is additive white Gaussian noise (AWGN) at the nth sampling instant with zero mean and variance σ^2. In vector form, (1.7) can be written as

$$\mathbf{y} = \mathbf{H}\mathbf{x} + \mathbf{w} \tag{1.8}$$

where $\mathbf{y}$ and $\mathbf{w}$ denote the time-domain received signal and AWGN noise, respectively,

and $\mathbf{H}$ is the channel matrix given by

$$\mathbf{H} = \begin{bmatrix} h(0,0) & 0 & \dots & h(0,1) \\ h(1,1) & h(1,0) & \dots & h(1,2) \\ \vdots & \vdots & \ddots & \vdots \\ h(L-1,L-1) & h(L-1,L-2) & \dots & 0 \\ \vdots & \vdots & \ddots & \vdots \\ 0 & 0 & \dots & h(N-1,0) \end{bmatrix}.$$

After removing the CP and performing a fast Fourier transform (FFT), we obtain

$$\mathbf{Y} = \mathbf{AX} + \mathbf{W} \tag{1.9}$$

where $\mathbf{Y} = [Y_0 \ \dots \ Y_{N-1}]^T$ is the frequency-domain received signal, $\mathbf{A} = \mathbf{F}^H\mathbf{HF}$, and $\mathbf{W} = \mathbf{F}^H\mathbf{w}$. The basic structure of an OFDM receiver is shown in Fig. 1.6.

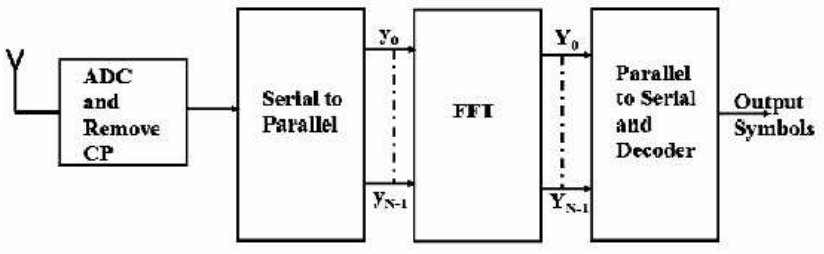

Figure 1.6: The basic structure of an OFDM receiver.

1.3 ICI Reduction for OFDM Systems

In a time invariant environment, the subcarriers in an OFDM system are orthogonal to each other. Thus $h(t;\tau_d)$ in (1.3) remains constant within one OFDM symbol duration, and $\mathbf{A}$ in (1.9) is a diagonal matrix. However, the orthogonality among subcarriers is destroyed in a fast fading environment, where the channel characteristics change over the duration of one OFDM symbol. This channel variation introduces different Doppler frequencies for the channel paths, which induces inter-carrier interference. This in turn results in a reduction in the effective signal to noise ratio due to the reduced carrier to interference ratio, and degrades system performance [16].

In this case, the received signal on the kth subcarrier can be written as

$$Y_k = A_{k,k}X_k + \sum_{m=0,m\neq k}^{N-1} A_{k,m}X_m + W_k \tag{1.10}$$

where $k = 0,\ \ldots,\ N-1$, $A_{k,m}$ denotes the (k,m)th element of $\mathbf{A}$, and $\sum_{m=0,m\neq k}^{N-1} A_{k,m}X_m$ represents the inter-carrier interference caused by other subcarriers. Thus the received signal at a given subcarrier depends not only on the transmitted signal at this subcarrier but also the transmitted signals from other subcarriers [17].

From (1.10), the signal to interference ratio (SIR) for the kth subcarrier is given by

$$SIR_k = \frac{E[|S_k|^2]}{E[|I_k|^2]} \text{ for } k = 0,\ \ldots,\ N-1 \tag{1.11}$$

where $S_k = A_{k,k}X_k$, and $I_k = \sum_{m=0,m\neq k}^{N-1} A_{k,m}X_m$. Because each path is statistically independent to each other, the individual ICI components $A_{k,m}X_m$, (for $k = 0,\ \ldots,\ N-1,\ m \neq k$) with respect to subcarrier k are uncorrelated. Consequently, for sufficiently large N, the ICI components can be modelled as zero mean additive Gaussian noise using the central limit theorem [16].

Assume

$$E[|S_k|^2] = E_s \text{ for } k = 0,\ \ldots,\ N-1 \tag{1.12}$$

is the signal energy on the kth subcarrier. Consequently, the variance of the ICI is bounded as [18]

$$Var(I_k) \leq \frac{1}{12}(2\pi f_d T_s)^2 E_s \text{ for } k = 0,\ \ldots,\ N-1 \tag{1.13}$$

where f_d is the Doppler frequency and T_s denotes the OFDM symbol duration. This in turn leads to a lower bound on the SIR for the kth subcarrier as

$$SIR_k \geq \frac{12}{(2\pi f_d T_s)^2} \text{ for } k = 0,\ \ldots,\ N-1 \tag{1.14}$$

Generally, a one tap equalizer is implemented in the OFDM system to take the advantage of the orthogonality among subcarriers. However, the orthogonality is destroyed due to corruption of ICI in a fast fading environment, and the system

performance degrades with increasing Doppler frequency. Thus a joint detection (JD) algorithm is desired at the receiver to mitigate the effects of ICI and improve the system performance.

Recently a number of algorithms have been proposed to mitigate the ICI and improve system performance over doubly-selective channels. In [18], Li and Cimini provide universal bounds on the ICI in an OFDM system over time-varying fading channels, which are evaluated and compared with the exact ICI. An ICI suppression algorithm using parallel cancelling with frequency-domain equalization techniques is presented in [19]. In [20], a block decision feedback equalizer (DFE) algorithm is described which utilizes signals from several neighbouring subcarriers to eliminate the ICI for a certain subcarrier. Kou et al. [21] proposed a low complexity ICI reduction algorithm based on an iterative optimization scheme, but it is appropriate only for OFDM systems with 4-QAM or QPSK.

1.4 Channel Estimation in OFDM Systems

Channel estimation has been investigated extensively in single carrier communication systems. In these systems, the wireless channel is typically modelled as a time-varying finite impulse response (FIR) filter with unknown channel coefficients [22]. Many single carrier channel estimation algorithms can be applied directly to OFDM systems. However, the unique properties of OFDM systems make it possible to develop new algorithms to take advantage of subcarrier orthogonality.

In an OFDM system, the serial data stream is divided and modulated onto the orthogonal subcarriers. For coherent detection of OFDM symbols, the receiver requires reliable channel information. Channel information can be estimated by utilizing pilot symbols in the time or frequency domain [23]. A typical arrangement of pilot symbols in the time or frequency domain is illustrated in Fig 1.7. The time domain channel can be modelled as a FIR filter, as in single carrier systems, where the delays and channel coefficients can be estimated from time domain received samples, which are then transformed to the frequency domain to obtain the channel frequency response (CFR). For frequency domain pilot-aided channel estimation, the common approach is to estimate the channel frequency response at pre-defined pilot tones/subcarriers. Then various methods can be utilized to obtain the channel response at other subcarriers.

Methods using low-order polynomial interpolation based on the channel frequency

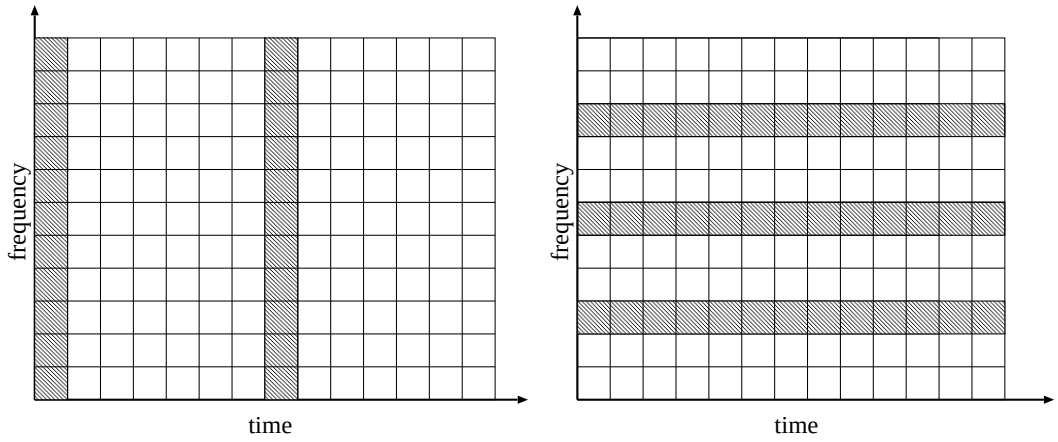

Figure 1.7: Typical training symbol and pilot subcarrier arrangement.

response at pilot tones have been proposed [24]. However, the performance of these methods depends on the spacing between pilots, so the channel response may not be very accurate with wide pilot spacing if the channel varies quickly. An alternative way to obtain the channel frequency response is to exploit the channel correlation among subcarriers. For example, minimum mean-square error (MMSE) estimation performs Wiener filtering using knowledge of second-order statistics of the channel [25]. However, the performance is poor if the channel statistics are not accurate.

1.5 Contributions and Organization of the Thesis

In Chapter 2, two ICI reduction algorithms are proposed for OFDM systems over doubly-selective channels. First, based on maximum likelihood (ML) criterion, the OFDM ICI reduction problem over time-varying channels is formulated as a combinatorial optimization problem. Two relaxation methods are utilized to convert the ICI reduction problem into convex quadratic programming (QP) problems. Next, a low complexity ICI reduction algorithm applicable to M-QAM signal constellations for OFDM systems is proposed. The ICI reduction problem is formulated as a QP problem with non-convex constraints. A successive method is then utilized to deduce a sequence of reduced-size QP problems. For the proposed algorithms, the QP problems are solved by limiting the search in the 2-dimensional subspace spanned by its steepest-descent and Newton directions to reduce the computational complexity. Furthermore, a low-bit descent search (LBDS) is employed to improve system performance. Performance results are given which demonstrate that the proposed ICI

reduction algorithms provide excellent performance with reasonable computational complexity.

In the design of most ICI reduction algorithms for OFDM systems, perfect channel information at the receiver is assumed. However, some robust channel estimation methods require a certain number of pilot symbols, which results in bandwidth loss and overhead, and can be excessive in fast fading channels. A low complexity joint semiblind detection algorithm based on the channel correlation and noise variance is proposed in Chapter 3. The detection problem is relaxed to a continuous non-convex quadratic programming problem. Then an iterative method is utilized to deduce a sequence of reduced-size quadratic programming problems, and the LBDS method is employed to improve the solution of the derived QP problems . Results are presented which demonstrate that the proposed algorithm provides similar performance with lower computational complexity compared to that of a sphere decoder.

A channel estimation method for OFDM systems is developed in Chapter 4 where the channel is assumed to be time-invariant within one OFDM symbol. This method utilizes the noncircularity of the input signals to obtain an estimate of the channel coefficients. It takes advantage of the nonzero cyclostationary statistics of the transmitted signals, which in turn allows blind polynomial channel estimation using second-order statistics of the OFDM symbol. A set of polynomial equations are formulated based on the correlation of the received signal. An estimate of the time domain channel coefficients can then be easily computed by solving these equations. Performance results are presented which show that the proposed algorithm provides better performance than the LMMSE solution at high signal to noise ratios (SNRs) with low computational complexity. Near-optimal performance can be achieved with large OFDM systems.

Chapter 5 presents a CS-based time-domain channel estimation method for OFDM systems over sparse channels. The channel estimation problem under consideration is formulated as a small-scale l_1-minimization problem which is convex and admits fast and reliable solvers for its globally optimal solution. It is demonstrated that the magnitudes as well as delays of the significant taps of a sparse channel model can be estimated with satisfactory accuracy by using fewer pilot tones than the channel length. Moreover, it is shown that a fast Fourier transform (FFT) matrix of extended size can be used as a set of appropriate basis vectors under which the channel sparsity can be enhanced. This allows the proposed method to be applicable to less-sparse OFDM channels. In addition, a total-variation (TV) minimization based method is

introduced to provide an alternative way to solve the original sparse channel estimation problem. The performance of the proposed method is compared to several established channel estimation algorithms.

Chapter 6 concludes the thesis, provides some concluding remarks and suggestions for future work and extensions.

Chapter 2

Intercarrier Interference Reduction Algorithms for OFDM Systems

In OFDM systems, the orthogonality of the subcarriers may be lost due to fast variation of the wireless channel, which in turn results in intercarrier interference [14]. In this chapter, we consider an N-subcarrier OFDM system with complex signals where the modulation for each subcarrier is M-QAM, as described in Section 2.2. A WSSUS channel model is assumed where the channel is time-varying within one OFDM symbol duration, and the length of the channel impulse response is no longer than that of the CP. The ICI reduction algorithms are utilized at the receiver after removing the CP and performing an FFT.

In this chapter, two ICI reduction algorithms are proposed for OFDM systems over doubly-selective channels. First, based on the ML criterion, the OFDM ICI reduction problem over time-varying channels is formulated as a combinatorial optimization problem. Two relaxation methods are utilized to convert the ICI reduction problem into convex QP problems. Next, a low complexity ICI reduction algorithm applicable to M-QAM signal constellations for OFDM systems is proposed. The ICI reduction problem is formulated as a QP problem with non-convex constraints. A successive method is then utilized to deduce a sequence of reduced-size QP problems. The QP problem involved in the proposed algorithms are in turn solved by limiting the search in the 2-dimensional subspace spanned by its steepest-descent and Newton directions to reduce the computational complexity. Furthermore, a low-bit descent search is employed to improve the system performance. Performance results are given which demonstrate that the proposed ICI reduction algorithms provide excellent

performance with reasonable computational complexity.

The rest of chapter is organized as follows. The ICI problem is formulated in Section 2.1, and several ICI algorithms are reviewed to establish the background on joint detection in OFDM systems over fast fading channels. Section 2.3 describes the proposed integer QP based relaxation algorithms for ICI reduction in a 4-QAM OFDM system. A successive ICI reduction algorithm for higher order QAM OFDM systems is presented in Section 2.3. A low-bit descent search method is given in Section 2.4 to improve the performance of the proposed algorithms. Simulations are carried out and the results are described in Section 2.5. Finally, some conclusions are given in Section 2.6.

2.1 Review of ICI Reduction Algorithms

2.1.1 Maximum Likelihood Joint Detection

Maximum likelihood detection is defined as maximizing the joint *a posteriori* probability by selecting the information signal which has minimum Euclidean distance from that of the received signal [26]. Based on the ML detection criterion, the ICI reduction problem for OFDM systems can be formulated as the optimization problem

$$\text{minimize } \|\mathbf{Y} - \mathbf{AX}\|_2^2 \tag{2.1a}$$

$$\text{subject to: } X_k \in \mathcal{M}, \text{ for } k = 0,\ 1,\ \ldots,\ N-1 \tag{2.1b}$$

where $\mathbf{Y} = [Y_0\ \ldots\ Y_{N-1}]^T$ is the frequency-domain received signal, $\mathbf{A} = \mathbf{F}^H\mathbf{HF}$, $\mathbf{F}$ is the IFFT matrix with elements $f_{n,k} = \frac{1}{\sqrt{N}}\exp(\frac{j2\pi kn}{N})$, $\mathbf{H}$ is the channel matrix, and $\mathbf{W} = \mathbf{F}^H\mathbf{w}$. $\mathcal{M}$ contains the constellation points of the modulation used. The computational effort required to solve the problem in (2.1) increases exponentially with the number of variables involved, and becomes prohibitive even for moderate N. Various algorithms have been proposed to suppress the ICI from the received signal and improve system performance [18]-[21]. Several algorithms are reviewed below to establish the background on ICI reduction in OFDM systems.

2.1.2 Minimum Mean Square Error (MMSE) Detector

An MMSE detector has been proposed for ICI reduction in [27], in which an equalizer matrix $\mathbf{G}$ is utilized to minimize the mean-square error between the unknown transmitted symbols $\mathbf{X}$ and the received data $\mathbf{Y}$

$$\text{minimize } E[\|\mathbf{X} - \mathbf{G}^H\mathbf{Y}\|_2^2] \tag{2.2}$$

The coefficient matrix $\mathbf{G}$ can be obtained as

$$\mathbf{G} = (E_s\mathbf{A}\mathbf{A}^H + \sigma^2\mathbf{I}_N)^{-1}\mathbf{A} \tag{2.3}$$

where $\mathbf{I}_N$ is an $N\times N$ identity matrix. Thus the transmitted signal $\mathbf{X}$ can be estimated as

$$\hat{\mathbf{X}} = \Phi\{\mathbf{A}^H(E_s\mathbf{A}\mathbf{A}^H + \sigma^2\mathbf{I}_N)^{-1}\mathbf{Y}\} \tag{2.4}$$

However, the MMSE detector is implemented to utilize all FFT output samples, and the number of OFDM subcarrier N is usually very large [27]. This results in a high computational complexity of $O(N^3)$.

2.1.3 Low Complexity MMSE ICI Suppression

To reduce the high computational complexity of the MMSE detector, a low complexity MMSE detector is presented in [20] which is based on the observation that the ICI for a particular subcarrier most likely comes from neighbouring subcarriers. Assume X_k is the transmitted symbol. Let $M = 2L+1$ where L is a positive integer, and define an $M\times 1$ vector $\boldsymbol{\psi}_k$ with the ith element $\psi_k(i) = [(k-L-1+i) \mod N]+1\ i = 1\ \ldots\ M$. Let $\mathbf{Y}_k = \mathbf{Y}(\boldsymbol{\psi}_k)$, $\mathbf{A}_k = \mathbf{A}(\boldsymbol{\psi}_k, :)$, and $\mathbf{W}_k = \mathbf{W}(\boldsymbol{\psi}_k)$. From (1.9), we have

$$\mathbf{Y}_k = \mathbf{A}_k\mathbf{X} + \mathbf{W}_k \text{ for } k = 0,\ \ldots,\ N-1 \tag{2.5}$$

Consequently, an estimate of the transmitted signal X_k can be obtained by choosing an equalizer matrix $\mathbf{G}_k$ which minimizes the cost function

$$\text{minimize } E[\|X_k - \mathbf{G}_k^H\mathbf{Y}_k\|_2^2] \tag{2.6}$$

and the coefficient matrix $\mathbf{G}_k$ can be determined as

$$\mathbf{G}_k = (E_s \mathbf{A}_k \mathbf{A}_k^H + \sigma^2 \mathbf{I}_N)^{-1} \mathbf{A}_k \tag{2.7}$$

Thus the transmitted signal X_k can be estimated as

$$\hat{\mathbf{X}}_k = \Phi\{\mathbf{A}_k^H (E_s \mathbf{A}_k \mathbf{A}_k^H + \sigma^2 \mathbf{I}_N)^{-1} \mathbf{Y}_k\} \tag{2.8}$$

It has been shown that with a proper choice of M, $M \ll N$ [20], (2.8) has comparable performance to that of (2.4) with significantly reduced computational complexity of $O(N^2 M)$.

2.1.4 Decision Feedback Detection

A decision feedback equalizer is also proposed in [20] to improve the performance of the linear MMSE detector in Section 2.1.3. For this algorithm, The symbol X_k with the largest energy (by ordering the norm of the columns of $\mathbf{A}$) is first determined by using (2.8) based on the signal model (2.6), and the remaining symbols are then detected in either a forward or a backward order. After detection of the current symbol, the next symbol is detected by substracting the previous detected symbol $\hat{X}_k$ from the received signal vector, and characterized using (2.8) with the updated received signal vector. This is repeated until all the symbols have been determined. It has been shown that the DFE algorithm can achieve better performance than that of the MMSE detection algorithm in Section 2.1.3, and the computational complexity $O(N^2 M)$ has the same order as that of the MMSE receiver [20].

2.2 Integer QP Relaxation Based Algorithms for ICI Reduction in OFDM Systems

In the multiuser detection of direct sequence code division multiple access (DS-CDMA) systems [28] [29], problem (2.1) can be solved more efficiently by using suboptimal detectors. The variables in (2.1) are complex-valued. If we define $\mathbf{Y} = \mathbf{Y}_r + j\mathbf{Y}_i$, $\mathbf{A} = \mathbf{A}_r + j\mathbf{A}_i$, and $\mathbf{X} = \mathbf{X}_r + j\mathbf{X}_i$, then (2.1) can be reformulated into an optimization

problem with real-valued variables as

$$\text{minimize } \|\hat{\mathbf{Y}} - \hat{\mathbf{A}}\mathbf{z}\|_2^2 \tag{2.9a}$$

$$\text{subject to: } z_k \in \hat{\mathcal{M}}, \text{ for } k = 0,\ 1,\ \ldots,\ N-1 \tag{2.9b}$$

where $\hat{\mathbf{Y}} = \begin{bmatrix} \mathbf{Y}_r \\ \mathbf{Y}_i \end{bmatrix}$, $\mathbf{z} = \begin{bmatrix} \mathbf{X}_r \\ \mathbf{X}_i \end{bmatrix}$, and $\hat{\mathbf{A}} = \begin{bmatrix} \mathbf{A}_r & -\mathbf{A}_i \\ \mathbf{A}_i & \mathbf{A}_r \end{bmatrix}$.

In what follows, the OFDM system is assumed to employ 4-QAM modulation, which corresponds to $\hat{\mathcal{M}} = \{\pm 1\}$. Clearly, (2.9) is a convex quadratic optimization problem with discrete variables and can be expressed as

$$\text{minimize } \mathbf{z}^T\mathbf{Q}\mathbf{z} + \mathbf{q}^T\mathbf{z} \tag{2.10a}$$

$$\text{subject to: } z_k = \{-1,\ 1\}, \text{ for } k = 0, \ldots, 2N-1 \tag{2.10b}$$

where $\mathbf{Q} = \hat{\mathbf{A}}^T\hat{\mathbf{A}}$, and $\mathbf{q} = -2\hat{\mathbf{A}}^T\hat{\mathbf{Y}}$.

2.2.1 Convex Relaxation

Since the vector $\mathbf{z}$ in the ML problem (2.10) is a discrete set, we have a combinatorial problem with exponential computational complexity. It has been shown [28] that this type of ML detection problem can be solved more efficiently by expanding the discrete feasible set into a continuous and convex feasible region. Two convex relaxation methods are then utilized that allow us to consider convex QP problems that admit a fast solution which yields good performance. The first QP problem minimizes a convex quadratic objective function subject to the solution being contained within an n-dimensional box centered at the origin. The second QP problem minimizes the same objective function subject to the solution being contained within an n-dimensional ball centered at the origin with radius $\sqrt{2N}$. The feasible regions of both problems are depicted in Fig. 2.1.

Bounded constraint relaxation

The discrete constraints in (2.10b) imply that $-1 \leq z_k \leq 1,\ \text{for } k = 0, \ldots, 2N-1$. Thus the ICI reduction problem (2.10) can be relaxed into a bounded constraint

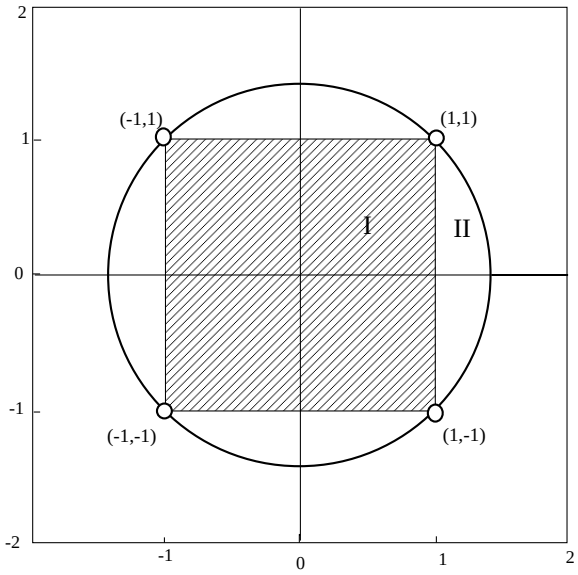

Figure 2.1: The feasible set defined by (2.10b) (points on the circle), the feasible region defined by (2.11b) (I), and the feasible region defined by (2.12b) (I+II) [29]

optimization problem

$$\text{minimize } \mathbf{z}^T\mathbf{Q}\mathbf{z} + \mathbf{q}^T\mathbf{z} \tag{2.11a}$$

$$\text{subject to: } -1 \leq z_k \leq 1, \text{ for } k = 0, \ldots, 2N-1 \tag{2.11b}$$

Obviously, problem (2.11) is a *convex* QP problem which can be solved efficiently to provide suboptimal performance to that of (2.10).

Quadratic convex relaxation

The constraints in (2.10b) imply that $z^T z \leq 2N$, thus, the ICI reduction problem (2.10) is relaxed into the problem

$$\text{minimize } \mathbf{z}^T\mathbf{Q}\mathbf{z} + \mathbf{q}^T\mathbf{z} \tag{2.12a}$$

$$\text{subject to: } \mathbf{z}^T\mathbf{z} \leq 2N \tag{2.12b}$$

Clearly, problem (2.12) is a *convex* QP minimization problem. A unique global solution can be obtained using efficient interior-point QP solvers with reduced computational complexity.

Efficient optimization algorithms are available in the literature [30] to solve the

minimization problems (2.11) and (2.12). Once the solution $\mathbf{z}^*$ of (2.11) or (2.12) is obtained, the solution of (2.10) can be approximated as $\text{sign}(\mathbf{z}^*)$.

2.2.2 2-Dimensional Search Method

To further reduce the computational complexity, the solutions of (2.11) or (2.12) can be obtained by limiting the search to the 2-dimensional subspace spanned by its steepest-descent direction (i.e., negative gradient of the objective function) and Newton direction. In doing so, we set

$$\mathbf{z} = \eta_1 \mathbf{v}_1 + \eta_2 \mathbf{v}_2 \tag{2.13}$$

where $\mathbf{v}_1 = \mathbf{q},\ \mathbf{v}_2 = \mathbf{Q}^{-1}\mathbf{q}$, and η_1, η_2 are two scalar variables. Then, problem (2.11) is converted to the *2-dimensional* problem

$$\text{minimize } \boldsymbol{\eta}^T \mathbf{S} \boldsymbol{\eta} + \mathbf{p}^T \boldsymbol{\eta} \tag{2.14a}$$

$$\text{subject to : } -1 \leq V_k \boldsymbol{\eta} \leq 1 \tag{2.14b}$$

where $\boldsymbol{\eta} = [\eta_1\ \eta_2]^T$, $\mathbf{S} = \mathbf{V}^T\mathbf{Q}\mathbf{V}$, $\mathbf{p} = \mathbf{V}^T\mathbf{q}$, V_k is the kth row of the matrix $\mathbf{V}$, and $\mathbf{V} = [\mathbf{v}_1\ \mathbf{v}_2]$.

Similarly, problem (2.12) can be reformulated to the *2-dimensional* problem

$$\text{minimize } \boldsymbol{\eta}^T \mathbf{S} \boldsymbol{\eta} + \mathbf{p}^T \boldsymbol{\eta} \tag{2.15a}$$

$$\text{subject to : } \boldsymbol{\eta}^T \mathbf{R} \boldsymbol{\eta} \leq 2N \tag{2.15b}$$

where $\mathbf{R} = \mathbf{V}^T\mathbf{V}$. If we denote the solution of problem (2.14) or (2.15) as $\boldsymbol{\eta}^*$, the solution $\mathbf{z}^*$ of problem (2.11) or (2.12) can be calculated using (2.13) accordingly, and $\text{sign}(\mathbf{z}^*)$ is then taken as the solution of (2.10).

2.3 A Successive ICI Reduction Algorithm for OFDM Systems

Here we consider the ICI reduction problem for OFDM systems with higher-order modulation schemes. In what follows, the OFDM system is assumed to employ 16-QAM modulation, which corresponds to $\hat{\mathcal{M}} = \{\pm 1,\ \pm 3\}$ in problem (2.9). Obviously,

(2.9) is a QP problem with discrete variables and can be expressed as

$$\text{minimize } \hat{\mathbf{X}}^T\hat{\mathbf{Q}}\hat{\mathbf{X}} + \hat{\mathbf{q}}^T\hat{\mathbf{X}} \tag{2.16a}$$

$$\text{subject to: } \hat{X}_k = \{\pm 1,\ \pm 3\},\ \text{for } k = 0,\ \ldots,\ 2N-1 \tag{2.16b}$$

where $\hat{\mathbf{Q}} = \hat{\mathbf{A}}^T\hat{\mathbf{A}}$, and $\hat{\mathbf{q}} = -2\hat{\mathbf{A}}^T\hat{\mathbf{Y}}$. The variable set in (2.16b) can be characterized as

$$\hat{\mathbf{X}} = 2\boldsymbol{\alpha} + \boldsymbol{\beta} \tag{2.17}$$

where $\boldsymbol{\alpha}$ and $\boldsymbol{\beta}$ are $2N$-dimensional vectors with components $\alpha_k,\ \beta_k \in \{-1,\ 1\}$, for $k = 0,\ \ldots,\ 2N-1$. Consequently, problem (2.16) assumes the form

$$\text{minimize } \mathbf{z}^T\mathbf{Q}\mathbf{z} + \mathbf{q}^T\mathbf{z} \tag{2.18a}$$

$$\text{subject to: } z_k = \{-1,\ 1\},\ \text{for } k = 0, \ldots, 4N-1 \tag{2.18b}$$

where $\mathbf{z} = \begin{bmatrix}\boldsymbol{\alpha}\\ \boldsymbol{\beta}\end{bmatrix}$, $\mathbf{Q} = \begin{bmatrix}4\hat{\mathbf{Q}} & 2\hat{\mathbf{Q}}\\ 2\hat{\mathbf{Q}} & \hat{\mathbf{Q}}\end{bmatrix}$, and $\mathbf{q} = \begin{bmatrix}2\hat{\mathbf{q}}\\ \hat{\mathbf{q}}\end{bmatrix}$.
By realizing that the constraints in (2.18b) imply $\mathbf{z}^T\mathbf{z} = 4N$, problem (2.18) can be relaxed to

$$\text{minimize } \mathbf{z}^T\mathbf{Q}\mathbf{z} + \mathbf{q}^T\mathbf{z} \tag{2.19a}$$

$$\text{subject to: } \mathbf{z}^T\mathbf{z} = 4N \tag{2.19b}$$

Note that (2.19) is an optimization problem with *continuous* variables. It follows from the definitions that $\hat{\mathbf{Q}}$ is a positive definite matrix and $\mathbf{Q}$ is a positive semidefinite matrix. Because of the non-convex constraint in (2.19b), however, (2.19) is not a convex QP problem. Nevertheless, an efficient solution method can be developed for problem (2.19).

2.3.1 A Successive ICI Reduction Algorithm

This Section presents an ICI reduction algorithm based on the QP formulation (2.19). The proposed algorithm is recursive in nature, as only some binary components of $\mathbf{z}$ in (2.18) are determined in each iteration by solving a corresponding non-combinatorial problem of type (2.19). Algorithmic details of a given, say the ith, iteration are described as follows. Suppose that prior to the ith iteration several binary components

of vector $\mathbf{z}$ have already been determined. Let $\mathbf{z}_i$ be the reduced-size vector that collects all undecided components of $\mathbf{z}$, Ω_i be the index set corresponding to $\mathbf{z}_i$, and N_i be the size of $\mathbf{z}_i$. By substituting the known binary components of $\mathbf{z}$ into (2.19), a reduced-size problem similar to (2.19) is obtained as

$$\text{minimize } \mathbf{z}_i^T \mathbf{Q}_i \mathbf{z}_i + \mathbf{q}_i^T \mathbf{z}_i \tag{2.20a}$$

$$\text{subject to: } \mathbf{z}_i^T \mathbf{z}_i = 4N_i \tag{2.20b}$$

The problem in (2.20) is solved by limiting the search in the 2-dimensional subspace spanned by its steepest-descent direction and Newton direction. In doing so, we set

$$\mathbf{z}_i = \eta_1^{(i)} \mathbf{v}_1^{(i)} + \eta_2^{(i)} \mathbf{v}_2^{(i)} \tag{2.21}$$

where $\mathbf{v}_1^{(i)} = \mathbf{q}_i$, $\mathbf{v}_2^{(i)} = \mathbf{Q}_i^{-1}\mathbf{q}_i$, and $\eta_1^{(i)}$, $\eta_2^{(i)}$ are two scalar variables. Then (2.20) is reduced to the *2-dimensional* problem

$$\text{minimize } \boldsymbol{\eta}_i^T \boldsymbol{S}_i \boldsymbol{\eta}_i + \mathbf{p}_i^T \boldsymbol{\eta}_i \tag{2.22a}$$

$$\text{subject to : } \boldsymbol{\eta}_i^T \mathbf{R}_i \boldsymbol{\eta}_i = 4N_i \tag{2.22b}$$

where $\boldsymbol{\eta}_i = [\eta_1^{(i)}\ \eta_2^{(i)}]^T$, $\mathbf{S}_i = \mathbf{V}_i^T \mathbf{Q}_i \mathbf{V}_i$, $\mathbf{p}_i = \mathbf{V}_i^T \mathbf{q}_i$, $\mathbf{R}_i = \mathbf{V}_i^T \mathbf{V}_i$, and $\mathbf{V}_i = [\mathbf{v}_1^{(i)}\ \mathbf{v}_2^{(i)}]$. It follows from the Karush-Kuhn-Tucker (KKT) conditions of (2.22) that the solution of (2.22) satisfies

$$2\mathbf{S}_i \boldsymbol{\eta}_i + \mathbf{p}_i + 2\lambda_i \mathbf{R}_i \boldsymbol{\eta}_i = 0 \tag{2.23a}$$

$$\boldsymbol{\eta}_i^T \mathbf{R}_i \boldsymbol{\eta}_i = 4N_i \tag{2.23b}$$

where λ_i is a Lagrange multiplier. From (2.23a), the optimal $\boldsymbol{\eta}_i$ is given by

$$\boldsymbol{\eta}_i^* = -\frac{1}{2}(\mathbf{S}_i + \lambda_i^* \mathbf{R}_i)^{-1} \mathbf{p}_i \tag{2.24}$$

where using (2.23b), λ_i^* is determined as the solution of the one-variable algebraic equation

$$g(\lambda_i) = \sum_{k=0}^{N_i - 1} \frac{\hat{p}_k^2}{(\lambda_i + s_k)^2} = 16N_i \tag{2.25}$$

where s_k is the kth eigenvalue of $\hat{\mathbf{S}}_i = \mathbf{R}_i^{-\frac{1}{2}}\mathbf{S}_i\mathbf{R}_i^{-\frac{1}{2}}$, which admits an eigen-decomposition $\hat{\mathbf{S}}_i = \mathbf{U}_i\mathbf{\Sigma}_i\mathbf{U}_i^T$, and $\hat{p}_k$ is the kth component of vector $\hat{\mathbf{p}}_i = \mathbf{U}_i^T\mathbf{R}_i^{-\frac{1}{2}}\mathbf{p}_i$. Since $g(\lambda_i)$ in (2.25) is monotonically decreasing with λ_i, and $g(\lambda_i) - 16N_i$ changes its sign on the interval $(-s_l, \frac{\|\hat{\mathbf{p}}_i\|}{1.5\sqrt{4N_i}} - s_l)$ with s_l being the smallest value of s_k such that $\hat{p}_l \neq 0$, the unique solution λ_i^* of (2.25) can be effectively identified by a bisection search method. Using (2.21), the solution of (2.20) can be then determined.

Next, the magnitudes of the components of $\mathbf{z}_i^*$ are examined. If $|z_k^*|$ exceeds a given threshold ρ, the corresponding variable is detected as $\text{sign}(z_k^*)$, otherwise component z_k^* remains undetermined and will be considered as a design variable in the next iteration. The components just detected are then used in (2.20) to produce a similar QP problem of reduced size where the vector $\mathbf{z}_i$ contains only the undecided variables. This iterative process continues until all the variables have been identified to produce an estimate of the transmitted data.

We conclude this section with a remark to stress that the proposed algorithm is essentially a successive two-variable optimization process. Thus it is considerably more efficient than the algorithm in [21].

2.3.2 Two Implementation Issues

There are two issues in constructing vector $\mathbf{v}_2^{(i)} = \mathbf{Q}_i^{-1}\mathbf{q}_i$. The first is the existence of $\mathbf{Q}_i^{-1}$. At least in the first iteration where $\mathbf{Q}_i$ is the entire matrix $\mathbf{Q}$, $\mathbf{Q}^{-1}$ may not exist since $\mathbf{Q}$ is merely positive semidefinite (see (2.18)). This problem can be readily fixed by adding $\epsilon\mathbf{I}$ with a small $\epsilon > 0$ to $\mathbf{Q}$ so that the slightly modified $\mathbf{Q} + \epsilon\mathbf{I}$ becomes positive definite, and thus nonsingular. Note that this modification does not affect the solution because the modification amounts to changing the objective function in (2.20a) to $\mathbf{z}_i^T(\mathbf{Q}_i + \epsilon\mathbf{I})\mathbf{z}_i + \mathbf{q}_i^T\mathbf{z}_i$, which in conjunction with the constraint in (2.20b) equals $\mathbf{z}_i^T\mathbf{Q}_i\mathbf{z}_i + \mathbf{q}_i^T\mathbf{z}_i + 4N_i\epsilon$, and adding a constant to the objective function does not alter the solution. As the iterations continue, matrix $\mathbf{Q}_i$ may or may not be singular, and the technique outlined above can be used in case $\mathbf{Q}_i$ is singular.

The second issue is the evaluation of $\mathbf{Q}_i^{-1}$, which is numerically intensive when the matrix size is large. This problem can be fixed using the well-known formula for inverting a four-block matrix [31], as given below. Suppose the inverse of matrix $\mathbf{Q}_{i-1}$ is known. Since $\mathbf{Q}_i$ is a principal submatrix of $\mathbf{Q}_{i-1}$, simple row-and-column

permutations of $\mathbf{Q}_i$ gives

$$\mathbf{P}\mathbf{Q}_{i-1}\mathbf{P} = \begin{bmatrix} \mathbf{Q}_i & \mathbf{B} \\ \mathbf{B}^T & \mathbf{C} \end{bmatrix}. \tag{2.26}$$

Applying the formula for inverting a four-block matrix to (2.26), we can write

$$\mathbf{P}\mathbf{Q}_{i-1}^{-1}\mathbf{P} = \begin{bmatrix} \mathbf{Q}_i^{-1} + \mathbf{Q}_i^{-1}\mathbf{B}\tilde{\mathbf{C}}^{-1}\mathbf{B}^T\mathbf{Q}_i^{-1} & -\mathbf{Q}_i^{-1}\mathbf{B}\tilde{\mathbf{C}}^{-1} \\ -\tilde{\mathbf{C}}^{-1}\mathbf{B}^T\mathbf{Q}_i^{-1} & \tilde{\mathbf{C}}^{-1} \end{bmatrix}. \tag{2.27}$$

Now partition $\mathbf{P}\mathbf{Q}_{i-1}^{-1}\mathbf{P}$, which is obtained by applying row-and-column permutations to $\mathbf{Q}_{i-1}$, into four blocks with sizes consistent with the right-hand side of (2.27), i.e.,

$$\mathbf{P}\mathbf{Q}_{i-1}^{-1}\mathbf{P} = \begin{bmatrix} \mathbf{D}_1 & \mathbf{D}_2 \\ \mathbf{D}_2^T & \mathbf{D}_3 \end{bmatrix}. \tag{2.28}$$

From (2.27) and (2.28), it follows that

$$\mathbf{Q}_i^{-1} = \mathbf{D}_1 - \mathbf{D}_2\mathbf{D}_3^{-1}\mathbf{D}_2^T \tag{2.29}$$

where the size of matrix $\mathbf{D}_3$ is $N_{i-1} - N_i$. Since the number of variables determined in each iteration is usually small, computing $\mathbf{D}_3^{-1}$ is considerably more economical than computing $\mathbf{Q}_i^{-1}$ directly.

2.3.3 Computational Complexity

For the sake of simplicity, only multiplications are considered here. The algorithm in Section 2.3.1 involves computing (i) the inverse of the initial matrix $\mathbf{Q}$ in (2.19); (ii) the inverse of the reduced size matrices $\mathbf{Q}_i$ for $i = 1, 2, \ldots, K$ where K denotes the number of iterations performed to complete the detection process; (iii) the data set $\{\mathbf{S}_i, \mathbf{R}_i, \mathbf{p}_i\}$ for $i = 1, 2, \ldots, K$; and (iv) the solution of the problem in (2.22) for $i = 1, 2, \ldots, K$. The complexity of performing (i), (ii), and (iii) is $O(N^3)$, $O(kN^2)$, and $O(N^2/k)$, respectively, where k denotes the average number of variables detected in one iteration and $k \ll N$ for a typical threshold value. The complexity of performing (iv) is insignificant relative to the other three steps because it involves problems with only two variables.

2.3.4 Extension to 64-QAM OFDM Systems

With minor modifications, the proposed algorithm in Section 2.3.1 can readily be extended to 64-QAM OFDM systems. In this case, the ICI reduction problem can be formulated as

$$\text{minimize } \hat{\mathbf{X}}^T\hat{\mathbf{Q}}\hat{\mathbf{X}} + \hat{\mathbf{q}}^T\hat{\mathbf{X}} \tag{2.30a}$$

$$\text{subject to: } \hat{X}_k = \{\pm 1,\ \pm 3,\ \pm 5,\ \pm 7\}, \tag{2.30b}$$

$$\text{for } k = 0,\ \ldots,\ 2N-1$$

where $\hat{\mathbf{Q}} = \hat{\mathbf{A}}^T\hat{\mathbf{A}}$, $\hat{\mathbf{q}} = -2\hat{\mathbf{A}}^T\hat{\mathbf{Y}}$. The variable set in (2.30b) can be characterized as

$$\hat{\mathbf{X}} = 4\boldsymbol{\alpha} + 2\boldsymbol{\beta} + \boldsymbol{\gamma} \tag{2.31}$$

where $\boldsymbol{\alpha},\ \boldsymbol{\beta},$ and $\boldsymbol{\gamma}$ are $2N$-dimensional vectors with components $\alpha_k,\ \beta_k,$ and $\gamma_k \in \{-1,\ 1\}$, for $k = 0,\ \ldots,\ 2N-1$. Problem (2.30) then assumes the form

$$\text{minimize } \mathbf{z}^T\mathbf{Q}\mathbf{z} + \mathbf{q}^T\mathbf{z} \tag{2.32a}$$

$$\text{subject to: } z_k = \{-1, 1\},\ \text{for } k = 0, \ldots, 6N-1 \tag{2.32b}$$

with $\mathbf{z} = \begin{bmatrix}\boldsymbol{\alpha}\\ \boldsymbol{\beta}\\ \boldsymbol{\gamma}\end{bmatrix}$, $\mathbf{Q} = \begin{bmatrix}16\hat{\mathbf{Q}} & 8\hat{\mathbf{Q}} & 4\hat{\mathbf{Q}}\\ 8\hat{\mathbf{Q}} & 4\hat{\mathbf{Q}} & 2\hat{\mathbf{Q}}\\ 4\hat{\mathbf{Q}} & 2\hat{\mathbf{Q}} & \hat{\mathbf{Q}}\end{bmatrix}$, and $\mathbf{q} = \begin{bmatrix}4\hat{\mathbf{q}}\\ 2\hat{\mathbf{q}}\\ \hat{\mathbf{q}}\end{bmatrix}$.

The relaxation and solution technique described in Sections 2.3.1-2.3.2 can then be applied to problem (2.32) with straightforward modifications.

2.4 Performance Enhancement by Low-Bit Descent Search

In LBDS, a given binary sequence is associated with an objective function to be minimized. The search process evaluates, compares, and determines the optimal sign switches of a relatively small number of sequence components to yield maximum reduction in the objective function in (2.10). LBDS has been applied recently to various problems [32]. As will be demonstrated by simulation, the performance of the proposed algorithm can be considerably enhanced using 1-bit or 2-bit, or a combined

1-bit-and-2-bit LBDS, at an insignificant extra cost in computational complexity.

It turns out [32] that one-bit descent search can be carried out by evaluating $\mathbf{z} \odot \boldsymbol{\xi}$ (here $\odot$ denotes component-wise multiplication), where $\boldsymbol{\xi} = \tilde{\mathbf{Q}}\mathbf{z} + \mathbf{q}/2$, and $\tilde{\mathbf{Q}}$ are generated from matrix $\mathbf{Q}$ with its diagonal components set to zero. Index k^* is then identified as where the corresponding component ξ_{k^*} has maximum value, and the sign of z_{k^*} is switched to obtain an improved solution. Similarly, a 2-bit LBDS is performed by computing matrix $\mathbf{G} = \boldsymbol{\xi}\boldsymbol{e}^T + \mathbf{e}^T\boldsymbol{\xi} - 2\mathbf{Q} \odot (\mathbf{z}\mathbf{z}^T)$, where $\mathbf{e}$ is the all-one vector. The index (k^*, m^*) is identified as where G_{k^*,m^*} has maximum value, and an improved solution is then obtained by switching the signs of the k^*th and m^*th components of $\mathbf{z}^*$.

2.5 Simulation Results

The proposed algorithms were applied to an OFDM system with $N = 64$ subcarriers and a bandwidth of 200kHz. The length of the cyclic prefix was chosen to be $N_p = N/8$. A two-ray WSSUS fading channel was employed, where each path is an independent complex Gaussian random process with Jakes' Doppler spectrum. The delay of the first path was set to zero, and the delay of the second path was randomly generated with uniform distribution from $\{T_c, \ \ldots, \ N_pT_c\}$. The normalized Doppler frequency of the channel is denoted as f_dT_s. Simulations were carried out to evaluate the performance in terms of bit error rate (BER) and computational complexity. The BER performance of the conventional one-tap equalizer and a 25-tap DFE algorithm [20] are provided for comparison purposes. Perfect channel information was assumed through the simulations, and combined 1-bit-and-2-bit LBDS was adopted to improve the performance of the proposed algorithms. The computational complexity of the algorithms are compared based on the CPU time under the same test environment (DELL Precision T7400), and the execution time of the optimization algorithms are measured using MATLAB command *cputime*.

2.5.1 Performance Evaluation of the Integer QP Relaxation Methods

For the integer QP relaxation based ICI reduction algorithms, 4-QAM modulation is employed. The proposed algorithms were implemented using the MATLAB SeDuMi toolbox [33]. The BER performance of an OFDM system with $f_dT_s = 0.1$ and the

bounded constraint relaxation method is shown in Fig. 2.2. It can be observed that the one-tap equalizer provides unsatisfactory performance over time-varying channels, but the bounded constraint relaxation methods considerably mitigate the intercarrier interference. The performance can be further improved by employing the LBDS method. Both the n-dimensional and 2-dimensional algorithms offer superior performance to that with the DFE algorithm, but with higher computational complexity. Because the solution of (2.14) is an approximation to that of (2.11), the n-dimensional algorithm outperforms the 2-dimensional algorithm, however, it is more complex. For example, at an E_b/N_0 of 25dB, the DFE algorithm has a BER of 9×10^{-5}, while the 2-dimensional bounded constraint relaxation algorithm with LBDS has a BER of 5×10^{-5} (with a 20% increase in computational complexity). The n-dimensional algorithm has a BER of 2.5×10^{-5} with LBDS (with a 40% increase in computational complexity).

The BER performance of the quadratic convex relaxation algorithms is given in Fig. 2.3. This shows that these algorithms exhibit behavior similar to that of the bounded constraint relaxation algorithms, and offer better performance than the one-tap equalizer and the DFE algorithm. However, the performance is slightly worse with the quadratic convex relaxation algorithms. This is because the optimization problem in (2.12) can be obtained by relaxing (2.11), so one would expect the bounded constraint relaxation algorithm to offer superior performance at a cost of slightly higher computational complexity. For example, with $E_b/N_0 = 25$dB, the 2-dimensional quadratic convex relaxation algorithm with LBDS has a BER of 7×10^{-5} (with a 18% increase in computational complexity over that with the DFE algorithm), while the n-dimensional algorithm with LBDS offers a BER of 4.5×10^{-5} (with a 35% increase in computational complexity).

Simulations were also carried out to determine the impact of normalized Doppler spread f_dT_s on performance. The BER of the 2-dimensional bounded constraint relaxation algorithm for $f_dT_s = 0.05,\ 0.1$, and 0.3 is plotted in Fig. 2.4. It can be observed that the performance of the 2-dimensional bounded constraint relaxation algorithm degrades as the Doppler spread increases, while time diversity can be achieved after combining with the LBDS method. For example, E_b/N_0 of 25dB is required to achieve a BER of 10^{-4} for $f_dT_s = 0.05$ with LBDS, while with $f_dT_s = 0.1$, only E_b/N_0 of 24dB is required to achieve the same BER. The required E_b/N_0 is lowered to 22.5dB to obtain the same BER with $f_dT_s = 0.3$. This improvement with increasing f_dT_s can be attributed to the increased temporal diversity introduced by the

larger Doppler spread [34]. Similar diversity gains can be achieved by employing the quadratic convex relaxation algorithm.

2.5.2 Performance Evaluation of the Successive ICI Reduction Algorithm

For the proposed successive ICI reduction algorithm, 16-QAM modulation was employed. The BER performance was evaluated in an OFDM system with $f_dT_s = 0.05$, and the results are shown in Fig. 2.5. It can be observed that the proposed algorithm considerably mitigates intercarrier interference. The proposed algorithm outperforms the DFE algorithm with a slightly increased computational complexity, and the performance improvement over the DFE algorithm increases as Doppler spread increases, as shown in Figs. 2.5 - 2.7. This is because the DFE algorithm only considers the ICI components of the K neighboring subcarriers of the desired subcarrier, and the ICI components outside this range are neglected. However, the proposed algorithm utilizes all the ICI components in the detection process. For example, at an SNR of 35dB, the DFE algorithm has a BER of 8×10^{-5}, while the proposed algorithm with $\rho = 0.8 \max |\mathbf{z}_i^*|$ has a BER of 5×10^{-5} (with a 25% increase in computational complexity). which can be further improved to a BER of 4×10^{-5} with LBDS (and a further 1% increase in computational complexity).

A larger threshold ρ provides better performance at a cost of increased computational complexity, as shown in Figs. 2.5 - 2.7. The proposed algorithm exhibits an error floor at high SNR for a smaller threshold, but this can be effectively suppressed by performing LBDS with a slightly increased computational complexity. For a larger threshold, the system has comparable performance with and without LBDS, and the increase in computational complexity using LBDS is insignificant, i.e., for the OFDM system with Doppler spread $f_dT_s = 0.1$, the algorithm with $\rho = 0.5 \max |\mathbf{z}_i^*|$ requires 15% more CPU time than that with the DFE algorithm which provides a BER of 0.002 at an SNR of 35dB. This can be improved to 2×10^{-5} by performing LBDS, which requires 20% more CPU time than the DFE algorithm. In addition, the algorithm with $\rho = 0.8 \max |\mathbf{z}_i^*|$ requires 25% more CPU time than the DFE algorithm, but achieves a BER of 4×10^{-5}, which can be improved to 1.5×10^{-5} by performing LBDS with 26% more CPU time than the DFE algorithm.

Simulations were also carried out to determine the impact of normalized Doppler spread f_dT_s on system performance. The BER of the proposed algorithm for $f_dT_s =$

0.1 and $f_dT_s = 0.3$ is depicted in Figs. 2.6 and 2.7, respectively. It can be observed that the system performance improves as Doppler spread increases. For example, for $\rho = 0.8 \max |\mathbf{z}_i^*|$, an SNR of 33dB is required to achieve a BER of 10^{-4} for the case $f_dT_s = 0.1$ with LBDS, while with $f_dT_s = 0.3$, an SNR of 31.4dB is required to achieve the same BER. This improvement with increasing f_dT_s can be attributed to the increased temporal diversity introduced by the larger Doppler spread [34]. Similar diversity gains can be achieved in 64-QAM OFDM systems by employing the proposed algorithm. Fig. 2.8 shows that an SNR of 40dB is required to achieve a BER of 10^{-4} for the case $f_dT_s = 0.05$ with LBDS, while with $f_dT_s = 0.3$, an SNR of 37dB is required to achieve the same BER.

2.6 Conclusions

In this chapter, the OFDM ICI reduction problem over doubly-selective fading channels was first formulated as a combinatorial optimization problem with integer constraints. Then, several ICI reduction algorithms were proposed. First, two relaxation methods were utilized to convert the discrete ML detection problem into convex QP problems. Next, a low complexity ICI reduction algorithm for OFDM systems with QAM signal constellations was proposed. The combinatorial optimization problem for ICI suppression was relaxed to a QP problem with non-convex constraints. A successive method was then utilized to deduce a sequence of reduced-size QP problems. To reduce the computational complexity, the QP problems were solved by limiting the search in the 2-dimensional subspace spanned by its steepest-descent and Newton directions for the proposed algorithms.

A low-bit descent search was employed to improve the performance of the proposed algorithms. Simulations results were presented which demonstrate that the integer QP relaxation based algorithms provide excellent performance with reasonable computational complexity. For the successive ICI reduction algorithm, the results showed that excellent performance can be obtained with low computational complexity. For all of the algorithms, temporal diversity can be achieved with increased Doppler spread.

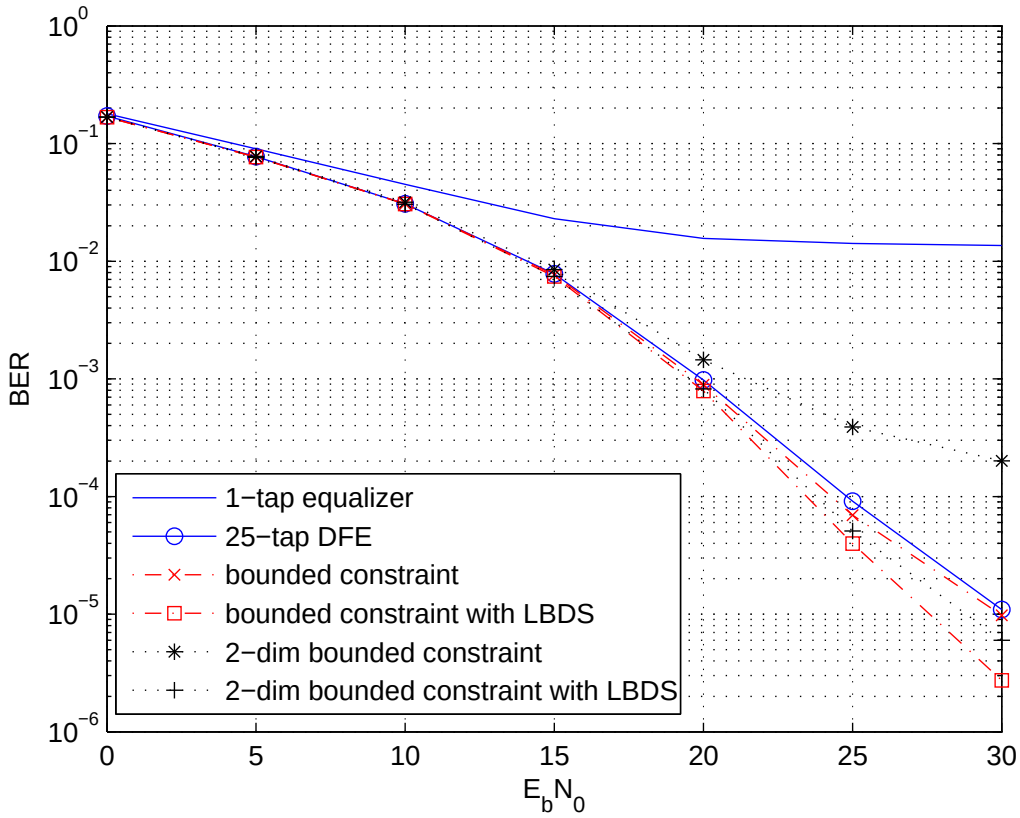

Figure 2.2: BER performance of the bounded constraint relaxation method with $f_dT_s = 0.1$ in a 4-QAM OFDM system.

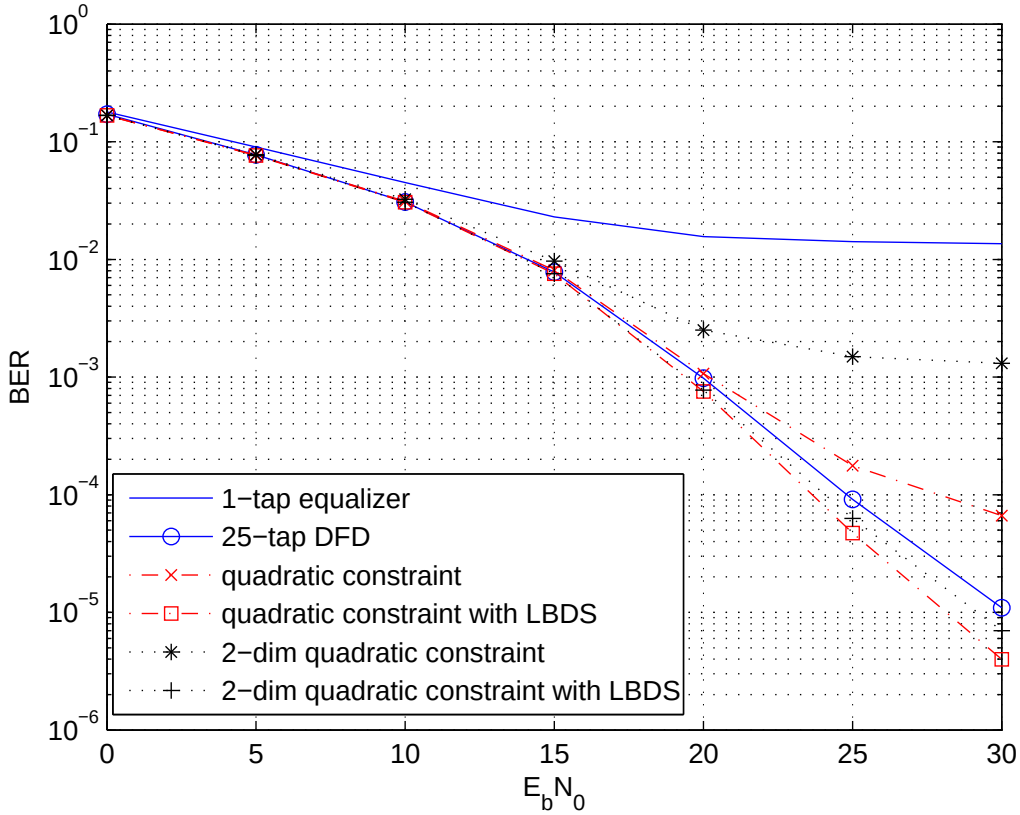

Figure 2.3: BER performance of the quadratic constraint relaxation method with $f_dT_s = 0.1$ in a 4-QAM OFDM system.

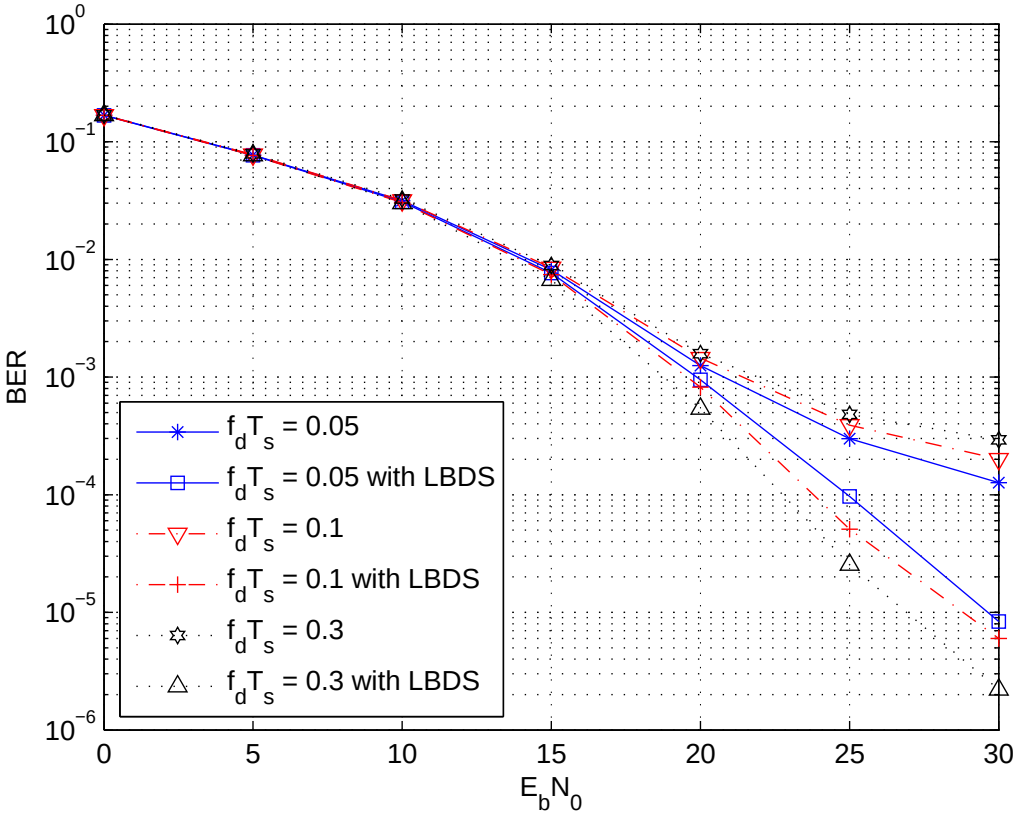

Figure 2.4: BER performance of the 2-dimensional bounded constraint relaxation method with various Doppler spreads in a 4-QAM OFDM system.

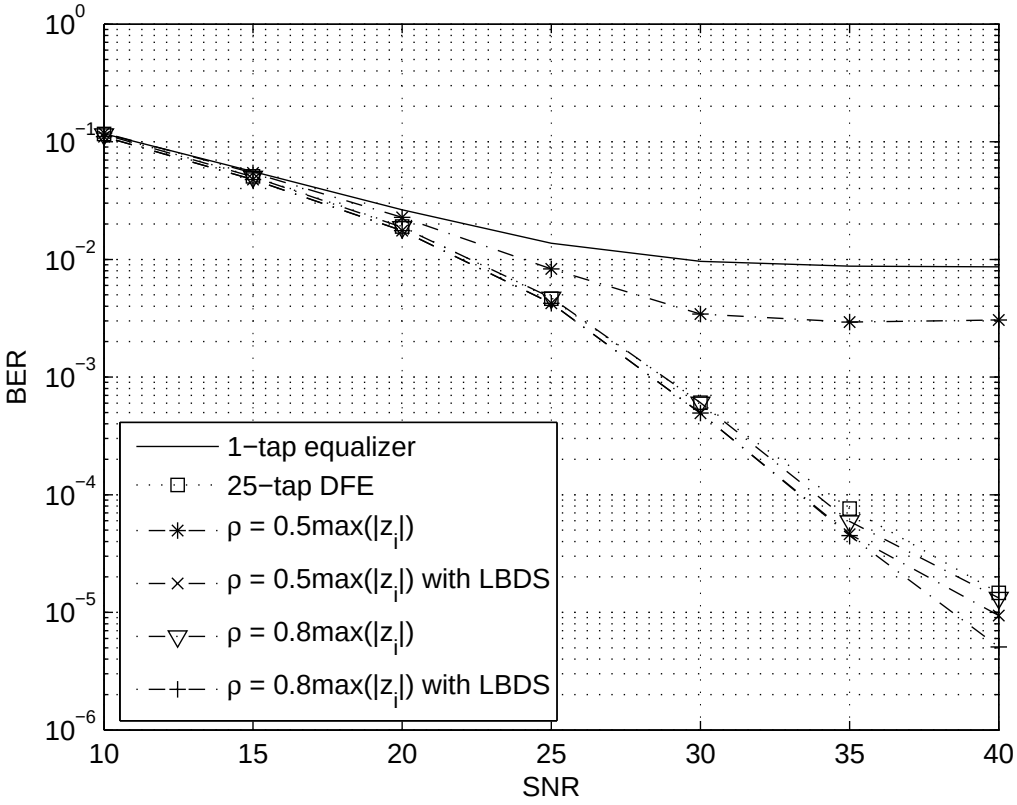

Figure 2.5: BER performance of the successive ICI reduction algorithm with $f_d T_s = 0.05$ in a 16-QAM OFDM system.

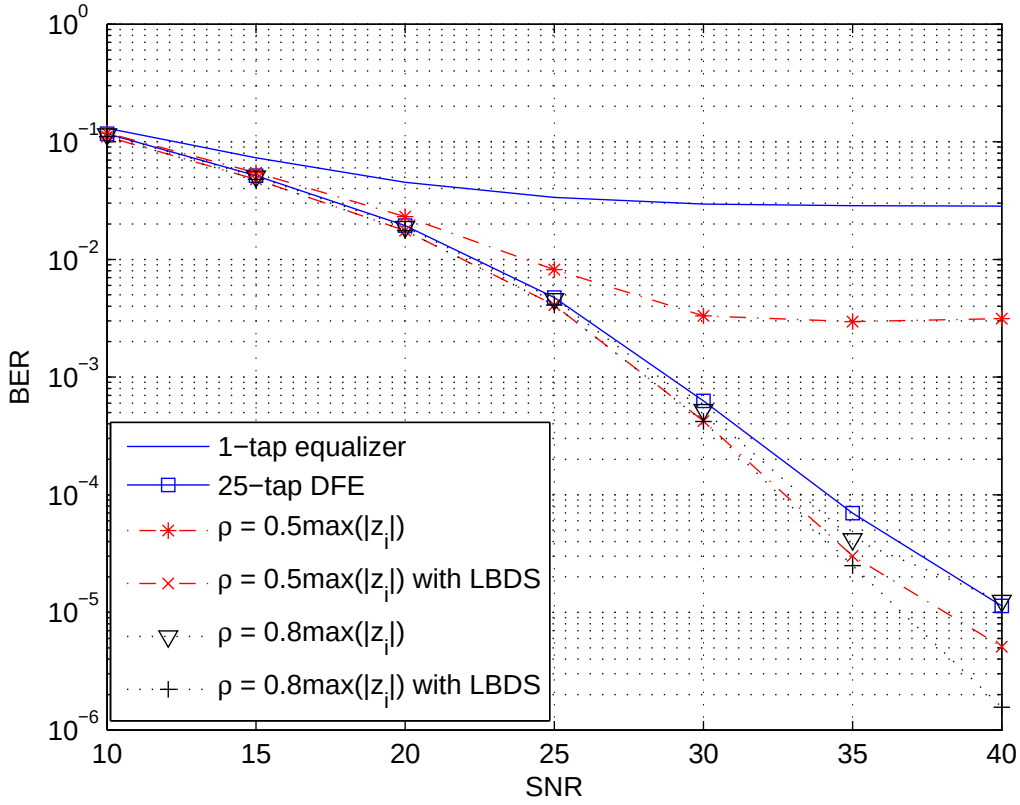

Figure 2.6: BER performance of the successive ICI reduction algorithm with $f_d T_s = 0.1$ in a 16-QAM OFDM system.

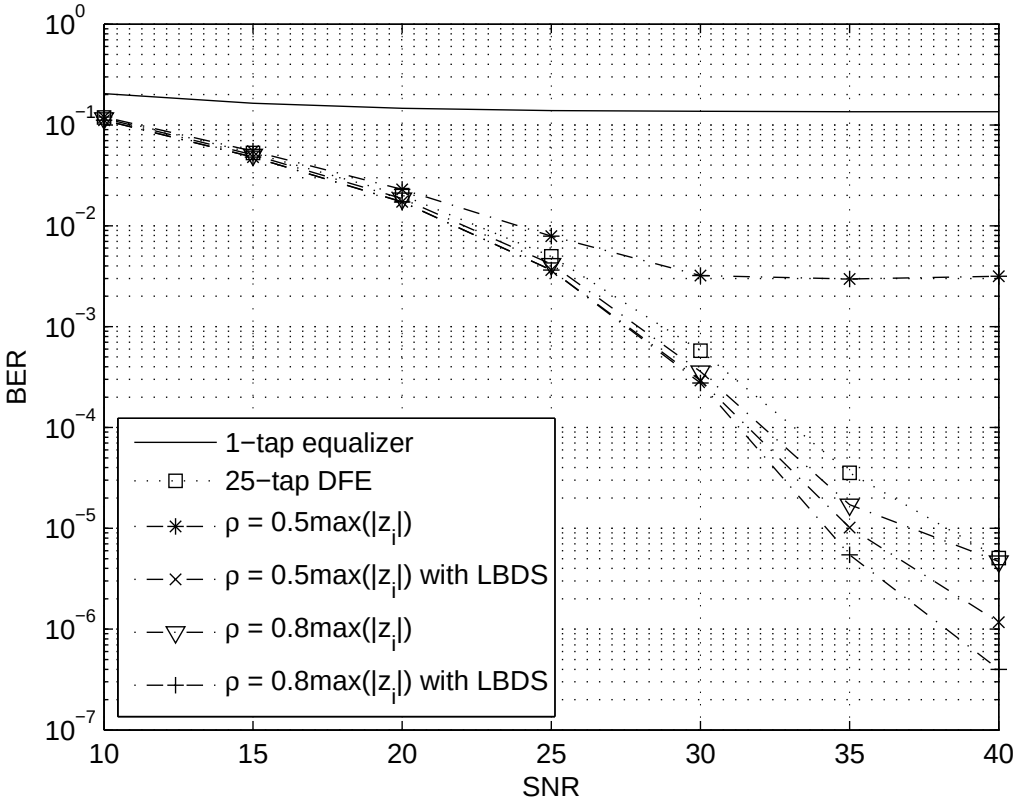

Figure 2.7: BER performance of the successive ICI reduction algorithm with $f_d T_s = 0.3$ in a 16-QAM OFDM system.

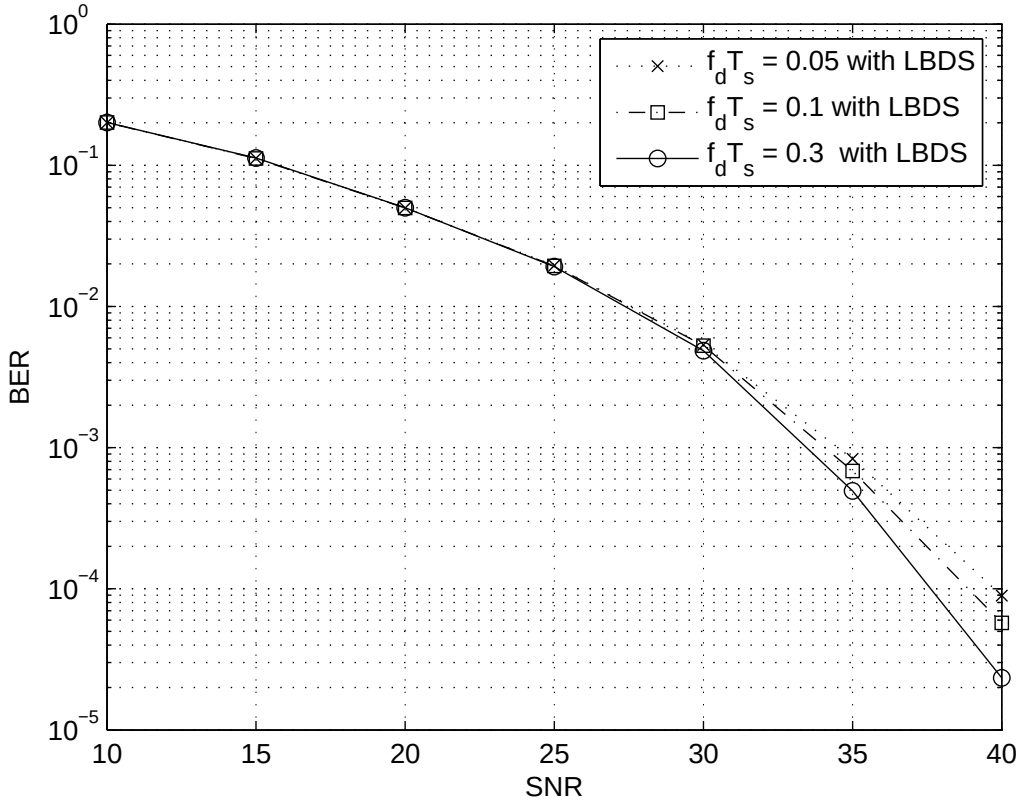

Figure 2.8: BER performance of the successive ICI reduction algorithm with various Doppler spreads in a 64-QAM OFDM system.

Chapter 3

Low Complexity Joint Semiblind Detection for OFDM Systems over Time-Varying Channels

In the design of most ICI reduction algorithms for OFDM systems [19]-[21], perfect channel information is assumed at the receiver. Many channel estimation methods have been proposed for OFDM systems based on pilot symbols [14] [27]. In most cases, channel estimation with pilot symbols is a robust method. However, there are disadvantages such as bandwidth loss and overhead, which can be excessive in fast fading channels. This motivates the use of joint blind or semiblind detection methods for OFDM systems. These methods exploit the statistical or deterministic properties of the channel to detect the transmitted signals without estimating the channel [35]-[37].

There have been several recent investigations on the joint channel estimation and data detection problem in communication systems. In [35], a joint maximum-likelihood channel estimation and signal detection problem for single-input multiple-output (SIMO) systems is formulated and solved via sphere decoding. A blind joint detection problem is formulated in [36] as an integer programming problem based on a regression model. Three ML data detectors for OFDM systems over fast fading channels with the assumption of known channel correlation are proposed in Cui and Tellambura [37].

A sphere decoder for joint semiblind detection provides near-optimal performance with low computational complexity compared to an exhaustive search [37]. However,

the complexity is still high, so there is a need for a suboptimal detector which yields a fast solution with good performance. In this chapter, an iterative joint semiblind detection (IJSD) algorithm for OFDM systems over time-varying channels is proposed. The detection problem is first relaxed to a continuous non-convex quadratic programming problem. A sequence of reduced-size QP problems are then deduced and solved by limiting the search in the 2-dimensional subspace spanned by its steepest-descent and Newton directions to reduce the computational complexity. Furthermore, a low-bit descent search is employed to improve the system performance.

The rest of chapter is organized as follows. The semiblind joint detection problem in OFDM systems over fast fading channels is formulated as a discrete optimization problem in Section 3.1, and an interative joint semiblind detection algorithm is presented in Section 3.2. Simulations are carried out and the results are described in Section 3.3. Finally, some conclusions are given in Section 3.4.

3.1 Joint Semiblind Detection Problem

Here we consider the problem of joint ML channel estimation and signal detection in an N-subcarrier OFDM system, where the channel is time-varying within one OFDM symbol duration, and the channel information is partly known in terms of the channel correlation and noise variance.

In this chapter, we consider a doubly selective fading channel model [7]. Thus, we have a wide sense stationary uncorrelated scattering channel with impulse response given by

$$h(t;\tau) = \sum_{l=0}^{L-1} h(t;\tau_l)\delta(\tau - \tau_l) \tag{3.1}$$

where τ_l is the lth path delay with $\tau_0 < \tau_1 < \ \ldots \ < \tau_{L-1}$, and $h(t;\tau_l)$ is a complex Gaussian process with zero mean and variance σ_l^2. In a rich scattering environment, the channel autocorrelation function is separable in terms of time and delay [7], where the time-correlation function of the channel can be characterized based on Jakes' model [9] as

$$E\{h_{l_1}(t+\Delta t)h_{l_2}^*(t)\} = \sigma_l^2 r_t(\Delta t)\delta(l_1 - l_2) \tag{3.2}$$

where $r_t(\Delta_t) = J_0(2\pi f_d \Delta_t)$, and $J_0(\cdot)$ denotes the zeroth-order Bessel function of the

first kind. The frequency-domain correlation of the channel is given by

$$r_f(\Delta f) = \sum_{l=0}^{L-1} \sigma_l^2 e^{-j2\pi\Delta f \tau_l} \tag{3.3}$$

For simplicity, we assume $\tau_l = lT_c$.

As shown in Section 1.2.3, the OFDM system model in the frequency domain can be described as

$$\mathbf{Y} = \mathbf{AX} + \mathbf{W} \tag{3.4}$$

where $\mathbf{Y} = [Y_0 \ \ldots \ Y_{N-1}]^T$ is the frequency-domain received signal, $\mathbf{A} = \mathbf{F}^H\mathbf{HF}$, $\mathbf{W} = \mathbf{F}^H\mathbf{w}$, where $(\cdot)^H$ denotes conjugate transpose of a vector or matrix, and $\mathbf{H}$ and $\mathbf{w}$ denote the time-domain channel matrix and AWGN noise, respectively.

In a fast fading environment, the channel varies within one OFDM symbol, so orthogonality of the subcarriers does not hold, and the received signal contains both the transmitted signal and ICI from other subcarriers [14]. According to the central limit theorem, the received signal $\mathbf{Y}$ can be modeled as an i.i.d. zero mean complex Gaussian random variable. Thus, the autocorrelation matrix of $\mathbf{Y}$ in (3.4) can be written as [37]

$$\mathbf{R}_{YY} = \sigma_{ICI}^2(\mathbf{X}_D\mathbf{R}_f\mathbf{X}_D^H + \sigma_{en}^2\mathbf{I}_N) \tag{3.5}$$

where $\mathbf{X}_D = \text{diag}(\mathbf{X})$

$$[\mathbf{R}_f]_{(i,j)} = r_f((i-j)/NT_c) \tag{3.6}$$

$$\sigma_{ICI}^2 = \frac{1}{N^2}\sum_{n_1=0}^{N-1}\sum_{n_2=0}^{N-1} r_t[(n_1-n_2)T_c] \tag{3.7}$$

and

$$\sigma_{en}^2 = \frac{((\sum_{l=0}^{L-1}\sigma_l^2)(1-\sigma_{ICI}^2)+\sigma^2)}{\sigma_{ICI}^2} \tag{3.8}$$

The correlation within the received signal is utilized to develop the semiblind joint detector for OFDM systems in the frequency-domain. By maximizing the log-likelihood function of the received signal conditioned on the transmitted signal, joint semiblind detection can be formulated as the following minimization problem

$$\text{minimize } \mathbf{Y}^H\mathbf{R}_{YY}^{-1}\mathbf{Y} \tag{3.9a}$$

$$\text{subject to: } X_k \in \mathcal{M} \text{ for } k = 0, \ \ldots, \ N-1 \tag{3.9b}$$

where $\mathcal{M}$ contains the symbols from the modulation used.

Assuming BPSK or QPSK modulation, we have $|X_k| = 1$. Thus the minimization problem (3.9) is equivalent to the problem [37]

$$\text{minimize } \mathbf{X}^T \mathbf{Y}_D^H \{\sigma_{ICI}^2 (\mathbf{R}_f + \sigma_{en}^2 \mathbf{I}_N)\}^{-1} \mathbf{Y}_D \mathbf{X}^* \tag{3.10a}$$

$$\text{subject to: } X_k \in \mathcal{M} \text{ for } k = 0, \ \ldots, \ N-1 \tag{3.10b}$$

where $\mathbf{X}^*$ denotes the conjugate of the transmitted signal $\mathbf{X}$. Note that this semiblind detector exhibits a phase ambiguity, where $\mathbf{X}e^{j\phi}$, $\phi \in [0, 2\pi)$, satisfies (3.10). One or more pilot tones can be employed to compensate for this ambiguity.

3.2 An Iterative Joint Semiblind Detection Algorithm

Define $\hat{\mathbf{Q}} = \mathbf{Y}_D^H \{\sigma_{ICI}^2 (\mathbf{R}_f + \sigma_{en}^2 \mathbf{I}_N)\}^{-1} \mathbf{Y}_D$. It can be seen that $\hat{\mathbf{Q}}$ is a positive definite Hermitian matrix. However, the computational effort required to solve the semiblind problem (3.10) increases exponentially with the number of subcarriers. In [37], a sphere decoder was proposed to solve this problem and provide near-optimal performance. Although the computational complexity of the sphere decoder is reduced by examining lattice points inside a hypersphere [38][39], it is desirable to seek a suboptimal detector which provides comparable results to that of the sphere decoder with lower computational complexity.

For simplicity, only the algorithm for a QPSK OFDM system is described. The algorithm for BPSK can be obtained with a straightforward modification. As (3.10) is a complex-valued optimization problem, we convert it into the following real-valued optimization problem

$$\text{minimize } \|\mathbf{M}\mathbf{z}\| \tag{3.11a}$$

$$\text{subject to: } z_k \in \{-\frac{\sqrt{2}}{2}, \ \frac{\sqrt{2}}{2}\} \text{ for } k = 0, \ \ldots, \ 2N-1 \tag{3.11b}$$

where $\mathbf{M} = \begin{bmatrix} \text{real}(\hat{\mathbf{M}}) & \text{imag}(\hat{\mathbf{M}}) \\ \text{imag}(\hat{\mathbf{M}}) & -\text{real}(\hat{\mathbf{M}}) \end{bmatrix}$, $\hat{\mathbf{Q}} = \hat{\mathbf{M}}^H \hat{\mathbf{M}}$, and $\mathbf{z} = \begin{bmatrix} \text{real}(\mathbf{X}) \\ \text{imag}(\mathbf{X}) \end{bmatrix}$.

Clearly, the above problem is equivalent to a quadratic programming problem of

the form

$$\text{minimize } \mathbf{z}^T\mathbf{Q}\mathbf{z} \tag{3.12a}$$

$$\text{subject to: } z_k \in \{-1,\ 1\} \text{ for } k = 0,\ \ldots,\ 2N-1 \tag{3.12b}$$

where $\mathbf{Q} = \mathbf{M}^T\mathbf{M}$.

Problem (3.12) is a combinatorial optimization problem with exponential computational complexity with respect to the number of subcarriers. This type of ML detection problem can be solved more efficiently by expanding the discrete feasible set into a continuous feasible region, as shown in Fig. 3.1. The constraints in (3.12b) imply $\mathbf{z}^T\mathbf{z} = 2N$, which corresponds to a $2N$-dimensional sphere centered at the origin with radius $\sqrt{2N}$. Thus problem (3.12) can be converted to

$$\min \mathbf{z}^T\mathbf{Q}\mathbf{z} \tag{3.13a}$$

$$\text{subject to: } \mathbf{z}^T\mathbf{z} = 2N \tag{3.13b}$$

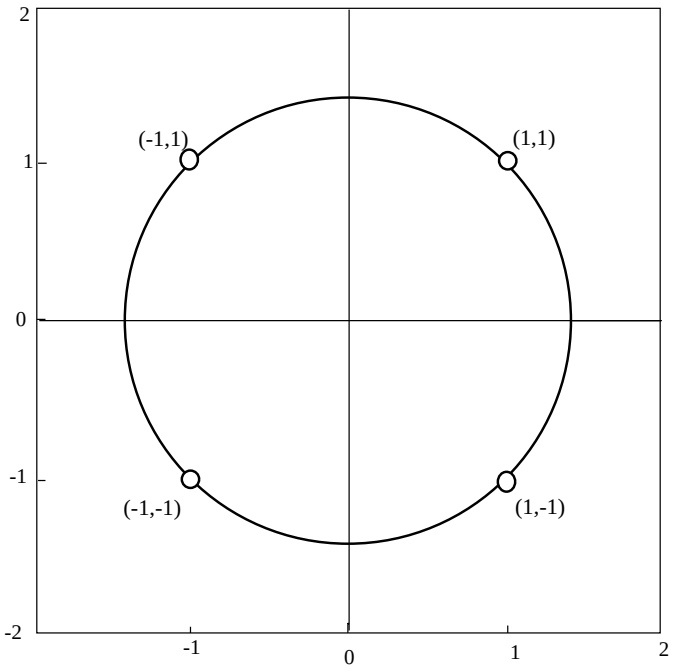

Figure 3.1: The feasible regions defined by (3.12b) and (3.13b).

The receiver has knowledge that a particular QPSK symbol was transmitted on some pre-defined subcarriers, and this can be utilized to solve problem (3.13). Let $\mathbf{z}_d$

be the vector of unknown transmitted data, Ω_d be the index set corresponding to $\mathbf{z}_d$, and N_d be the size of $\mathbf{z}_d$. The corresponding pilot symbol vector is denoted as $\mathbf{z}_p$, Ω_p is the index set associated with $\mathbf{z}_p$, and N_p is the size of $\mathbf{z}_p$. By substituting the known pilot tones $\mathbf{z}_p$ from the variable vector $\mathbf{z}$, $\mathbf{Q}_d$ and $\mathbf{q}_d$ can be obtained from $\mathbf{Q}$ with respect to Ω_d and Ω_p, respectively. Consequently we have a quadratic optimization problem of the form

$$\text{minimize } \mathbf{z}_d^T \mathbf{Q}_d \mathbf{z}_d + \mathbf{q}_d^T \mathbf{z}_d \tag{3.14a}$$

$$\text{subject to: } \mathbf{z}_d^T \mathbf{z}_d = N_d \tag{3.14b}$$

3.2.1 Basic Algorithm

The variables in (3.14) can be iteratively detected, where only some binary components of $\mathbf{z}_d$ are determined in each iteration by solving a corresponding non-combinatorial problem of type (3.14). Suppose that prior to the ith iteration some binary components of vector $\mathbf{z}_d$ have been determined. Let $\mathbf{z}_i$ be the reduced-size vector that collects all undecided components of $\mathbf{z}_d$, Ω_i be the index set corresponding to $\mathbf{z}_i$, and N_i be the size of $\mathbf{z}_i$ during the ith iteration, respectively. By substituting the known binary components of $\mathbf{z}_d$ into (3.14), a reduced-size problem similar to (3.14) is obtained as

$$\text{minimize } \mathbf{z}_i^T \mathbf{Q}_i \mathbf{z}_i + \mathbf{q}_i^T \mathbf{z}_i \tag{3.15a}$$

$$\text{subject to: } \mathbf{z}_i^T \mathbf{z}_i = N_i \tag{3.15b}$$

The computational complexity is reduced by realizing that the variable set in problem (3.15) can be expressed with respect to a 2-dimensional subspace spanned by its steepest-descent direction (i.e., negative gradient of the objective function) and Newton direction. In doing so, we express

$$\mathbf{z}_i = \eta_1^{(i)} \mathbf{v}_1^{(i)} + \eta_2^{(i)} \mathbf{v}_2^{(i)} \tag{3.16}$$

where $\mathbf{v}_1^{(i)} = \mathbf{q}_i$, $\mathbf{v}_2^{(i)} = \mathbf{Q}_i^{-1}\mathbf{q}_i$, and $\eta_1^{(i)}$, $\eta_2^{(i)}$ are two scalar variables. Then (3.15) is converted to a *2-dimensional* problem

$$\text{minimize } \boldsymbol{\eta}_i^T \boldsymbol{S}_i \boldsymbol{\eta}_i + \mathbf{p}_i^T \boldsymbol{\eta}_i \tag{3.17a}$$

$$\text{subject to : } \boldsymbol{\eta}_i^T \mathbf{R}_i \boldsymbol{\eta}_i = N_i \tag{3.17b}$$

where $\boldsymbol{\eta}_i = [\eta_1^{(i)}\ \eta_2^{(i)}]^T$, $\mathbf{S}_i = \mathbf{V}_i^T \mathbf{Q}_i \mathbf{V}_i$, $\mathbf{p}_i = \mathbf{V}_i^T \mathbf{q}_i$, $\mathbf{R}_i = \mathbf{V}_i^T \mathbf{V}_i$, and $\mathbf{V}_i = [\mathbf{v}_1^{(i)}\ \mathbf{v}_2^{(i)}]$. Consequently, the solution of (3.17) must satisfy the KKT conditions

$$2\mathbf{S}_i \boldsymbol{\eta}_i + \mathbf{p}_i + 2\lambda_i \mathbf{R}_i \boldsymbol{\eta}_i = 0 \tag{3.18a}$$

$$\boldsymbol{\eta}_i^T \mathbf{R}_i \boldsymbol{\eta}_i = N_i \tag{3.18b}$$

where λ_i is a Lagrange multiplier at the ith iteration. It follows that the optimal $\boldsymbol{\eta}_i$ can be obtained from (3.18a) as

$$\boldsymbol{\eta}_i^* = -\frac{1}{2}(\mathbf{S}_i + \lambda_i^* \mathbf{R}_i)^{-1} \mathbf{p}_i \tag{3.19}$$

and (3.18b) can be rewritten as

$$g(\lambda_i) = \sum_{k=0}^{N_i - 1} \frac{\hat{p}_k^2}{(\lambda_i + s_k)^2} = 4N_i \tag{3.20}$$

where s_k is the kth eigenvalue of $\hat{\mathbf{S}}_i = \mathbf{R}_i^{-\frac{1}{2}} \mathbf{S}_i \mathbf{R}_i^{-\frac{1}{2}}$, which admits an eigen-decomposition $\hat{\mathbf{S}}_i = \mathbf{U}_i \boldsymbol{\Sigma}_i \mathbf{U}_i^T$, and $\hat{p}_k$ is the kth component of vector $\hat{\mathbf{p}}_i = \mathbf{U}_i^T \mathbf{R}_i^{-\frac{1}{2}} \mathbf{p}_i$.

The only unknown variable λ_i in (3.18) can be determined by solving the one-variable optimization problem

$$\text{minimize } \left| \sum_{k=0}^{N_i - 1} \frac{\hat{p}_k^2}{(\lambda_i + s_k)^2} - 4N_i \right| \tag{3.21a}$$

$$\text{subject to: } -s_l \ \leq \ \lambda_i \ \leq \ \frac{\|\hat{\mathbf{p}}_i\|}{1.5\sqrt{4N_i}} - s_l \tag{3.21b}$$

with s_l being the smallest value of s_k such that $\hat{p}_l \neq 0$. The unique solution λ_i^* of (3.21) can be effectively identified via a bisection search.

Next, the magnitudes of the components of $\mathbf{z}_i^*$ are examined. If $|z_k^*|$ exceeds a given threshold $\rho = \alpha |z_i^*|_{max}$, the corresponding variable is claimed to be $\text{sign}(z_k^*)$,

otherwise component z_k^* remains undetermined and will be considered as a design variable in the next iteration. Based on the components just detected, a QP problem similar to (3.14) with reduced size is produced where the vector $\mathbf{z}_i$ contains only the undetermined variables. This iterative process continues until all the variables have been identified to produce an estimate of the transmitted data.

Note that the evaluation of $\mathbf{Q}_i^{-1}$ is numerically intensive when its size is large. This can be alleviated using the well-known formula for inverting a four-block matrix [31]. Thus the major portion of the computational complexity for the proposed algorithm is found to be in the order of $O(kN^2)$ for each iteration, where k denotes the average number of variables detected in one iteration, and $k \ll N$ for a typical threshold value.

The LBDS method presented in Section 2.4 is utilized to evaluate, compare, and determine the optimal sign switches of a relatively small number of components to yield maximum reduction in the objective function in (3.14). This results in an insignificant extra cost in computational complexity.

3.3 Simulation Results

The proposed IJSD algorithm was applied to an OFDM system with $N = 64$ subcarriers and a cyclic prefix of length $N_{cp} = N/8$. The carrier frequency of the OFDM system was 5GHz and the bandwidth of the system was set to 3MHz. The 6-ray COST 207 TU model with power profile [0.189, 0.379, 0.239, 0.095, 0.061, 0.037] and delay profile [0.0, 0.2, 0.5, 1.6, 2.3, 5.0] μs was employed for the simulation. Each path is an independent complex Gaussian random process with Jake's Doppler spectrum. One or more pilot tones was utilized to compensate for the phase ambiguity, and BPSK or QPSK modulation was used for both the data and pilot symbols. The channel correlation matrix was assumed to be perfectly known at the receiver. The normalized Doppler frequency of the channel is denoted as $f_d T_s$. The performance of the proposed joint detection algorithm is evaluated based on BER and computational complexity, in comparison with a sphere decoder [39]. The performance of the successive detector in Chapter 2 was used as the benchmark with the assumption of perfect channel state information (CSI). The computational complexity of the algorithms are compared based on the CPU time under the same test environment (DELL Precision T7400), and the execution time of the optimization algorithms are measured using MATLAB command *cputime*.

Table 3.1: Computational Complexity Comparison

Algorithm	Normalized CPU time	
	$\alpha = 0.8$	$\alpha = 0.5$
IJSD Without LBDS	0.55	0.45
IJSD With LBDS	0.57	0.5
Sphere decoder	1	

The BER performance was evaluated with $f_dT_s = 0.01$ for both BPSK and QPSK OFDM systems, as shown in Figs. 3.2 and 3.3. It can be observed that the IJSD algorithm provides comparable results to those of the sphere decoder with much less computational complexity. For example, for the QPSK OFDM system, at an E_b/N_0 of 30dB, the sphere algorithm has a BER of 6.4×10^{-4}, while the proposed algorithm with $\alpha = 0.8$ achieves a BER of 3×10^{-3} (with only 55% of the CPU time of the sphere decoder). This is improved to a BER of 8.5×10^{-4} with LBDS (and 57% of the CPU time of the sphere decoder).

A larger value of α can provide better performance at a cost of increased computational complexity, as shown in Fig. 3.4. The proposed algorithm exhibits a performance loss due to a smaller threshold, but this loss can be avoided by performing LBDS with a slightly increased computational complexity. For the QPSK OFDM system with Doppler spread $f_dT_s = 0.01$, the algorithm with $\alpha = 0.5$ only requires 45% of the CPU time of the sphere decoder at an E_b/N_0 of 30dB. The corresponding BER with $\alpha = 0.5$ is 4.5×10^{-3}. This can be improved to 9×10^{-4} by performing LBDS with 50% of the CPU time of the sphere decoder. Table 3.1 summarizes the computational complexity of the IJSD algorithm relative to that of the sphere decoder for a QPSK OFDM system at $E_b/N_0 = 30$dB, where the CPU time of the sphere decoder is normalized to one, and the CPU time of the proposed algorithms are given with respect to that of the sphere decoder.

Simulations were also carried out to determine the impact of normalized doppler spread f_dT_s on the system performance. The BER performance of the proposed algorithm for $f_dT_s = 0.001,\ 0.005,$ and 0.01 is depicted in Fig. 3.5. It can be observed that at lower SNR, the proposed algorithm provides similar performance for all values of Doppler spread. However, for smaller Doppler spreads, better performance was achieved at higher SNRs, e.g., at $E_b/N_0 = 30$dB, a BER of 8.5×10^{-4} was obtained for $f_dT_s = 0.01$ using the proposed algorithm with LBDS, while a BER of 2.5×10^{-4} can be achieved for $f_dT_s = 0.001$.

Simulations were also carried out to determine the impact of the number of pilot tones on performance. The BER of the proposed algorithm with LBDS for $f_d T_s = 0.01$ and 1, 2 and 4 pilot tones is shown in Fig. 3.6. It can be observed that there is an error floor at high signal-to-noise ratios with one pilot tone. The performance improves as the number of pilot tones increases, with the error floor significantly reduced. For example, with one pilot tone, the proposed algorithm with LBDS achieves a BER of 0.015 at an E_b/N_0 of 30dB, while with 2 pilot tones, a BER of 2.2×10^{-3} is obtained for the same E_b/N_0. The performance can be further improved to a BER of 8.5×10^{-4} by utilizing 4 pilot tones.

3.4 Conclusions

A low complexity joint semiblind detection algorithm for OFDM systems over time-varying channels has been proposed. The joint semiblind problem is relaxed to a continuous non-convex QP problem. An iterative method is then utilized to deduce a sequence of reduced-size QP problems by taking advantage of the pilot tones. These are solved by limiting the search in the 2-dimensional subspace to reduce the computational complexity. Furthermore, a low-bit descent search is employed to improve the system performance. Results were given which demonstrate that the proposed algorithm provides similar performance with lower computational complexity compared to that of a sphere decoder.

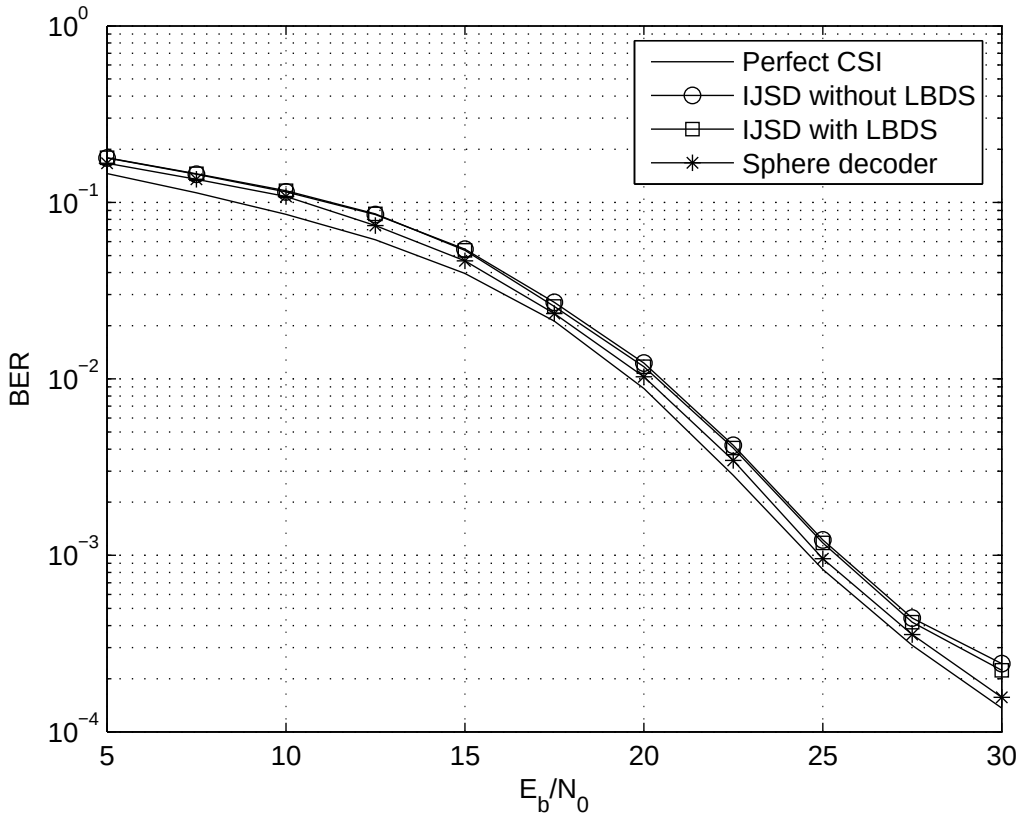

Figure 3.2: BPSK OFDM system performance with $f_d T_s = 0.01$, $\alpha = 0.8$ and 4 pilot tones.

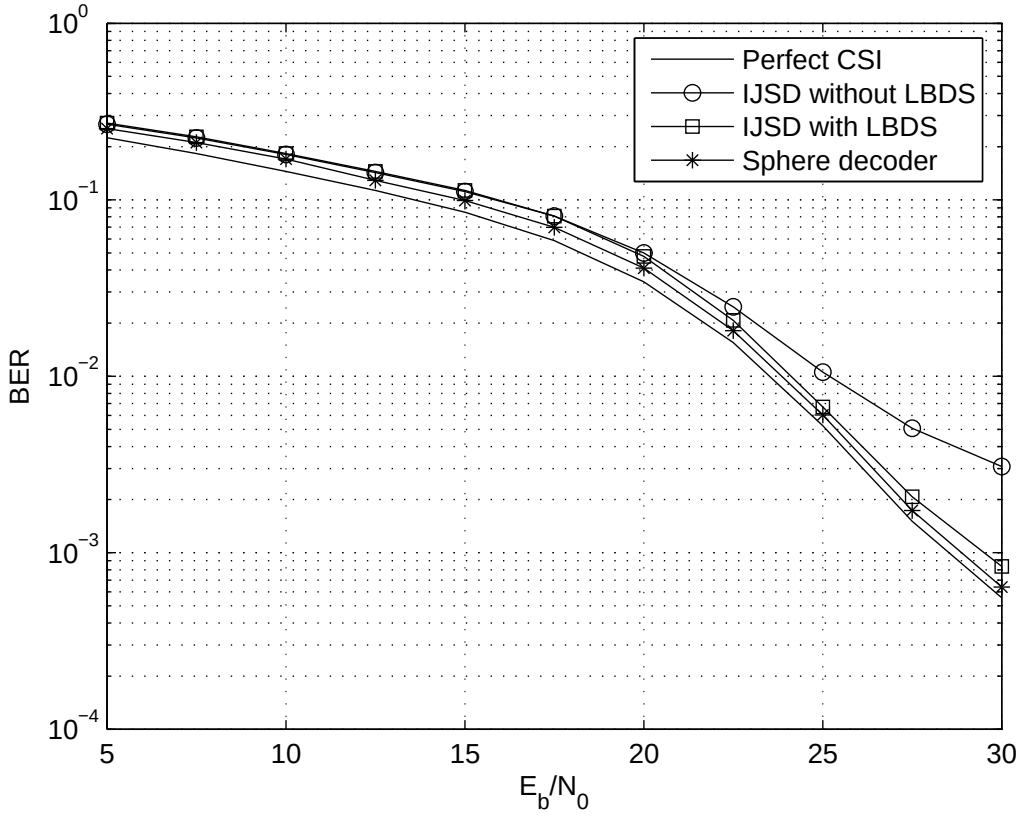

Figure 3.3: QPSK OFDM system performance with $f_d T_s = 0.01$, $\alpha = 0.8$ and 4 pilot tones.

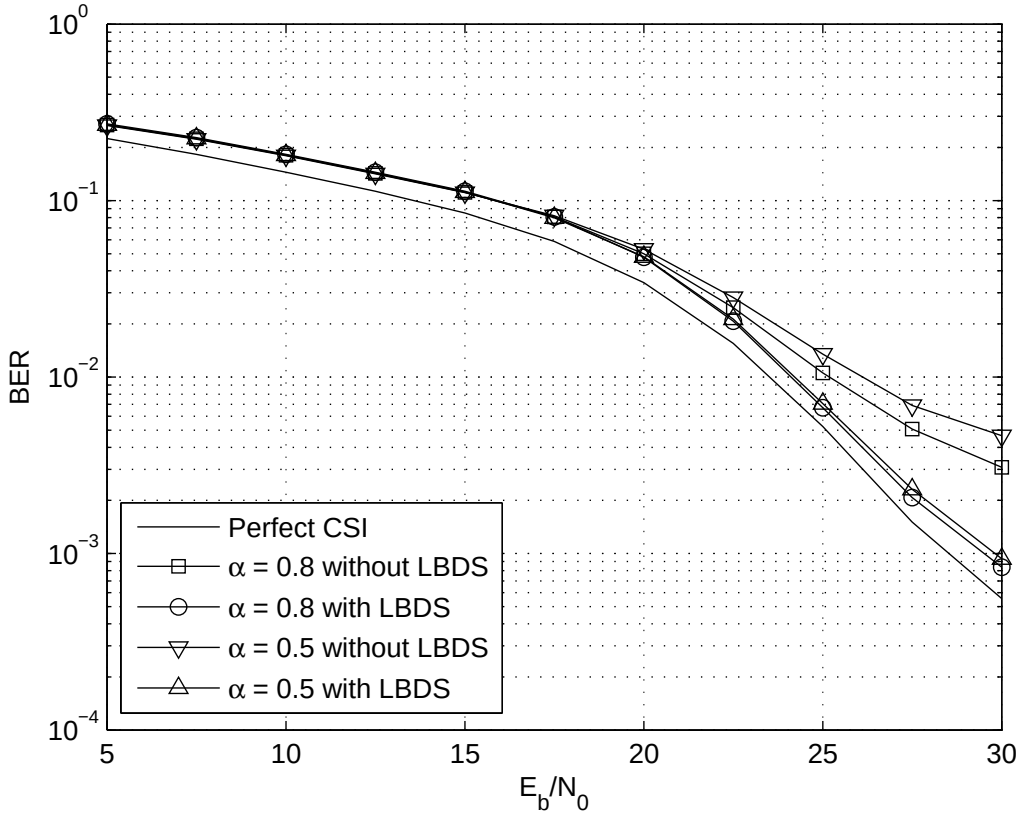

Figure 3.4: QPSK OFDM system performance with $f_d T_s = 0.01$, 4 pilot tones and various thresholds using the proposed IJSD algorithm.

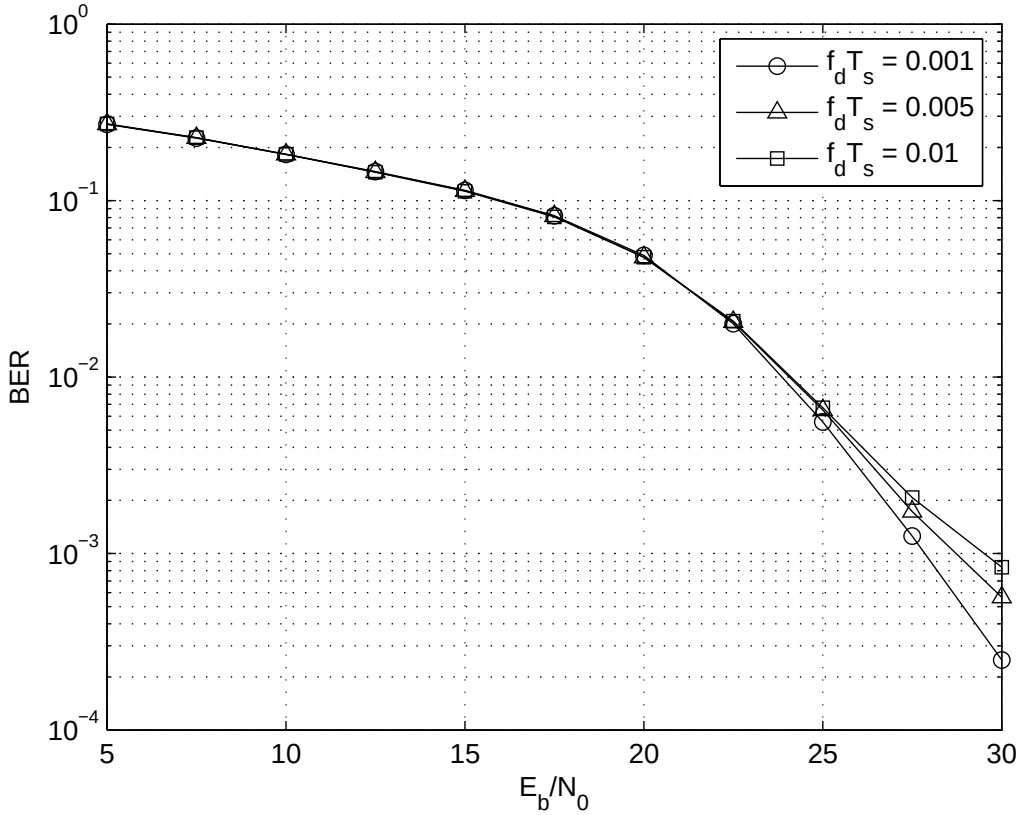

Figure 3.5: QPSK OFDM system performance with $\alpha = 0.8$, 4 pilot tones and various Doppler spreads using the proposed IJSD algorithm with LBDS.

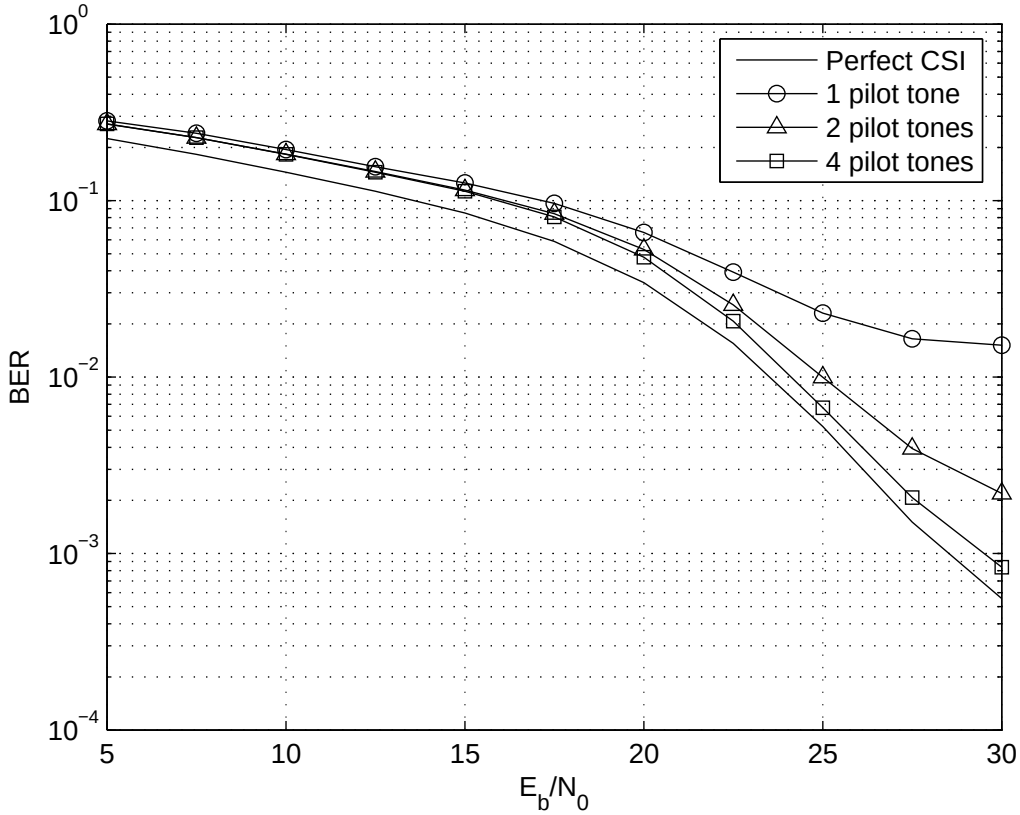

Figure 3.6: QPSK OFDM system performance with $f_d T_s = 0.01$, $\alpha = 0.8$ and various pilot tones using the proposed IJSD algorithm with LBDS.

Chapter 4

Blind Polynomial Channel Estimation for OFDM Systems

For coherent detection of OFDM symbols, the receiver requires reliable channel information. Channel information can be estimated by utilizing pilot symbols in the frequency or time domains [27]. For frequency domain pilot-aided channel estimation, a common approach is to estimate the channel frequency response at pre-defined pilot tones/subcarriers, and then various methods can be utilized to obtain the channel response at other subcarriers. Approaches which use low-order polynomial interpolation based on the channel frequency response at pilot tones are presented in [24]. However, the performance of these methods depends on the spacing between pilots, and the channel response is not accurate with wide pilot spacing if the channel varies quickly. An alternative means of obtaining the channel frequency response is to exploit the channel correlation among subcarriers. For example, minimum mean-square error estimation performs Wiener filtering using knowledge of the second-order statistics of the channel [25]. However, the performance is degraded if the channel statistics are not accurate.

Time-domain channel estimation determines the channel impulse response (CIR) by exploiting the fact that the number of channel taps is much less than the number of subcarriers. The number of unknown parameters is reduced significantly, thus fewer pilots can be employed while obtaining a more accurate estimate. However, finding the multipath channel delays remains a critical issue.

Recently, blind channel identification and equalization for OFDM system have attracted significant attention [11] [40]-[43]. These methods estimate the channel

information by exploiting the statistical behavior of the channel or received signals. Various blind estimation algorithms have been developed for OFDM systems. In Chang *et. al* [11], a regression model is employed to develop a joint blind detector for OFDM systems over time-varying channels. In Cui and Tellambura [40], joint blind and semiblind maximum likelihood detectors are developed to exploit the relationship between subcarriers. In Heath and Giannakis [41], the cyclostationarity introduced by the CP is exploited to identify the channel impulse response. A noise subspace method by utilizing the CP which results in faster convergence with smaller data blocks is presented in Cai and Akansu [42]. Furthermore, in Li and Roy [43], a method to estimate the channel information based on virtual carriers is proposed.

Based on the source characteristics, such as the noncircularity of the input signals, blind identification techniques can be used to obtain an estimate of the channel coefficients [44]. In this chapter, we take advantage of the nonzero cyclostationary statistics of the transmitted signals, which in turn allows blind polynomial channel estimation using second-order statistics of the OFDM symbol. A set of polynomial equations are formulated based on the correlation of the received signal. An estimate of the time domain channel coefficients can then be easily computed by solving these equations.

The rest of the chapter is organized as follows. The blind polynomial channel estimation algorithm for OFDM systems is formulated in Section 4.1, and an illustrative example is given in Section 4.2 to describe how the channel estimation problem is solved. Simulations are carried out and the results are described in Section 4.3. Finally, some conclusions are given in Section 4.4.

4.1 Blind Polynomial Channel Estimation for OFDM Systems

The concept of *circularity* was introduced in [45]. It is defined as a simple expression of the distribution, moments, and related statistical objects of a complex Gaussian random variable. Thus it in turn induces a correlation between the real and imaginary parts of the random variable [45]. A scalar random variable Z is referred to as *circular at order 2* if $E(Z^2) = 0$, and *noncircular at order 2* if $E(Z^2)$ is nonzero. A non-Gaussian random variable is referred to as circular if its distribution is invariant when multiplied by a unit modulus complex number [44].

In this chapter, we utilize the statistical property that discrete signals are noncircular at given orders (order-k for k-PSK random variables), to develop a polynomial channel estimation method for OFDM systems. In particular, we exploit the noncircularity at order 2 of the transmitted signal [44]. For example, for binary phase-shift keying (BPSK) modulated signals in a single carrier system, the noncircular and circular second-order correlations are given by

$$E[x_n x_{n+m}] = \delta(m) \tag{4.1}$$

where $\delta(m) = 1$ if $m = 0$ and $\delta(m) = 0$ elsewhere. Based on this property, a set of polynomial equations are derived such that the channel must satisfy

$$E[y(n)y(n-m)] = \sum_{l=0}^{L-1} h(l)h(l+m) \tag{4.2}$$

In what follows, BPSK modulation is employed in the OFDM system. Assume the transmitted signals X_k are i.i.d. and follow a uniform distribution. The channel is time-invariant within one OFDM symbol, and the receiver has knowledge of the channel length. Due to the noncircular statistics of the transmitted signal X_k, we have $\mathbf{R} = E[\mathbf{X}\mathbf{X}^T]$ with $R_{i,j} = \delta(i-j)$. Consequently, the correlation of the time domain signal $\mathbf{x}$ is

$$E[\mathbf{x}\mathbf{x}^T] = \mathbf{F}\mathbf{F}^T \tag{4.3}$$

where

$$E[x(m)x(n)] = \frac{1}{N}\sum_{k=0}^{N-1} e^{\frac{j2\pi k(m+n)}{N}} = \mathbf{F}_m^T \mathbf{F}_n \tag{4.4}$$

and $\mathbf{F}_m$ is the mth column of matrix $\mathbf{F}$. Thus, the correlation $E[\mathbf{x}\mathbf{x}^T]$ in (4.4) has the following structure

$$E[\mathbf{x}\mathbf{x}^T] = \begin{bmatrix} 1 & 0 & 0 & \dots & 0 \\ 0 & 0 & 0 & \dots & 1 \\ \vdots & \vdots & \vdots & \ddots & \vdots \\ 0 & 0 & 1 & \dots & 0 \\ 0 & 1 & 0 & \dots & 0 \end{bmatrix}$$

The noise and the transmitted signal are independent, and the real and imaginary

parts of the noise are also independent, so we have that

$$E[w(n)w(n-l)] = 0 \ \forall \ l \tag{4.5}$$

$$E[w(n)w(n-l)^*] = 0 \text{ for } l \neq 0 \tag{4.6}$$

and

$$E[|w(n)|^2] = \sigma_n^2 \tag{4.7}$$

Thus, for the received signals in the time domain, the correlation is given by

$$E[\mathbf{y}\mathbf{y}^T] = \mathbf{H}\mathbf{F}\mathbf{F}^T\mathbf{H}^T \tag{4.8}$$

where

$$E[y(n)y(n-l)] = \mathbf{F}_n^T\mathbf{h}\mathbf{h}^T\mathbf{F}_{n-l} \tag{4.9}$$

Similarly, the circular second-order correlation of the transmitted signal in the time domain is obtained as

$$E[\mathbf{x}\mathbf{x}^H] = \mathbf{I}_N \tag{4.10}$$

As a consequence, the circular correlation of the received signals in the time domain is given by

$$E[\mathbf{y}\mathbf{y}^H] = \mathbf{H}\mathbf{H}^H + \sigma_n^2\mathbf{I}_N \tag{4.11}$$

where

$$E[y(n)y(n-l)^*] = \sum_{l=0}^{L-1} h(l)^* h(m+l) + \sigma_n^2\delta(l) \tag{4.12}$$

Based on a similar concept, equivalent equations can be formulated for higher order PSK or QAM OFDM systems with some minor modifications. For such systems, the real and imaginary parts of the signal are considered separately at the receiver, because the real and imaginary parts of X_k have a deterministic square.

4.2 An Example

Without restricting the generality, we use a simple example to illustrate how to obtain a set of polynomial equations with respect to the channel coefficients. Assume a 6-subcarrier OFDM system with a channel of length $L = 3$. Then $\mathbf{h} = [h_0 \ h_1 \ h_2]^T$, and

the channel matrix is given by

$$\mathbf{H} = \begin{bmatrix} h_0 & 0 & 0 & 0 & h_2 & h_1 \\ h_1 & h_0 & 0 & 0 & 0 & h_2 \\ h_2 & h_1 & h_0 & 0 & 0 & 0 \\ 0 & h_2 & h_1 & h_0 & 0 & 0 \\ 0 & 0 & h_2 & h_1 & h_0 & 0 \\ 0 & 0 & 0 & h_2 & h_1 & h_0 \end{bmatrix}$$

After removing the CP, the noncircular and circular correlation of the received signal in the time domain have structures given in (4.13) and (4.14), respectively.

$$E[\mathbf{y}\mathbf{y}^T] = \begin{bmatrix} h_0^2 & 2h_0h_1 & h_1^2+2h_0h_2 & 2h_1h_2 & h_2^2 & 0 \\ 2h_0h_1 & h_1^2+2h_0h_2 & 2h_1h_2 & h_2^2 & 0 & h_0^2 \\ h_1^2+2h_0h_1 & 2h_1h_2 & h_2^2 & 0 & h_0^2 & 2h_0h_2 \\ 2h_1h_2 & h_2^2 & 0 & h_0^2 & 2h_0h_1 & h_1^2+2h_0h_2 \\ h_2^2 & 0 & h_0^2 & 2h_0h_1 & h_1^2+2h_0h_2 & 2h_1h_2 \\ 0 & h_0^2 & 2h_0h_1 & h_1^2+2h_0h_2 & 2h_1h_2 & h_2^2 \end{bmatrix} \tag{4.13}$$

$$E[\mathbf{y}\mathbf{y}^H] =$$

$$\begin{bmatrix} \|\mathbf{h}\|^2+\sigma_n^2 & h_0h_1^*+h_1h_2^* & h_0h_2^* & 0 & h_2h_0^* & h_2h_1^*+h_1h_0^* \\ h_2h_1^*+h_1h_0^* & \|\mathbf{h}\|^2+\sigma_n^2 & h_0h_1^*+h_1h_2^* & h_0h_2^* & 0 & h_2h_0^* \\ h_2h_0^* & h_2h_1^*+h_1h_0^* & \|\mathbf{h}\|^2+\sigma_n^2 & h_0h_1^*+h_1h_2^* & h_0h_2^* & 0 \\ 0 & h_2h_0^* & h_2h_1^*+h_1h_0^* & \|\mathbf{h}\|^2+\sigma_n^2 & h_0h_1^*+h_1h_2^* & h_0h_2^* \\ h_0h_2^* & 0 & h_2h_0^* & h_2h_1^*+h_1h_0^* & \|\mathbf{h}\|^2+\sigma_n^2 & h_0h_1^*+h_1h_2^* \\ h_0h_1^*+h_1h_2^* & h_0h_2^* & 0 & h_2h_0^* & h_2h_1^*+h_1h_0^* & \|\mathbf{h}\|^2+\sigma_n^2 \end{bmatrix} \tag{4.14}$$

It can be seen that both $E[\mathbf{y}\mathbf{y}^T]$ and $E[\mathbf{y}\mathbf{y}^H]$ are circulant matrices with respect to the vectors $\mathbf{v}_{nc} = [h_0^2 \quad 2h_0h_1 \quad h_1^2+2h_0h_2 \quad 2h_1h_2 \quad h_2^2 \quad 0]$ and $\mathbf{v}_c = [\|\mathbf{h}\|^2 + \sigma_n^2 \quad h_0h_1^*+h_1h_2^* \quad h_0h_2^* \quad 0 \quad h_2h_0^* \quad h_2h_1^*+h_1h_0^*]$, respectively. Both vectors have $2L-1$ nonzero components, thus we obtain a system of $2L-1$ second-order polynomial equations which correspond to the L unknown channel coefficients. Note that $\mathbf{v}_{nc}$ is only related to the channel coefficients, and the polynomial system based on the

noncircular correlation is easier to solve. Based on the noncircular correlation $E[\mathbf{y}\mathbf{y}^T]$, the polynomial system of equations is

$$\begin{cases} f_1(\mathbf{h}) &= h_0^2 - \alpha_1 = 0 \\ f_2(\mathbf{h}) &= 2h_0h_1 - \alpha_2 = 0 \\ f_3(\mathbf{h}) &= h_1^2 + 2h_0h_3 - \alpha_3 = 0 \\ f_4(\mathbf{h}) &= 2h_1h_2 - \alpha_4 = 0 \\ f_5(\mathbf{h}) &= h_2^2 - \alpha_5 = 0 \end{cases} \tag{4.15}$$

with $\alpha_i = \mathbf{v}_{nc}(i)$.

Several solutions are possible using the first, second and fifth equations in (4.15). The other two equations allow a unique solution of the channel coefficients, up to a sign. From this example, it can be seen that it is possible to identify a complex-valued channel by using the noncircular second-order statistics or circular second-order correlation with only simple computations. It is worth noting that the computational complexity of the proposed method is $O(N^2)$, which corresponds to the calculation of the correlation matrix $\mathbf{y}\mathbf{y}^T$.

We now summarize the polynomial channel estimation method as follows.

Step 1: Obtain the received signal $\mathbf{y}$, and compute the correlation product $\mathbf{y}\mathbf{y}^T$.

Step 2: Shift the rows of $\mathbf{y}\mathbf{y}^T$ with respect to the first row and average them over the subcarriers to obtain an approximation of $\mathbf{v}_{nc}$.

Step 3: Solve the polynomial system of equations based on the noncircular correlation of the received signals to obtain an estimate of the channel coefficients.

Step 4: Use the estimated channel coefficients for detection.

4.3 Performance Evaluation

The proposed blind polynomial channel estimation algorithm was applied to an OFDM system with BPSK modulation. The carrier frequency of the OFDM system was 5 GHz and the bandwidth of the system was set to 200 kHz. A WSSUS channel was employed with an exponential multipath intensity profile, i.e., $\sigma_d^2 = \exp(-d/D)/\sum_{d=0}^{D-1}\sigma_d^2$. The simulations were carried out for various numbers of channel taps, where each tap is an independent complex Gaussian random process

with Jake's Doppler spectrum. Two pilot tones were utilized to compensate for the sign ambiguity. The channel length is assumed to be known at the receiver, and a one-tap zero forcing (ZF) equalizer was employed to detect the received signals. The normalized Doppler frequency of the channel was set to $f_d T_s = 0.001$. The performance of the proposed algorithm was evaluated based on the mean-square error and bit error rate.

Fig. 4.1 shows the BER performance of a 6-tap OFDM system for different channel estimation methods with $N = 128$ subcarriers. It can be observed that the blind polynomial channel estimation algorithm outperforms the least minimum mean-square error (LMMSE) solution at high SNRs with similar computational complexity. For example, for the proposed method, a BER of 10^{-3} was achieved at $E_b/N_0 = 25.5$dB, with approximately 0.5dB loss compared to that with perfect channel state information. To obtain the same BER with the LMMSE method, $E_b/N_0 = 27$dB is necessary, and additional information such as the noise variance and other channel statistics are required.

Simulations were carried out to determine the impact of the channel length on the system performance. The MSE of the proposed algorithm for various channel lengths and $N = 128$ is depicted in Fig. 4.2. It can be observed that the proposed algorithm achieves better performance with a shorter channel length. This is because $\mathbf{v}_{nc}$ has more nonzero components with a longer length channel, which results in higher computational errors. For example, the proposed algorithm achieves an MSE of 10^{-3} at $E_b/N_0 = 17$dB in a 3-tap channel, while the same MSE was achieved at $E_b/N_0 = 22$dB in a 5-tap channel.

The BER performance of the proposed algorithm with various values of N in a 6-tap channel is shown in Fig. 4.3. It can be observed that the BER performance improves as the number of subcarriers increases. The reason is that the proposed algorithm solves the polynomial equations based on the approximate noncircular second-order statistics. As the number of subcarriers increases, the effect of noise on the calculation $\mathbf{v}_{nc}$ from $\mathbf{y}\mathbf{y}^T$ is reduced. For example, with $N = 64$, the proposed algorithm achieves a BER of 10^{-3} at $E_b/N_0 = 28$dB, with approximately a 1.5dB loss compared to perfect CSI. With $N = 256$, the same BER can be reached at $E_b/N_0 = 26$dB with almost no loss compared to perfect CSI.

4.4 Conclusions

Based on the source characteristics, such as the noncircular characteristics of the input signals, blind channel identification techniques can be developed to obtain a system of polynomial equations. In this chapter, the nonzero cyclostationary statistics of the transmitted signal were exploited to allow blind polynomial channel estimation using the second-order statistics. A set of polynomial equations was formulated based on the correlation of the received signals. The solution of these equations is easily obtained as the channel coefficients in the time domain. Performance results were presented which show that the proposed algorithm provides better performance than the LMMSE algorithm at high SNRs, and it has low computational complexity. Near-optimal performance can be achieved with large OFDM systems.

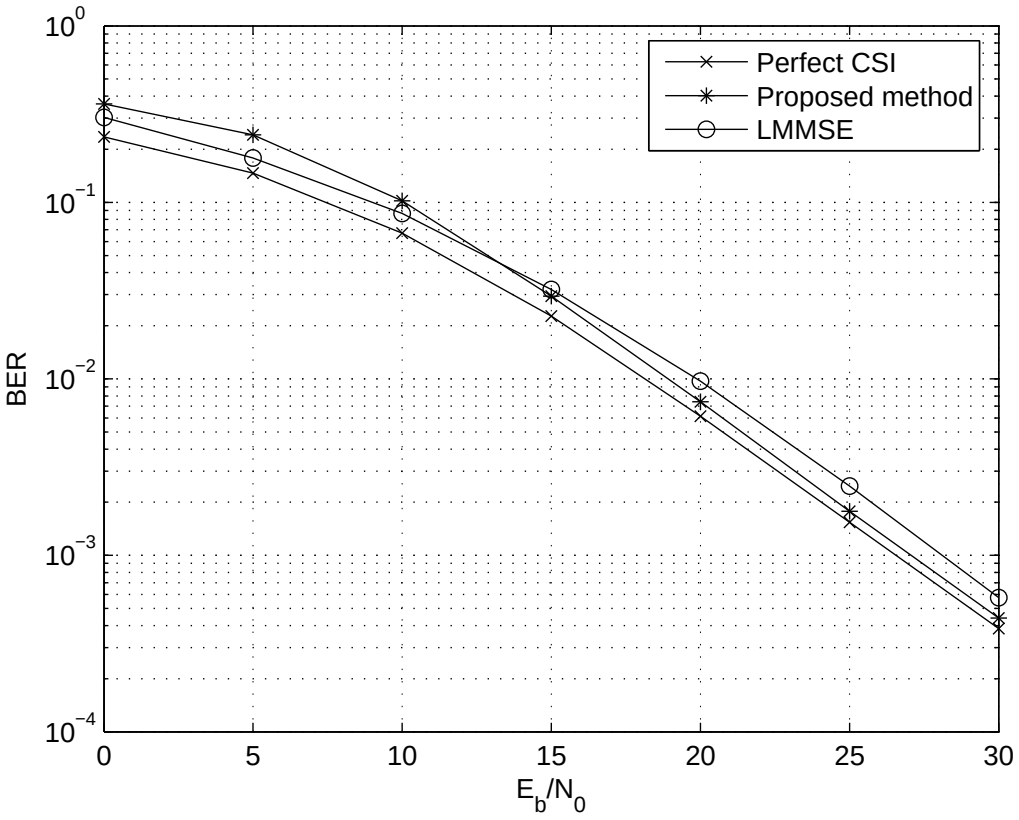

Figure 4.1: BER performance of a 6-tap 128-subcarrier OFDM system.

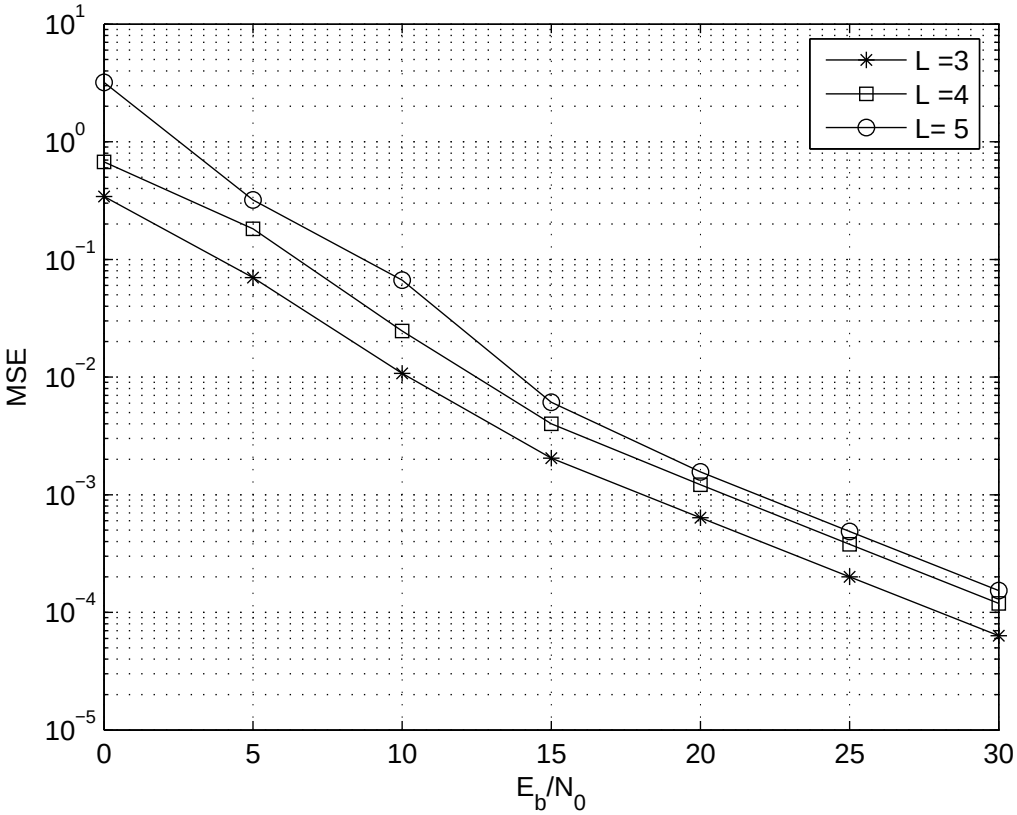

Figure 4.2: Mean-square error of the proposed method for a 128-subcarrier OFDM system with various channel lengths.

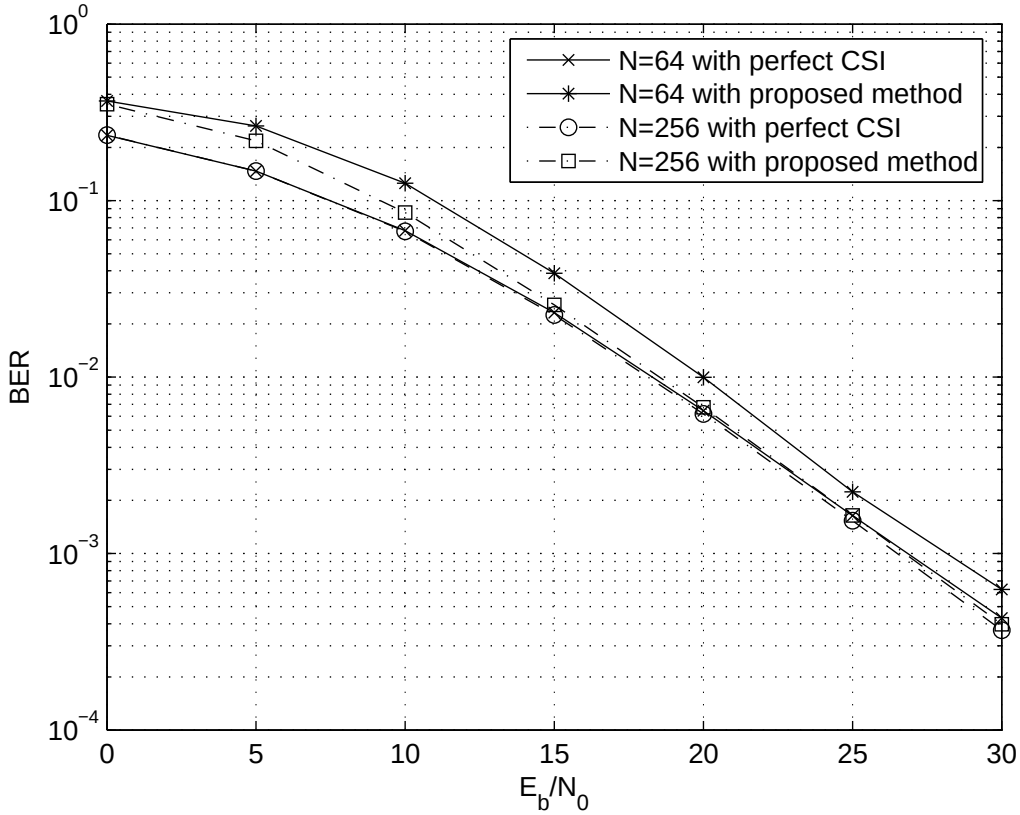

Figure 4.3: BER performance of the proposed method for an OFDM system with various numbers of subcarriers and a 6-tap channel.

Chapter 5

OFDM Channel Estimation Using Compressive Sensing

Wireless channels tend to be sparse due to the high-speed data transmission, i.e., only a few of the multipath channel taps have significant energy. The sparsity of a multipath channel can be defined as the ratio of the time duration (in OFDM samples), spanned by the multipath signal to the number of these signals [46]. To improve the accuracy of the sparse channel estimation, the length of the CIR and the delays of the significant multipath components are required to be known [47]. There have been a number of algorithms proposed to estimate the sparse channel in OFDM systems. In [48], an effective delay acquisition technique is developed, however the pilots need to be equally spaced. In [49], the multiple signal characterization (MUSIC) algorithm widely used for spectrum analysis is employed for channel estimation, again assuming equally spaced pilots. A delay subspace tracking algorithm applicable for OFDM is proposed in [50], which can also exploit sparse multipath channels. A generalized Akaike information criterion (GAIC)-based sparse channel estimation algorithm is proposed in [51]. The system performance is improved by combining a LS channel estimator and GAIC method, and it is iterative in nature. However, the channel length has to be determined in advance to detect the positions of the significant taps.

Recently, compressive sensing (CS) has been introduced to efficiently reconstruct sparse signals from a limited number of samples (measurements) [52]-[55]. The methodology of CS has been applied in numerous research fields, such as coding, information theory, high-dimensional geometry, statistical signal processing, machine learning, Bayesian inference, multi-band signal processing, imaging, analog-to-information

conversion, biosensing, geophysical data analysis, radar, astronomy, metrology, and communications [52]-[55]. Based on this methodology, CS can be employed to take advantage of the inherent sparsity of wireless channels. This is significant because fewer pilot tones to estimate the channel impulse response results in more subcarriers for data transmission.

Several authors have proposed CS based methods for channel estimation in both signal-carrier and multi-carrier communication systems. In [56] and [57], a matching pursuit algorithm is presented for channel estimation in a single-carrier system, however, the focus was on simulation and implementation issues. The channel estimation techniques presented in [56] and [58] estimate the delay-Doppler sparsity of the channel. Sharp and Scaglione propose a channel estimation method in [59], which forms an overcomplete basis for the non-sparse channel impulse responses. This in turn leads to a sparse coefficient vector. In [60] and [61], CS-based techniques are proposed for the estimation of delay-Doppler sparsity in pulse-shaping multicarrier systems with doubly selective channels. He and Song [62] propose an optimal pilot pattern for sparse channel estimation in OFDM systems by minimizing the mutual coherence of the measurement matrix, and the first path is assumed to be always nonzero. In [63], a continuous time path-based channel model is assumed in OFDM systems. A dictionary with finer time resolution than that of baseband sampling rate is employed to improve the performance of the orthogonal matching pursuit (OMP) and basis pursuit (BP) algorithms.

In this chapter, a CS-based time-domain channel estimation method for OFDM systems over sparse channels is presented. Employing a CS framework, the channel estimation problem under consideration is formulated as a small-scale l_1-minimization problem which is convex and admits fast and reliable solvers for the globally optimal solution. It is demonstrated that the magnitudes as well as delays of the significant taps of a sparse channel model can be estimated with satisfactory accuracy by using fewer pilot tones than the channel length. Moreover, it is shown that an FFT matrix of extended size can be used as a set of appropriate basis vectors under which the channel sparsity can be enhanced. This technique allows the proposed method to also be applicable to less-sparse OFDM channels. In addition, a total-variation minimization based method is introduced to provide an alternative way to solve the original sparse channel estimation problem. The performance of the proposed method is compared to several established channel estimation algorithms.

This chapter is organized as follows. A brief introduction to compressive sensing

necessary for the subsequent development is given in Section 5.1. In Section 5.2, the CS-based channel estimation method and a minimum total-variation method for OFDM channel estimation are proposed. The simulation environment and performance results are presented in Section 5.3, followed by some conclusions in Section 5.4.

5.1 Compressive Sensing and TV Minimization

5.1.1 Compressive Sensing: Concepts and Key Results

Compressive sensing refers to a collection of methods to represent a signal with a limited number of measurements and recover the signal from these measurements. Research in CS remains very active, and as a result, it is now well understood that if a signal is measured by independent random projections, then it can be reconstructed using these measurements as long as certain conditions between the dimension and sparsity of the signal and the number of measurements collected are satisfied [53]-[55].

A discrete-time signal $\boldsymbol{x}$ of length N is said to be K-sparse if it contains K nonzero components with $K \ll N$. Although most real-world signals do not look sparse under the canonical basis, many natural and man-made signals admit sparse representations with respect to an appropriate basis [64]. For this reason, in the rest of the chapter we focus on the class of K-sparse signals. The acquisition of a sparse signal $\boldsymbol{x}$ in CS theory is performed by obtaining inner products of $\boldsymbol{x}$ with M different waveforms $\{\boldsymbol{\phi}_1,\ \boldsymbol{\phi}_2,\ \cdots,\ \boldsymbol{\phi}_M\}$, namely, $y_k = \langle \boldsymbol{\phi}_k,\ \boldsymbol{x} \rangle$ for $k = 1,\ 2,\ \ldots,\ M$. If we let $\boldsymbol{y} = [y_1\ y_2\ \cdots\ y_M]^T$ and

$$\boldsymbol{\Phi} = \begin{bmatrix} \boldsymbol{\phi}_1 \\ \boldsymbol{\phi}_2 \\ \vdots \\ \boldsymbol{\phi}_M \end{bmatrix},$$

then the data acquisition process in a compressive sensing framework can be described as

$$\boldsymbol{y} = \boldsymbol{\Phi}\boldsymbol{x} \tag{5.1}$$

The size of the measurement matrix $\boldsymbol{\Phi}$ in (5.1) is $M \times N$, typically with $M \ll N$. In this way, the signal $\boldsymbol{x}$ is "sensed" by a reduced or "compressed" number of measurements, hence the name compressive sensing.

With $M < N$, (5.1) is an underdetermined system of linear equations, hence reconstructing signal $\boldsymbol{x}$ from measurement $\boldsymbol{y}$ is in general an *ill-posed* problem. However, if one searches for the sparsest solution of (5.1), it can be obtained by solving the constrained problem

$$\text{minimize } \|\boldsymbol{x}\|_0 \tag{5.2a}$$

$$\text{subject to: } \boldsymbol{\Phi x} = \boldsymbol{y} \tag{5.2b}$$

where $\|\boldsymbol{x}\|_0$ is the so-called l_0 norm of $\boldsymbol{x}$ defined by $\|\boldsymbol{x}\|_0 = \sum_{i=1}^{N} |x_i|^0$, which counts the number of nonzero components in $\boldsymbol{x}$. Unfortunately, (5.2) is a combinatorial optimization problem whose computational complexity grows exponentially with signal size N. A key result in CS theory ([53]-[55]) is that if $\boldsymbol{x}$ is K-sparse, $\{\boldsymbol{\phi}_1,\ \boldsymbol{\phi}_2,\ \cdots,\ \boldsymbol{\phi}_M\}$ are independent and identically distributed (i.i.d.) random measurements with zero mean and variance $1/N$, and the number of measurements, M, satisfies the condition

$$M \geq cK \log(N/K) \tag{5.3}$$

with c a small constant, then $\boldsymbol{x}$ can be reconstructed by solving the convex problem

$$\text{minimize } \|\boldsymbol{x}\|_1 \tag{5.4a}$$

$$\text{subject to: } \boldsymbol{\Phi x} = \boldsymbol{y} \tag{5.4b}$$

where $\|\boldsymbol{x}\|_1 = \sum_{i=1}^{N} |x_i|$ denotes the l_1-norm of $\boldsymbol{x}$.

For real-valued data $\{\boldsymbol{\Phi},\ \boldsymbol{y}\}$, (5.4) is a linear programming problem; for complex-valued $\{\boldsymbol{\Phi},\ \boldsymbol{y}\}$, (5.4) can be cast as a second-order cone programming problem [65], both of which can be solved using reliable and efficient algorithms. In practice, it may well be that the measurements are inaccurate. The model in (5.1) in this case needs to be modified to

$$\boldsymbol{y} = \boldsymbol{\Phi x} + \boldsymbol{e} \tag{5.5}$$

where $\boldsymbol{e}$ is the measurement error with $\|\boldsymbol{e}\|_2 \leq \sigma$. Accordingly, the l_1-minimization problem associated with model (5.5) is given by

$$\text{minimize } \|\boldsymbol{x}\|_1 \tag{5.6a}$$

$$\text{subject to: } \|\boldsymbol{\Phi x} - \boldsymbol{y}\|_2 \leq \sigma \tag{5.6b}$$

which is a convex problem that can be re-formulated as an SOCP problem for fast solution [65].

5.1.2 Signal Reconstruction via TV Minimization

An alternative model to recover a K-sparse signal $\boldsymbol{x}$ is to minimize the signal's total variation subject to measurement fidelity [66]. The TV of a discrete signal $\boldsymbol{x}$ is defined as

$$\|\boldsymbol{x}\|_{TV} = \sum_{i=1}^{N-1} |x_{i+1} - x_i| \tag{5.7}$$

A TV-minimization based method reconstructs a sparse signal $\boldsymbol{x}$ by solving the constrained problem

$$\text{minimize } \|\boldsymbol{x}\|_{TV} \tag{5.8a}$$

$$\text{subject to: } \boldsymbol{\Phi x} = \boldsymbol{y} \tag{5.8b}$$

Similarly, for a sparse signal $\boldsymbol{x}$ with noise measurements as modeled in (5.5), a TV-minimization based algorithm recovers $\boldsymbol{x}$ by solving the convex problem

$$\text{minimize } \|\boldsymbol{x}\|_{TV} \tag{5.9a}$$

$$\text{subject to: } \|\boldsymbol{\Phi x} - \boldsymbol{y}\|_2 \leq \sigma \tag{5.9b}$$

Depending on whether the variables in (5.8) and (5.9) are real-valued or complex-valued, these problems can be re-formulated as a linear programming (LP) or second-order cone programming (SOCP) problem for fast solution [65].

5.2 Sparse Channel Estimation

For an OFDM system, if the channel is time-invariant within one OFDM symbol, the matrix $\mathbf{A}$ in (1.9) is a diagonal matrix, and we can rewrite (1.9) with respect to the channel impulse response as

$$\mathbf{Y} = \sqrt{N}\mathbf{X}_D\mathbf{F}^H\boldsymbol{h}_N + \mathbf{W} \tag{5.10}$$

where $\mathbf{X}_D$ is a diagonal matrix of transmitted data in the frequency domain, i.e., $\mathbf{X}_D = \text{diag}(X)$, and $\boldsymbol{h}_N = [h(0)\ h(1)\ \ldots\ h(L-1)\ 0\ \ldots\ 0]^T$ is the time domain

channel impulse response with length N.

For coherent detection in OFDM systems, reliable channel information is required to fully recover the transmitted signals. Generally, pilot symbols are transmitted at pre-determined subcarriers, and an approximation of the channel information can be obtained using various channel estimation methods [25] [27]. However, the number of pilots needed must be equal to or greater than the number of channel taps. Channels in OFDM systems tend to be sparse due to the high-speed data transmission, i.e., only a few of the multipath channel taps have significant energy. Thus it is natural to consider using fewer pilot symbols, but still obtain reliable channel estimation. Channel estimation requires that the nonzero channel tap amplitudes and positions be determined, and as will be shown, compressive sensing can provide a near-optimal solution for these parameters.

5.2.1 Sparse Channel Estimation with l_1-Minimization

We assume the length of the OFDM channel is L, but contains only K nonzero taps, where $K \ll L$. Thus the channel vector $\boldsymbol{h} = [h(0)\ h(1)\ \ldots\ h(L-1)]^T$ is a sparse vector. According to the theory of compressive sensing, with proper measurement samples $\mathbf{Y}_M$, an approximation of the channel information can be obtained by solving the following l_1-minimization problem

$$\text{minimize } \|\boldsymbol{h}\|_1 \tag{5.11a}$$

$$\text{subject to: } \|\boldsymbol{\Phi h} - \mathbf{Y}_M\|_2 \leq \sqrt{M}\sigma \tag{5.11b}$$

where $\mathbf{Y}_M$ denotes the received signal at the pilot subcarriers with size $M \times 1$, and $\boldsymbol{\Phi}$ denotes the submatrix of $\sqrt{N}\mathbf{X}_D\mathbf{F}^H$ corresponding to the pilot subcarriers with size $M \times L$, $M < L$. σ is the standard derivation of the AWGN, and the derivation of constraint (5.11b) is given in Appendix A.

The variables in (5.11) are complex-valued. If we define $\mathbf{Y}_M = \mathbf{Y}_{M_r} + \mathrm{j}\mathbf{Y}_{M_i}$, $\boldsymbol{\Phi} = \boldsymbol{\Phi}_r + \mathrm{j}\boldsymbol{\Phi}_i$, and $\boldsymbol{h} = \boldsymbol{h}_r + \mathrm{j}\boldsymbol{h}_i$, then (5.11) becomes an optimization problem with

real-valued data as

$$\text{minimize } \sum_{k=1}^{L} \delta_k \tag{5.12a}$$

$$\text{subject to: } \|\hat{\mathbf{I}}_k \hat{\boldsymbol{h}}\|_2 \ \leq \delta_k \text{ for } k = 1, \ldots, \ L \tag{5.12b}$$

$$\|\hat{\boldsymbol{\Phi}} \hat{\boldsymbol{h}} - \hat{\mathbf{Y}}_M\|_2 \leq \sqrt{M}\sigma \tag{5.12c}$$

where $\hat{\boldsymbol{h}} = \begin{bmatrix} \boldsymbol{h}_r \\ \boldsymbol{h}_i \end{bmatrix}$, $\hat{\mathbf{Y}}_M = \begin{bmatrix} \mathbf{Y}_{M_r} \\ \mathbf{X}_{M_i} \end{bmatrix}$, and $\hat{\boldsymbol{\Phi}} = \begin{bmatrix} \boldsymbol{\Phi}_r & -\boldsymbol{\Phi}_i \\ \boldsymbol{\Phi}_i & \boldsymbol{\Phi}_r \end{bmatrix}$. The matrix $\hat{\mathbf{I}}_k$ has the form $\hat{\mathbf{I}}_k = \begin{bmatrix} \mathbf{I}_k & \mathbf{0}_L \\ \mathbf{0}_L & \mathbf{I}_k \end{bmatrix}$,

where $\mathbf{I}_k$ denotes the kth row of an $L \times L$ identity matrix, and $\mathbf{0}_L$ is an all zero row vector of length L.

Consequently, the optimization problem (5.12) can be converted into a SOCP problem as

$$\text{minimize } \mathbf{c}_0^T \tilde{\mathbf{h}} \tag{5.13a}$$

$$\text{subject to: } \|\tilde{\mathbf{I}}_k \tilde{\mathbf{h}}\|_2 \ \leq \mathbf{c}_k^T \tilde{\mathbf{h}} \text{ for } k = 1, \ldots, \ L \tag{5.13b}$$

$$\|\tilde{\boldsymbol{\Phi}} \tilde{\mathbf{h}} - \hat{\mathbf{Y}}_M\|_2 \leq \sqrt{M}\sigma \tag{5.13c}$$

where $\tilde{\mathbf{h}} = [\delta_1 \ \delta_2 \ \ldots \ \delta_L \ \hat{\mathbf{h}}^T]^T$, $\tilde{\mathbf{I}}_k = [\mathbf{0}_{2\times L} \ \hat{\mathbf{I}}_k]$, and $\tilde{\boldsymbol{\Phi}} = [\mathbf{0}_{2M\times L} \ \hat{\boldsymbol{\Phi}}]$. We have $\mathbf{c}_0 = [1 \ 1 \ \ldots \ 1 \ 0 \ \ldots \ 0]^T$, and $\mathbf{c}_k$ is a zero vector of length $3L$, except the kth component is set to one. This SOCP problem can be solved, for example, using the MATLAB-compatible toolbox SeDuMi [33].

5.2.2 Sparse OFDM Channel Estimation by Increasing the FFT Matrix Size

The previous Section presented sparse channel estimation using l_1-minimization. However, the accuracy of the solution degrades as the channel becomes less sparse. We propose using an FFT matrix of increased size to facilitate reducing the solution sensitivity with respect to the channel sparsity. To be specific, note that the OFDM system model in (5.10) is equivalent to

$$\mathbf{Y} = \sqrt{2N}\mathbf{X}_D \mathbf{F}_{2N}'^H \boldsymbol{h}_{2N} + \mathbf{W} \tag{5.14}$$

where $\mathbf{F}'_{2N}$ is a matrix which contains the odd columns of a size $2N$ FFT matrix, and the length $2N$ vector $\boldsymbol{h}_{2N}$ has the form $\boldsymbol{h}_{2N} = [\mathbf{h}_N \dots \ \mathbf{0}_N]^T$, where $\mathbf{0}_N$ is a all zero vector with length N. Thus the sparsity of the channel vector increases from $\frac{K}{L}$ to $\frac{K}{2L}$.

This approach leads to a minimization problem based on the system model in (5.14) with respect to the extended channel vector $\boldsymbol{h}' = [h(0)\ h(1)\ \dots\ h(L-1)\ \mathbf{0}_L]^T$. According to the theory of compressive sensing, with proper measurement samples $\mathbf{Y}_M$, approximate channel information can be obtained by solving the following l_1-norm minimization problem

$$\text{minimize } \|\boldsymbol{h}'\|_1 \tag{5.15a}$$

$$\text{subject to: } \|\boldsymbol{\Phi}'\boldsymbol{h}' - \mathbf{Y}_M\|_2 \leq \sqrt{M}\sigma \tag{5.15b}$$

where $\mathbf{Y}_M$ denotes the received signal at the pilot subcarriers with size $M \times 1$, and $\boldsymbol{\Phi}'$ denotes the submatrix of $\sqrt{2N}\mathbf{X}_D\mathbf{F}'^H_{2N}$ corresponding to the pilot subcarriers with size $M \times 2L$. Consequently, problem (5.15) can be reformulated as in (5.12) and (5.13), and converted into an SOCP problem.

In principle, one can extend the original FFT matrix to an even larger size to further increase the sparsity of the channel vector. However, this results in reduced estimation accuracy, hence a proper compromise needs to be made with regard to the length of the extended FFT matrix and the estimation accuracy.

5.2.3 Sparse Channel Estimation Using TV Minimization

Define the TV of the channel $\boldsymbol{h}$ as

$$\|\boldsymbol{h}\|_{TV} = \sum_{i=1}^{L-1} |h_{i+1} - h_i| \tag{5.16}$$

The TV-minimization method recovers the channel information $\boldsymbol{h}$ by minimizing the total variation as defined above subject to measurement fidelity, namely

$$\text{minimize } \|\boldsymbol{h}\|_{TV} \tag{5.17a}$$

$$\text{subject to: } \|\boldsymbol{\Phi}\boldsymbol{h} - \mathbf{Y}_M\|_2 \leq \sqrt{M}\sigma \tag{5.17b}$$

The variables in (5.17) are complex-valued, but the above problem can be converted into a real-valued optimization problem as

$$\text{minimize } \sum_{k=1}^{L} \delta_k \tag{5.18a}$$

$$\text{subject to: } \|\mathbf{P}\boldsymbol{\Upsilon}_k \hat{\boldsymbol{h}}\|_2 \leq \delta_k \text{ for } k = 1, \ldots, L \tag{5.18b}$$

$$\|\hat{\boldsymbol{\Phi}}\hat{\boldsymbol{h}} - \hat{\mathbf{Y}}_M\|_2 \leq \sqrt{M}\sigma \tag{5.18c}$$

where $\hat{\boldsymbol{h}} = \begin{bmatrix} \boldsymbol{h}_r \\ \boldsymbol{h}_i \end{bmatrix}$, $\hat{\mathbf{Y}}_M = \begin{bmatrix} \mathbf{Y}_{M_r} \\ \mathbf{X}_{M_i} \end{bmatrix}$, and $\hat{\boldsymbol{\Phi}} = \begin{bmatrix} \boldsymbol{\Phi}_r & -\boldsymbol{\Phi}_i \\ \boldsymbol{\Phi}_i & \boldsymbol{\Phi}_r \end{bmatrix}$. For each k, the matrix $\boldsymbol{\Upsilon}_k$ is a $4 \times 2L$ matrix zero matrix except for elements $\Upsilon_{1,k},\ \Upsilon_{2,k+1},\ \Upsilon_{3,L+k},\ \Upsilon_{4,L+k+1}$ which are set to one, and

$$\mathbf{P} = \begin{bmatrix} \frac{\sqrt{2}}{2} & -\frac{\sqrt{2}}{2} & 0 & 0 \\ -\frac{\sqrt{2}}{2} & \frac{\sqrt{2}}{2} & 0 & 0 \\ 0 & 0 & \frac{\sqrt{2}}{2} & -\frac{\sqrt{2}}{2} \\ 0 & 0 & -\frac{\sqrt{2}}{2} & \frac{\sqrt{2}}{2} \end{bmatrix} \tag{5.19}$$

By defining $\tilde{\mathbf{h}} = [\delta_1\ \delta_2\ \ldots\ \delta_L\ \hat{\mathbf{h}}^T]^T$, $\tilde{\boldsymbol{\Upsilon}}_k = [\mathbf{0}_{4\times L}\ \boldsymbol{\Upsilon}_k]$, $\tilde{\boldsymbol{\Phi}} = [\mathbf{0}_{2M\times L}\ \hat{\boldsymbol{\Phi}}]$, $\mathbf{c}_0 = [1\ 1\ \ldots\ 1\ 0\ \ldots\ 0]^T$, and $\mathbf{c}_k$ is a vector of length $3L$ with all components zero except $c_k(k) = 1$, the problem in (5.18) can then be expressed as a standard SOCP problem as given below

$$\text{minimize } \mathbf{c}_0^T \tilde{\boldsymbol{h}} \tag{5.20a}$$

$$\text{subject to: } \|\mathbf{P}\tilde{\boldsymbol{\Upsilon}}_k \tilde{\boldsymbol{h}}\|_2 \leq \mathbf{c}_k^T \tilde{\mathbf{h}} \text{ for } k = 1, \ldots, L \tag{5.20b}$$

$$\|\tilde{\boldsymbol{\Phi}}\tilde{\boldsymbol{h}} - \hat{\mathbf{Y}}_M\|_2 \leq \sqrt{M}\sigma \tag{5.20c}$$

Once the global solution of (5.20) is calculated, the real and imaginary parts of the channel information $\boldsymbol{h}$ can be extracted from the solution $\tilde{\boldsymbol{h}}$ as its last $2L$ components.

5.3 Performance Evaluation

The proposed CS-based channel estimation methods were simulated in a 4-QAM OFDM system. The channel length was assumed to be known at the receiver, while the positions of the nonzero taps were unknown. The pilot tones were arbitrary 4-QAM symbols, and the positions of these pilot were randomly selected.

The carrier frequency of the OFDM system was 5 GHz, the bandwidth of the system was set to 200 kHz, and the number of subcarriers was 128. A WSSUS channel was employed with an exponential multipath intensity profile, i.e., $\sigma^2 = \exp(-d/D)/\sum_{d=0}^{D-1}\sigma^2$. The simulations were carried out for various numbers of channel taps, where each tap was an independent complex Gaussian random process with Jake's Doppler spectrum. A one-tap ZF equalizer was employed to detect the received signals. The normalized Doppler frequency of the channel was set to $f_d T_s = 0.001$. The performance of the proposed algorithms were evaluated based on BER using the MATLAB SeDuMi toolbox [33]. The computational complexity of the algorithms are compared based on the CPU time under the same test environment, and the execution time of the optimization algorithms are measured using MATLAB command *cputime*.

Fig. 5.1 shows the BER performance of a 20-tap OFDM system with 2 nonzero taps for different channel estimation methods. The CS-based and TV-minimization channel estimation methods only used 14 pilot tones, while the LMMSE method employed 20 and 40 pilot tones, respectively. It can be observed that with a channel sparsity of $K \leq 0.1L$, the CS-based and TV-minimization channel estimation algorithms provide a near-optimal solution relative to the performance with perfect channel information, and both outperform the LMMSE solutions with considerably fewer pilot tones. The TV-minimization method has better performance at higher E_b/N_0 than that of the CS-based method with slightly increased computational complexity. For example, the CS-based method with 14 pilot tones achieves a BER of 10^{-3} at $E_b/N_0 = 21.3$ dB, an approximately 0.35 dB loss compared to that with perfect channel state information. To obtain the same BER with the LMMSE method with 40 pilot tones, $E_b/N_0 = 23$ dB is necessary. The TV-minimization method provides a near-optimal solution for E_b/N_0 greater than 25 dB.

The BER performance of the proposed algorithm with a larger size FFT matrix is depicted in Figs. 5.2 and 5.3. It can be observed that at a sparsity of $K \leq 0.2L$, the CS-based channel estimation method with a larger size FFT matrix still provides sub-optimal BER performance relative to that with perfect channel information, but the LMMSE method requires more than twice the number pilot tones to achieve similar performance. Furthermore, Fig. 5.3 shows that the BER performance of the proposed method is slightly improved compared with the performance with perfect channel information, as the channel in this case has a longer length. For example, with a 10-tap channel with 2 nonzero taps, the proposed algorithm achieves a BER

of 10^{-3} at $E_b/N_0 = 23.7$ dB, an approximately 2.7 dB loss compared to perfect CSI, while the LMMSE method with 20 pilot tones provides the same BER at 25 dB, as shown in Fig. 2. The BER performance loss at a BER of 10^{-3} is reduced to 2 dB for the proposed method compared to that with perfect channel information.

5.4 Conclusions

In this chapter, a CS-based time-domain channel estimation method for OFDM systems over sparse channels was presented. Employing a CS framework, the channel estimation problem under consideration was formulated as a small-scale l_1-minimization problem which is convex and admits fast and reliable solvers for the globally optimal solution. It was demonstrated that the magnitudes as well as delays of the significant taps of a sparse channel model can be estimated with satisfactory accuracy by using fewer pilot tones than the channel length. Moreover, an FFT matrix of extended size can be used as a set of appropriate basis vectors to enhance the channel sparsity. This technique allows the proposed method to also be applicable to less-sparse OFDM channels. In addition,we a TV minimization based method was introduced to provide an alternative way to solve the original sparse channel estimation problem. Simulation results were presented to evaluate the performance of the proposed method relative to several established channel estimation algorithms.

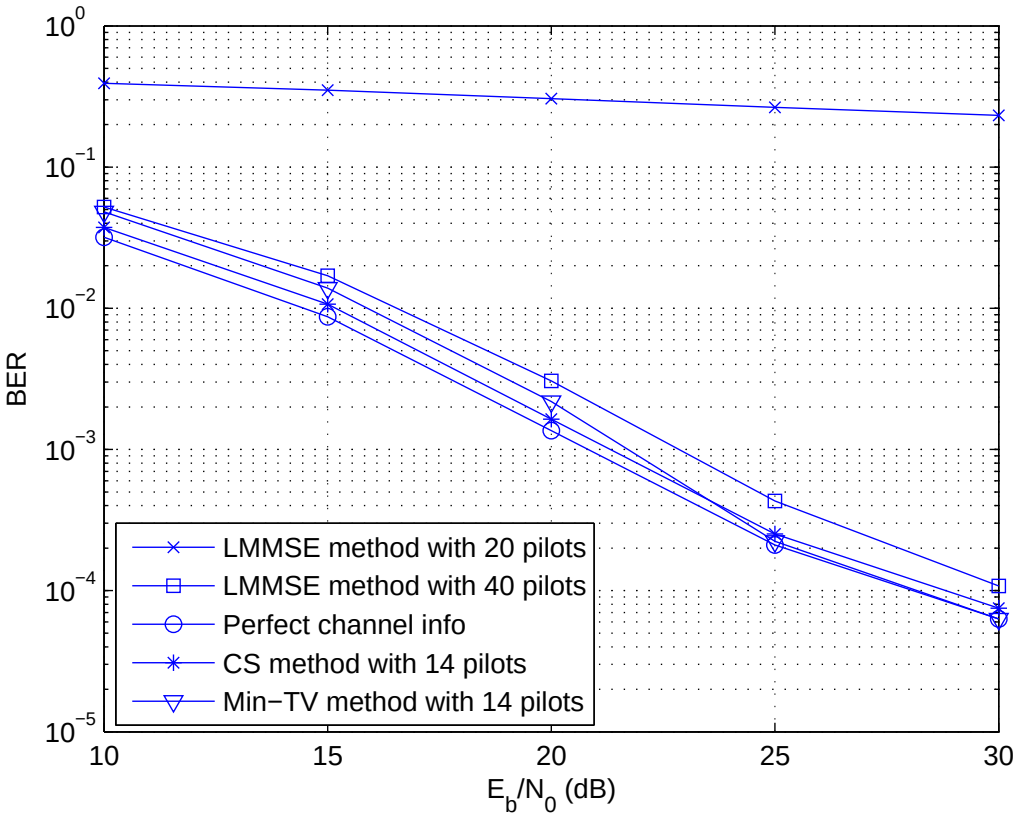

Figure 5.1: BER performance of a 20-tap 128-subcarrier OFDM system with 2 nonzero taps.

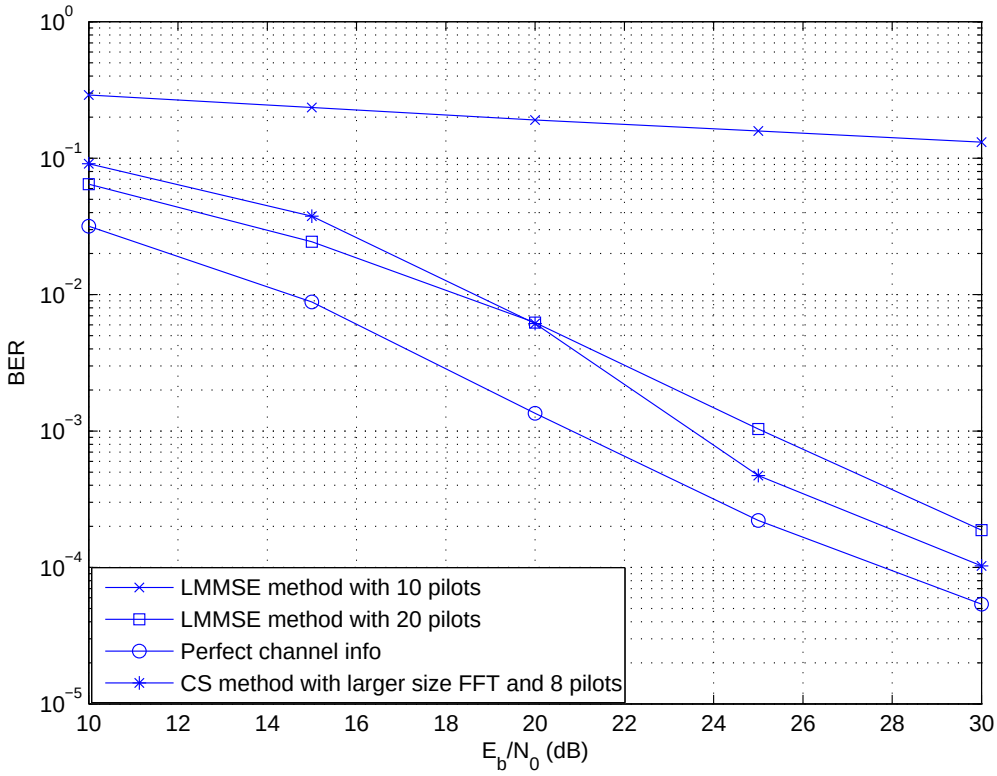

Figure 5.2: BER performance of a 10-tap 128-subcarrier OFDM system with 2 nonzero taps.

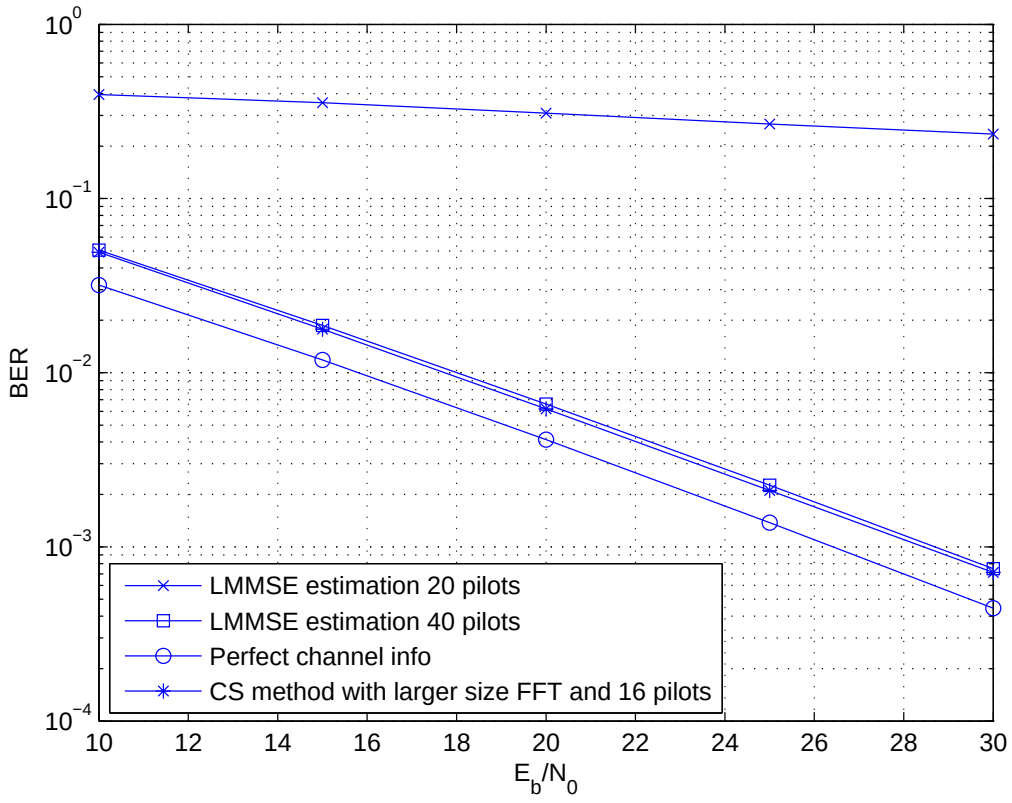

Figure 5.3: BER performance of a 20-tap 128-subcarrier OFDM system with 4 nonzero taps.

Chapter 6

Conclusions and Future Work

6.1 Conclusions

In Chapters 2 to 5, several signal detection and channel estimation algorithms were proposed for OFDM systems. In Chapter 2, several ICI reduction algorithms were presented for OFDM systems over fast fading channels, and Chapter 3 described a semiblind signal detection algorithm for OFDM systems with knowledge of the channel correlation and noise variance. Chapter 4 proposed a blind channel estimation algorithm for OFDM systems over time-invariant channels, and the algorithm described in Chapter 5 wass employed to estimate a sparse channel in OFDM systems.

6.1.1 Intercarrier Interference Reduction Algorithms for OFDM Systems

In this chapter, the OFDM ICI reduction problem was formulated as a combinatorial optimization problem based on ML criterion. As significant computational complexity is required to solve such problem, two relaxation methods were proposed to relax the maximum likelihood detection problem into convex quadratic programming problems, which leads to reduced computational complexity with sub-optimal performance. Furthermore, a low complexity ICI reduction algorithm which can be applied to QAM signal constellations was proposed to relax the ICI reduction problem into a QP problem with non-convex constraints. These algorithms employ a successive method which deduces a sequence of reduced-size QP problems, and the solutions are obtained by limiting the search in the 2-dimensional subspace spanned by its steepest-descent and Newton directions to reduce the computational complexity. A

low-bit descent search can also be employed to improve the system performance. The extension to higher-order quadrature amplitude modulation OFDM systems was also addressed.

It was demonstrated via simulation that the integer QP relaxation based algorithms provide excellent performance with reasonable computational complexity. The three proposed ICI reduction algorithms offer superior performance to that with the one-tap equalizer and the DFE algorithm, and the performance was further improved by employing the LBDS method. The performance of the 2-dimensional bounded constraint relaxation algorithm degrades as the Doppler spread increases, while time diversity can be achieved after combining with the LBDS method. Furthermore, the successive ICI reduction algorithm provides a performance improvement over the DFE algorithm, which increases as the Doppler spread increases. The algorithm exhibits an error floor at high SNR for a smaller threshold ρ, but this can be effectively suppressed by performing LBDS with a slightly increased computational complexity. For a larger threshold, the system has comparable performance with and without LBDS, and the increase in computational complexity using LBDS is insignificant. The system performance improves as the Doppler spread increases.

6.1.2 Low Complexity Joint Semiblind Detection for OFDM Systems over Time-Varying Channels

In this chapter, a low complexity joint semiblind detection algorithm for OFDM systems over time-varying channels was proposed based on the channel correlation and noise variance. The problem was relaxed to a continuous non-convex quadratic programming problem. Then an iterative method was utilized to deduce a sequence of reduced-size quadratic programming problems. The 2-dimensional subspace search and LBDS method were employed to improve system performance and reduce the computational complexity.

Simulations were carried out to demonstrate that the IJSD algorithm provides comparable results to those of the sphere decoder with much less computational complexity. A loss in performance was observed due to a smaller threshold, but this loss can be avoided by performing LBDS with a slightly increased computational complexity. It was shown that at lower SNRs, the proposed algorithm provides similar performance for all values of Doppler spread. However, for smaller Doppler spreads, better performance was achieved at higher SNRs. A small number of pilot tones is

required to solve the optimization problem, and the performance improves as the number of the pilot tones increases, with the error floor significantly reduced.

6.1.3 Blind Polynomial Channel Estimation for OFDM Systems

In this chapter, a blind polynomial channel estimation algorithm was described using the noncircular second-order statistics of the received OFDM signal. A set of polynomial equations was then formulated based on the correlation of the received signal. The solution of these equations provides an estimate of the channel coefficients.

The performance results given showed that proposed channel estimation algorithm outperforms the LMMSE algorithm at high SNRs with similar computational complexity. With a shorter channel length, the proposed algorithm can achieve better performance. Furthermore, the performance of the algorithm is near-optimal for larger size OFDM systems.

6.1.4 OFDM Channel Estimation Using Compressive Sensing

In this chapter, a CS-based time-domain channel estimation method for OFDM systems over sparse channels was presented. Employing a CS framework, the channel estimation problem under consideration was formulated as a small-scale l_1-minimization problem which is convex and admits fast and reliable solvers for the globally optimal solution. It was demonstrated that the magnitudes as well as delays of the significant taps of a sparse channel model can be estimated with satisfactory accuracy by using fewer pilot tones than the channel length. Moreover, an FFT matrix of extended size can be used as a set of appropriate basis vectors under which the channel sparsity can be enhanced. This technique allows the proposed method to be applied to less-sparse OFDM channels. In addition, a total-variation minimization based method was introduced to provide an alternative way to solve the original sparse channel estimation problem.

It was demonstrated via simulation that the proposed channel estimation algorithms offer a performance improvement over the LMMSE algorithm with fewer pilot tones. With a channel sparsity of $K \leq 0.1L$, the CS-based and TV-minimization channel estimation algorithms provide a near-optimal solution relative to the perfor-

mance with perfect channel information, and both outperform the LMMSE algorithm with considerably fewer pilot tones. The TV-minimization method has better performance at higher E_b/N_0 than that of the CS-based method with slightly increased computational complexity.

For a less sparse channel, the CS-based channel estimation method with a larger size FFT matrix still provides sub-optimal BER performance relative to that with perfect channel information, but the LMMSE algorithm requires more than twice the number pilot tones to achieve similar performance. The BER performance of the proposed method can be improved close to that with perfect channel information over a longer length channel.

6.2 Future Work

In what follows, several research topics are described as possible extensions to the results presented in this dissertation.

6.2.1 ICI Reduction for MIMO OFDM Systems

Recently, multiple antennas have been widely employed for use at both the transmitter and receiver to provide capacity gain, diversity gain, or both. Multiple-input multiple-output (MIMO) systems and related signal processing have attracted great attention in recent years, and are currently being proposed for the emerging fourth generation systems. Thus, efficient transmission and reception techniques for these systems are of interest.

MIMO technique can be combined with OFDM to convert a time-invariant frequency-selective channel into a set of orthogonal frequency-flat channels, which in turn enable simple equalization at the receiver [67]. However, the Doppler spread induced by high-mobility environments destroys the OFDM orthogonality among subcarriers, which results in intercarrier interference and degrades system performance. Furthermore, the effects of the time-varying channel become even more serious in MIMO-OFDM systems, because the data received at each subcarrier is affected by the ICI generated by the signal transmitted on adjacent subcarriers from all the transmit antennas [68] [69]. Thus, it is worthwhile to extend the results in Chapters 2 and 3 to MIMO-OFDM systems over time-varying channels, and to develop an optimization framework to obtain robust detection efficiently.

6.2.2 Channel Estimation in OFDM Systems over Doubly-Selective Channels

The channel estimation algorithms proposed in Chapter 4 and 5 assume that the channel is time-invariant within one OFDM symbol duration. However, in a high mobility environment, the channel is varying within an OFDM symbol duration, which increases the number of channel impulse responses to be estimated, and the estimation difficulty. Thus, it would be interesting to investigate pilot based or blind channel estimation over doubly-selective channels in an OFDM system. In [70], a channel estimation method was proposed which pre-cancels the ICI for the channel estimation using the channel of the previous symbol, and post-cancels the ICI for symbol detection with the more accurate channel information. The first symbol is assumed to be a preamble for initialization of the channel estimation method.

6.2.3 Channel Estimation in MIMO OFDM Systems

The channel estimation methods for single-input single-output (SISO) OFDM systems can be modified for use in MIMO OFDM systems. However, for an $N_t \times N_r$ MIMO OFDM system, the computational complexity of these channel estimation algorithms is increased by a factor of $N_t \times N_r$, and the solution may involve the inversion of a high-dimensional matrix. Thus channel estimation becomes a challenging problem in OFDM systems. It is worthwhile to design a low complexity channel estimation algorithm that utilizes fewer pilot tones to obtain reliable channel information for MIMO OFDM systems. In [71], a multichannel compressed sensing method is proposed for these systems to estimate the channel information by exploiting the sparsity of the individual OFDM channels as well as the joint sparsity of MIMO wireless channels.

Appendix A

Derivation of Constraint (5.11b)

Assume the white Gaussian noise has variance σ^2, so that

$$E(\mathbf{\Phi h} - \mathbf{Y}_M)^2 \leq \sigma^2$$

which is equivalent to

$$\frac{1}{M}\sum_{k=1}^{M}(\phi_k \mathbf{h} - Y_k)^2 \leq \sigma^2$$

Consequently, we have

$$\|\mathbf{\Phi} \boldsymbol{h} - \mathbf{Y}_M\|_2 = \sqrt{\sum_{k=1}^{M}(\phi_k \mathbf{h} - Y_k)^2} \leq \sqrt{M}\sigma$$

Bibliography

[1] ETSI, "Digital video broadcasting: framing structure, channel coding, and modulation for digital terrestrial television," *European Telecommunication Standard*, ETS 300–744, Aug. 1997.

[2] ETSI, "Radio broadcasting systems: digital audio broadcasting to mobile, portable and fixed receivers," *European Telecommunication Standard*, ETS 300–401, Feb. 1995.

[3] IEEE 802.11, "IEEE standard for wireless LAN: Medium access control (MAC) and physical layer (PHY) specifications", Nov. 1997.

[4] 3GPP, http://www.3gpp.org/article/lte, May 2011.

[5] IEEE 802.16, "IEEE standard for local and metropolitan area networks: Air interface for fixed broadband wireless access systems", June 2004.

[6] T. S. Rappaport, *Wireless Communications Principles and Practice,* 1st Ed., Prentice-Hall, 1996.

[7] J. G. Proakis, *Digital Communications*, 4th Ed., McGraw-Hill, 2001.

[8] M. Patzold, *Mobile Fading Channels: Modelling, Analysis, and Simulation*, 1st Ed., Wiley, 2002.

[9] W. C. Jakes, *Microwave Mobile Communications*, Wiley, 1974.

[10] R. V. Nee and R. Prasad, *OFDM for Wireless Multimedia Communications*, Artech House, 2000.

[11] R. W. Chang, "Synthesis of band-limited orthogonal signals for multichannel data transmission," *Bell System Technical Journal*, vol. 45, pp. 1775–1796, Dec. 1996.

[12] S. B. Weinstein and P. M. Ebert, "Data transmission by frequency division multiplexing using the discrete fourier transform," *IEEE Transactions on Communications*, vol. 19, pp. 628–634, Oct. 1971.

[13] A. Peled and A. Ruiz, "Frequency domain data transmission using reduced computational complexity algorithms," *Proceedings of IEEE International Conference on Acoustics, Speech, and Signal Processing*, pp. 964–967, Apr. 1980.

[14] A. R. S. Bahai, B. R. Saltzberg, and M. Ergen, *Multicarrier Digital Communications: Theory and Applications of OFDM,* Springer, 2004.

[15] Y. J. Kou, *Peak-to-Average Power-Ratio and Intercarrier Interference Reduction Algorithms for Orthogonal Frequency Division Multiplexing Systems,* Ph.D. Dissertation, University of Victoria, Dec. 2005.

[16] P. Robertson and S. Kaiser, "Analysis of the loss of orthogonality through Doppler spread in OFDM systems," *Proceedings of IEEE Global Telecommunications Conference*, pp. 701–706, 1999.

[17] M. Russell and G. L. S. Stuber, "Interchannel interference analysis of OFDM in a mobile environment," *Proceedings of IEEE Vehicular Technology Conference*, pp. 820–824, July 1995.

[18] Y. G. Li and L. J. Cimini Jr., "Bounds on the interchannel interference of OFDM in time-varying impairments," *IEEE Transactions on Communications*, vol. 49, no. 3, pp. 401–404, Mar. 2001.

[19] W.-S. Hou and B.-S. Chen, "ICI cancellation for OFDM communication systems in time-varying multipath fading channels," *IEEE Transactions on Wireless Communications*, vol. 4, no. 5, pp. 2100–2110, Sept. 2005.

[20] X. Cai and G. B. Giannakis, "Bounding performance and suppressing intercarrier interference in wireless mobile OFDM," *IEEE Transactions on Communications*, vol. 51, no. 12, pp. 2047–2056, Dec. 2003.

[21] Y. J. Kou, W.-S. Lu, and A. Antoniou, "An iterative intercarrier-interference reduction algorithm for OFDM systems," *Proceedings of IEEE Pacific Rim Conference on Communications, Computers, and Signal Processing*, pp. 538–541, Aug. 2005.

[22] H. Arslan and G. E. Bottomley, "Channel estimation in narrowband wireless communication systems," *Wireless Communications and Mobile Computing*, vol. 1, no. 2, pp. 201–219, Apr. 2001.

[23] M. K. Ozdemir and H. Arslan, "Channel estimation for wireless OFDM systems," *IEEE Communications Surveys and Tutorials*, vol. 9, pp. 18–48, 2007.

[24] S. G. Kang, Y. M. Ha, and E. K. Joo, "A comparative investigation on channel estimation algorithms for OFDM in mobile communications," *IEEE Transactions on Broadcasting*, vol. 49, no. 2, pp. 142–149, June 2003.

[25] O. Edfors, M. Sandell, J. J. van de Beek, S. K. Wilson, and P. O. Borjesson, "OFDM channel estimation by singular value decomposition," *Proceedings of IEEE Vehicular Technology Conference*, pp. 923–927, Apr. 1996.

[26] S. Verdú, *Multiuser Detection*, Cambridge University Press, 1998.

[27] Y.-S. Choi, P. J. Voltz and F. A. Cassara, "On channel estimation and detection for multicarrier signals in fast and selective Rayleigh fading channels," *IEEE Transactions on Communications*, vol. 49, no. 8, pp. 1375–1387, Aug. 2001.

[28] H. T. Peng, L. K. Rasmussen, and T. J. Lim, "Constrainted maximum-likelihood detection in CDMA," *IEEE Transactions on Communications*, vol. 49, pp. 142–152, Jan. 2002.

[29] A. Yener, R.D. Yates and S. Ulukus, "CDMA multiuser detection: a nonlinear programming approach," *IEEE Transactions on Communications*, vol. 50, no. 6, pp. 1016–1024, June 2002.

[30] S. Boyd and L. Vandenberghe, *Convex Optimization*, Cambridge University Press, 2004.

[31] R. A. Horn and C. R. Johnson, *Matrix Analysis*, Cambridge University Press, 1985.

[32] W.-S. Lu, "Design of FIR digital filters with discrete coefficients via convex programming," *Proceedings of IEEE International Symposium on Circuits and Systems*, pp. 1831–1834, May 2005.

[33] SeDuMi ver. 1.1, Advanced Optimization Laboratory, McMaster University, http://sedumi.mcmaster.ca/.

[34] N. J. Bass and D. P. Taylor, "Matched filter bounds for wireless communication over Rayleigh fading dispersive channel," *IEEE Transactions on Communications*, vol. 49, no. 9, pp. 1525–1528, Sept. 2001.

[35] H. Vikalo, B. Hassibi, and P. Stoica, "Efficient joint maximum-likelihood channel estimation and signal detection," *IEEE Transactions on Wireless Communications*, vol. 5, no. 7, pp. 1838–1845, July 2006.

[36] M.-X. Chang and Y. T. Su, "Blind and semiblind detection of OFDM signals in fading channels," *IEEE Transactions on Communications*, vol. 52, no. 5, pp. 744–754, May 2004.

[37] T. Cui and C. Tellambura, "Semi-blind equalization for OFDM systems over fast fading channels," *Proceedings of IEEE International Conference on Communications*, pp. 1137–1141, May 2005.

[38] E. Viterbo and J. Boutros, "A universal lattice code decoder for fading channels," *IEEE Transactions on Information Theory*, vol. 45, no. 5, pp. 1639–1642, July 1999.

[39] B. Hassibi and H. Vikalo, "On the sphere-decoding algorithm I: Expected complexity," *IEEE Transactions on Signal Processing*, vol. 53, no. 8, pp. 2806–2818, Aug. 2005.

[40] T. Cui and C. Tellambura, "Joint data detection and channel estimation for OFDM systems," *IEEE Transactions on Communications*, vol. 54, no. 4, pp. 670–679, Apr. 2006.

[41] R. W. Heath and G. B. Giannakis, "Exploiting input cyclostationarity for blind channel identification in OFDM systems," *IEEE Transactions on Signal Processing*, vol. 47, no. 3, pp. 848–856, Mar. 1999.

[42] X. Cai and A. N. Akansu, "A subspace method for blind channel identification in OFDM systems," *Proceedings of IEEE International Conference on Communications*, pp. 929–933, June 2000.

[43] C. Li and S. Roy, "Subspace-based blind channel estimation for OFDM by exploiting virtual carriers," *IEEE Transactions on Wireless Communications*, vol. 2, no. 1, pp. 141–150, Jan. 2003.

[44] O. Grellier, P. Comom, B. Mourrain, and P. Trebuchet, "Analytical blind channel identification," *IEEE Transactions on Signal Processing*, vol. 50, no. 9, pp. 2196–2207, Sep. 2002.

[45] B. Picinbono, "On circularity," *IEEE Transactions on Signal Processing*, vol. 42, no. 12, pp. 3473–3482, Dec. 1994.

[46] I. Kang, M. P. Fitz, and S. B. Gelfand, "Blind estimation of multipath channel parameters: A modal analysis approach," *IEEE Transactions on Communications*, vol. 47, no. 8, pp. 1140–1150, Aug. 1999.

[47] H. Minn and V.K. Bhargava, "An investigation into time-domain approach for OFDM channel estimation," *IEEE Transactions on Broadcasting*, vol. 46, no. 4, pp. 240–248, Dec. 2000.

[48] B. Yang, K. B. Letaief, R. S. Cheng and Z. Cao, "Channel estimation for OFDM transmission in multipath fading channels based on parametric channel modeling," *IEEE Transactions on Communications*, vol. 49, no. 3, pp. 467–478, Mar. 2001.

[49] M. Oziewicz, "On application of MUSIC algorithm to time delay estimation in OFDM channels," *IEEE Transactions on Broadcasting*, vol. 51, no. 2, pp. 249–255, June 2005.

[50] O. Simeone, Y. Bar-Ness, and U. Spagnolini, "Pilot-based channel estimation for OFDM systems by tracking the delay-subspace," *IEEE Transactions on Wireless Communications*, vol. 3, no. 1, pp. 315–325, Jan. 2004.

[51] M. R. Raghavendra and K. Giridhar, "Improving channel estimation in OFDM systems for sparse multipath channels," *IEEE Signal Processing Letters*, vol. 12, no. 1, pp. 52–55, Jan. 2005.

[52] E. Candés and T. Tao, "Near optimal signal recovery from random projections: Universal encoding strategies?" *IEEE Transactions on Information Theory*, vol. 52, no. 12, pp. 5406–5425, Dec. 2006.

[53] D. L. Donoho, "Compressed sensing," *IEEE Transactions on Information Theory*, vol. 52, no. 4, pp. 1289–1306, Apr. 2006.

[54] R. G. Baraniuk, "Compressive sensing," *IEEE Signal Processing Magazine*, vol. 24, no. 4, pp. 118–120 and 124, July 2007.

[55] E. Candès, J. Romberg, and T. Tao, "Robust uncertainty principles: Exact signal reconstruction from highly incomplete frequency information," *IEEE Transactions on Information Theory*, vol. 52, no. 2, pp. 489–509, Feb. 2006.

[56] S. F. Cotter and B. D. Rao, "Sparse channel estimation via matching pursuit with application to equalization," *IEEE Transactions on Communications*, vol. 50, no. 3, pp. 374–377, Mar. 2002.

[57] W. Li and J. C. Preisig, "Estimation of rapidly time-varying sparse channels," *IEEE Journal of Oceanic Engineering*, vol. 32, no. 4, pp. 927–939, Oct. 2007.

[58] W. U. Bajwa, J. Haupt, G. Raz, and R. Nowak, "Compressed channel sensing," *Proceedings of Conference on Information Sciences and Systems*, pp. 5–10, Mar. 2008.

[59] M. Sharp and A. Scaglione, "Estimation of sparse multipath channels," *Proceedings of IEEE Military Communications Conference*, pp. 1–7, Nov. 2008.

[60] G. Tauböck and F. Hlawatsch, "A compressed sensing technique for OFDM channel estimation in mobile environments: Exploiting channel sparsity for reducing pilots," *Proceedings of IEEE International Conference on Acoustics, Speech and Signal Processing*, pp. 2885–2888, Mar. 2008.

[61] G. Tauböck, F. Hlawatsch, and H. Rauhut, "Compressive estimation of doubly selective channels in multicarrier systems: Leakage effects and sparsity-enhancing processing," *IEEE Journal of Selected Topics in Signal Processing*, vol. 4, no. 2, pp. 255–271, 2010.

[62] X. He and R. Song, "Pilot pattern optimization for compressed sensing based sparse channel estimation in OFDM systems," *Proceedings of International Conference on Wireless Communications and Signal Processing*, pp. 1–5, Oct. 2010.

[63] C. R. Berger, S. Zhou and P. Willett, "Sparse channel estimation for OFDM: Over-complete dictionaries and super-resolution," *Proceedings of IEEE Workshop*

on Signal Processing Advances in Wireless Communications, pp. 196–200, June 2009.

[64] S. Mallat, *A Wavelet Tour of Signal Processing*, New York: Academic, 1999.

[65] A. Antoniou and W.-S. Lu, *Practical Optimization: Algorithms and Engineering Applications*, Springer, 2007.

[66] R. Berinde and P. Indyk, "Sparse Recovery using Sparse Random Matrices," *MIT-CSAIL Technical Report*, 2008.

[67] G. L. Stüber, J. R. Barry, S. W. McLaughlin, Y. Li, M. A. Ingram, and T. G. Pratt, "Broadband MIMO-OFDM wireless communications," *Proceedings of the IEEE*, vol. 92, no. 2, pp. 271–294, Feb. 2004.

[68] A. Stamoulis, S. N. Diggavi, and N. Al-Dhahir, "Intercarrier interference in MIMO OFDM," *IEEE Transactions on Signal Processing*, vol. 50, no. 10, pp. 2451–2464, Oct. 2002.

[69] R. Chen, Y. Y. Xu, H. B. Zhang, and H. W. Luo, "Iterative ICI mitigation method for MIMO OFDM systems," *IEICE Transactions on Communications*, vol. E89-B, no. 3, pp. 859–866, Mar. 2006.

[70] K. Kwak, S. Lee, H. Min, S. Choi, and D. Hong, "New OFDM channel estimation with dual-ICI cancellation in highly mobile channel," *IEEE Transactions on Wireless Communications*, vol. 9, no. 10, pp. 3155–3165, Oct. 2010

[71] D. Eiwen, G. Tauböck, F. Hlawatsch, H. Rauhut, and N. Czink, "Multichannel-compressive estimation of doubly selective channels in MIMO-OFDM systems: Exploiting and enhancing joint sparsity," *Proceedings of IEEE International Conference on Acoustics, Speech and Signal Processing*, pp. 3082–3085, Mar. 2010.

[72] Y. Peng, X. Yang, X. Zhang, W. Wang, and B. Wu, "Compressed MIMO-OFDM channel estimation," *Proceedings of IEEE International Conference on Communication Technology*, pp. 1291–1294, Nov. 2010.